

Dispersion and Modal Behavior of Different Optical Fiber Materials at Different Temperatures

Submitted by

Sajib Barua, Student No. 201016040

Farha Diba, Student No. 201016044

A K M Ahsan Habib, Student No. 201016060



**Electrical, Electronic and Communication Engineering
Military Institute of Science and Technology (MIST)**

Thesis submitted to the Faculty of the Electrical, Electronic and Communication Engineering, of
Military Institute of Science and Technology (MIST), in partial fulfillment of the requirements
for the degree of

B.Sc in Electrical, Electronic and Communication Engineering

Supervised by

Dr. Md. Shah Alam

Professor

Department of Electrical and Electronic Engineering
Bangladesh University of Engineering and Technology (BUET)
Dhaka-1000, Bangladesh

DECLARATION

This is to certify that the research work presented in this thesis paper is the outturn of the study, analysis and simulation carried out by the undersigned students of Electrical, Electronic and Communication Engineering, (EECE-8), Military Institute of Science and Technology (MIST), Mirpur cantonment, Mirpur-12, Dhaka-1216, under the direct supervision of Dr. Md. Shah Alam, professor, department of Electrical and Electronic Engineering (EEE), Bangladesh University of Engineering and Technology (BUET), Dhaka-1000, Bangladesh.

We declare that the thesis entitled “**Dispersion and modal behavior of different optical fiber materials at different temperatures**” and the work presented in the thesis are both our own and have been generated by us. We confirm that:

- This work is done wholly while in candidature for an under-graduate research degree at this university.
- Where we have quoted from the works of others, the source is always given. With the exception of such quotations; the thesis is entirely our own work.
- We have acknowledged all sources of help.
- This thesis work is not published anywhere.

SAJIB BARUA

Student No. 201016040
EECE-8, MIST

DR. MD. SHAH ALAM

Professor
Dept. of EEE, BUET

FARHA DIBA

Student No. 201016044
EECE-8, MIST

A K M AHOSAN HABIB

Student No. 201016060
EECE-8, MIST

CERTIFICATION

The thesis paper titled “**Dispersion and modal behavior of different optical fiber materials at different temperatures**” is submitted by the group mentioned to the Faculty of the Electrical, Electronic and Communication Engineering of Military Institute of Science And Technology (MIST), has been accepted as partially fulfillment of the requirements for the degree of B.Sc. in Electrical, Electronic and Communication Engineering On December 2013.

SAJIB BARUA

Student No. 201016040
EECE-8, MIST

DR. MD. SHAH ALAM

Professor
Dept. of EEE, BUET

FARHA DIBA

Student No. 201016044
EECE-8, MIST

A K M AHOSAN HABIB

Student No. 201016060
EECE-8, MIST

ACKNOWLEDGEMENT

We have the pleasure, at this final stage of our thesis, to thank some of the exceptional people who helped us throughout the thesis. Firstly, we would like to thank our supervisor Dr. Md. Shah Alam, professor, department of EEE, Bangladesh Engineering University and Technology (BUET), whose emphatic guidance, instruction and supervision motivated us to work on this subject. It is he who persuaded our intrusive mind to bring out some dynamic result of our work. Without his sensible and prudent judgment and observation, we could hardly fulfill our job.

We are grateful to Dr. Satya Prasad Majumder, Professor in the selection grade, Department of Electrical, Electronic and Communication Engineering (EECE), Military Institute of Science and Technology (MIST), for his immense help throughout the whole work.

We would, however like to thank MIST authority and the faculty members of EECE for broadening their supporting hands throughout the work.

ABSTRACT

Temperature dependent Sellmeier coefficients are necessary for determining different optical design parameters which are important for optical fiber communication system. These coefficients are calculated for fused Silica (SiO_2), Aluminosilicate and Vycor glasses, to find the dependence of chromatic dispersion on temperature and at any wavelengths encompassing the profile dispersion parameter. The zero-dispersion wavelengths, for single mode fiber is modeled and investigated for all three materials, considering step-index fiber model. Temperature effects on zero-dispersion wavelengths, are also investigated for a wide range (-120°C to 120°C) as well as including the relative refractive index difference. The two important modal properties, the effective area and power propagation through the fiber are calculated first solely and then considering the perfectly matched layer (PML). It was found that the power propagation increased and the corresponding effective area decreased due to the use of PML which strongly supports the theory of confinement of light within the core region. We calculated the dependence of modal birefringence and polarization mode dispersion upon wavelength for different fiber materials. We also determined the sensitivities of these two parameters to temperature. Our results show that in the analyzed spectral range both modal birefringence and polarization mode dispersion decreases with wavelength.

DEDICATION

To our respected Parents

TABLE OF CONTENTS

Declaration.....	i
Certification.....	ii
Acknowledgements.....	iii
Abstract.....	iv
Dedication.....	v
Table of Contents.....	vi
List of figures.....	ix
List of tables.....	xii
Chapter 1 General.....	1
1.1 Introduction.....	1
1.2 Optical fiber communication system.....	2
1.3 Optical spectral bands.....	4
1.4 Advantages of optical fiber communication.....	6
1.5 Applications of optical fiber.....	7
1.6 Objective of the work.....	9
1.7 Layout of the thesis.....	9
Chapter 2 Basics of Optical Fiber.....	10
2.1 Optical Fiber.....	10
2.2 Basic Structure of Optical Fiber.....	11
2.2.1 Core.....	11
2.2.2 Cladding.....	11
2.2.3 Coating.....	12
2.2.4 Strength members.....	12
2.2.5 Jacket.....	12
2.3 Optical Fiber Materials.....	12
2.3.1 Fused Silica.....	13
2.3.2 Vycor Glass (7913).....	13
2.3.3 Aluminosilicate (Al_2SiO_5).....	14
2.4 Refraction of Light.....	14
2.5 Refractive Index.....	15
2.6 Snell's Law.....	15

2.7 Total Internal Reflection (TIR).....	16
2.8 Critical Angle.....	17
2.9 Acceptance Angle.....	17
2.10 Cone of Acceptance.....	18
2.11 Numerical Aperture (NA).....	18
2.12 Types of Optical Fiber.....	19
2.12.1 Based on mode of propagation.....	20
2.12.2 Based on Fiber Index Profile.....	20
2.13 Fiber Optic Configuration.....	21
2.13.1 Single Mode Step Index Fiber.....	22
2.13.2 Multimode Step Index Fiber.....	22
2.13.3 Multimode Graded Index Fiber.....	23
2.14 Transmission Characteristics of Optical Fiber.....	23
2.14.1 Bandwidth–distance product (or bandwidth–length product).....	24
2.14.2 Material Absorption Losses.....	24
2.14.3 Linear scattering losses.....	26
2.14.4 Nonlinear scattering Losses.....	27
Chapter 3 Modal properties of optical fiber.....	29
3.1 Optical fiber as a cylindrical waveguide.....	29
3.2 Effective refractive index.....	33
3.3 Cutoff wavelength.....	34
3.4 Sellmeier Equation.....	35
3.5 Dispersion.....	38
3.5.1 Dispersion in single mode fibers.....	38
3.5.1.1 Material dispersion.....	38
3.5.1.2 Waveguide Dispersion.....	39
3.5.1.3 Chromatic dispersion or Total dispersion.....	39
3.5.1.4 Profile dispersion.....	40
3.6 Effective area.....	40
3.7 Complex refractive index.....	41
3.8 Perfectly Matched Layer (PML).....	41
3.9 Modal Birefringence.....	43
3.10 Polarization Mode Dispersion.....	43

Chapter 4 Simulation Results and Discussions.....	45
4.1 Temperature dependence of refractive indices.....	45
4.2 Effective Refractive Index.....	47
4.3 Dispersion.....	49
4.3.1 Material Dispersion.....	49
4.3.2 Chromatic Dispersion.....	53
4.3.3 Profile Dispersion.....	55
4.4 Effective Area.....	59
4.5 Power Flow.....	61
4.6 Perfectly Matched Layer (PML).....	63
4.6.1 Effective Area and Power Using PML.....	63
4.7 Birefringence.....	66
4.8 Polarization Mode Dispersion.....	68
Chapter 5 Conclusion.....	74
5.1 Conclusion.....	74
5.2 Scope of Future Work.....	74
References.....	75

LIST OF FIGURES

Figure 1.1 Optical fiber communication system	3
Figure 1.2 Spectrum of electromagnetic radiation.....	4
Figure 1.3 Optical windows.....	5
Figure 1.4 The route of the submarine cable, SEA-ME-WE 4.....	8
Figure 2.1 The optical fiber.....	10
Figure 2.2 Basic structure of an optical fiber.....	11
Figure 2.3 Refraction of Light.....	15
Figure 2.4 Total internal reflection.....	16
Figure 2.5 Cone of acceptance.....	18
Figure 2.6 Optical fiber configuration.....	23
Figure 2.7 Absorption in optical fiber.....	25
Figure 3.1 A step-index waveguide.....	30
Figure 3.2 PML region surrounding the waveguide structure.....	42
Figure 4.1 Refractive index vs. wavelength for three optical glasses.....	45
Figure 4.2 Refractive index vs. temperature for three optical glasses.....	45
Figure 4.3 Sellmeier coefficients vs. temperature for SiO ₂ glass.....	46
Figure 4.4 Sellmeier coefficients vs. temperature Aluminosilicate glass.....	46
Figure 4.5 Sellmeier coefficients vs. temperature Vycor glass.....	47
Figure 4.6 Effective mode index for Aluminosilicate with normalized electric field.....	47
Figure 4.7 Effective mode index vs. wavelength for SiO ₂ glass at 26 ⁰ C.....	48
Figure 4.8 Effective mode index as a function of temperature.....	49
Figure 4.9 Material dispersion at 26 ⁰ C for all three glasses.....	49
Figure 4.10 Material dispersion for SiO ₂ glass at 26 ⁰ C with zero dispersion wavelength.....	50
Figure 4.11 Material dispersion vs. wavelength for a wide range of temperature for SiO ₂ glass.....	51
Figure 4.12 Material dispersion vs. wavelength for a wide range of temperature for Aluminosilicate glass.....	51

Figure 4.13 Material dispersion vs. wavelength for a wide range of temperature for Vycor glass.....	52
Figure 4.14 Zero-dispersion wavelength vs. temperature.....	52
Figure 4.15 Chromatic dispersion vs. wavelength for 26 ⁰ C for SiO ₂ glass.....	53
Figure 4.16 Chromatic dispersion vs. wavelength for 26 ⁰ C for Aluminosilicate glass.....	54
Figure 4.17 Chromatic dispersion vs. wavelength for 26 ⁰ C for Vycor glass.....	54
Figure 4.18 Profile dispersion vs. wavelength for SiO ₂ glass.....	55
Figure 4.19 Profile dispersion vs. wavelength for Aluminosilicate glass.....	55
Figure 4.20 Profile dispersion vs. wavelength for Vycor glass.....	56
Figure 4.21 Profile dispersion vs. wavelength for SiO ₂ glass.....	56
Figure 4.22 Profile dispersion vs. wavelength for Aluminosilicate glass.....	57
Figure 4.23 Profile dispersion vs. wavelength for Vycor glass.....	57
Figure 4.24 Profile dispersion vs. wavelength for all three glasses.....	58
Figure 4.25 Total dispersion vs. wavelength considering profile dispersion at 26 ⁰ C for SiO ₂ glass.....	59
Figure 4. 26 Effective area vs. wavelength of SiO ₂ glass at different temperatures.....	60
Figure 4. 27 Effective area vs. wavelength of Aluminosilicate glass at different temperatures...60	60
Figure 4. 28. Effective area vs. wavelength of Vycor glass at different temperatures.....	61
Figure 4.29 Maximum power flow through the core.....	61
Figure 4.30 Power flow vs. wavelength of SiO ₂ glass at different temperatures.....	62
Figure 4.31 Power flow vs. wavelength of Aluminosilicate glass at different temperatures.....	62
Figure 4.32 Power flow vs. wavelength of Vycor glass at different temperatures.....	63
Figure 4.33 Perfectly matched layer (PML).....	64
Figure 4.34 Effective area vs. wavelength of Aluminosilicate glass at different temperatures using PML.....	64
Figure 4.35 Effective area vs. wavelength of Vycor glass at different temperatures using PML.....	65

Figure 4.36 Power flow vs. wavelength of Aluminosilicate glass at different temperatures using PML.....	65
Figure 4.37 Power flow vs. wavelength of Vycor glass at different temperatures using PML.....	66
Figure 4.38 Birefringence vs. wavelength for Aluminosilicate glass.....	66
Figure 4.39 Birefringence vs. wavelength for SiO ₂ glass.....	67
Figure 4.40 Birefringence vs. wavelength for Vycor glass.....	67
Figure 4.41 PMD vs. wavelength for SiO ₂ glass.....	68
Figure 4.42 PMD vs. wavelength for Aluminosilicate glass.....	68
Figure 4.43 PMD vs. wavelength for Vycor glass.....	69
Figure 4.44 PMD vs. wavelength for all three glasses at 45.2 ⁰ C.....	69
Figure 4.45 PMD vs. wavelength for all three glasses at 60 ⁰ C.....	70
Figure 4.46 PMD Coefficient vs. wavelength for Aluminosilicate glasses at 45.2 ⁰ C.....	71
Figure 4.47 PMD Coefficient vs. wavelength for Aluminosilicate glasses at 60 ⁰ C.....	71
Figure 4.48 PMD Coefficient vs. wavelength for SiO ₂ glasses at 45.2 ⁰ C.....	72
Figure 4.49 PMD Coefficient vs. wavelength for SiO ₂ glasses at 60 ⁰ C.....	72
Figure 4.50 PMD Coefficient vs. wavelength for Vycor glasses at 45.2 ⁰ C.....	73
Figure 4.51 PMD Coefficient vs. wavelength for Vycor glasses at 60 ⁰ C.....	73

LIST OF TABLES

Table 1.1.....	6
Table 2.1.....	14
Table 2.2.....	22
Table 3.1.....	32
Table 3.2.....	36
Table 3.3.....	36

Chapter 1

General

1.1 Introduction

In this information age, we are faced with the technological ability to communicate conveniently with anyone, anywhere and at any time in many different ways-voices, facsimile, data, e-mail, image and video-and all this at an affordable cost. Thus modern society has impressively been reduced to a global village and exchange of information has experienced an explosion enormously.

The introduction of microwaves in the 1920's for communication between two distant points, this technology has gone through a remarkable amount of development. However, these links were limited to distances within the 'line of sight' (roughly 30 kilometers). Thus, the need for orbiting satellites to relay information over long distances was conceived as real. Today satellites of all shapes and capabilities have been introduced to serve almost all the countries of the world. However, signals are weakened about a hundred times after travelling these large link distances, thus necessitating the usage of high gain antennas and powerful transmitters. A more relevant problem, however, is the delay and echo often experienced in long distance phone calls that use these satellites, popularly known as satphone.

The settlement of even increasing traffic needs the usages of higher frequency bands for satellite communications. The limitations on the performance of satellite communication systems at frequencies more than 10GHz result from a strong interaction of radio waves with rain and ice in the lower atmosphere. Attenuation due to rain dominates the power margin for system operating above 10GHz; hence multiple sites are conditioned to cope up high availability objectives. In addition, the capacity per beam is strongly reduced by rain. For example, to ensure the same quality of transmission during rainy period, the capacity may have to be halved. Conclusively, a substantial number of terrestrial relays (microwave radio links that operate only within 'line of sight' distances) are needed to transmit the information.

The fundamental shortfalls of satellite based system, accelerates the real interest in optical communication, which was aroused with the invention of the laser in early 1960's. This device provides a powerful coherent light source, together with the possibility of modulation at high frequencies. In addition the low beam divergence of the laser made enhanced free space optical transmission a practical outcome. The first modern optical communication experiments involved laser beam transmission through the atmosphere. However, it was realized that laser beams could not be sent in the open atmosphere for reasonably long distances to carry signals. This is due to fact that the light beam is severely attenuated and distorted owing to scattering and absorption by the atmosphere.

Thus, for reliable long-distance light-wave communication in terrestrial environments it would be necessary to provide a transmission medium that could protect the signal-carrying light beams from the shortfalls of the terrestrial environment.

In 1966, Kao and Hockham made an extremely important suggestion; they noted that optical fibers based on silica glass could provide necessary transmission medium if metallic and other impurities could be removed from the silica. The proposals for optical communication via dielectric waveguides from glass to avoid degradation of optical signal while propagating through the atmosphere, were made almost simultaneously in 1966 by Kao and Hockham and Werts. These systems were considered as a replacement of earlier coaxial cables or carrier transmission systems. Early systems exhibited very high attenuation (1000 dB/km), implying a power loss by a factor of 100 in traversing only 20m of the fiber, and therefore the actual breakthrough in optical transmission remained in the verse of theory. This high loss was primarily due to the trace amounts of impurities present in the glass. There also serious problems involved in jointing the fiber cables to achieve low loss for better performance.

The 1966 paper of Kao and Hockham triggered the beginning of research into removing traces of impurities present the glass. In 1970, Kapron, Kech and Maurer (at Corning Glass, USA) were successfully produced silica fibers with a loss of about 17 dB/km at the helium-neon (He-Ne) laser wavelength of 633nm. Since then technology has advanced with tremendous rapidity. By 1985 glass fibers were routinely being produced with extremely low losses; less than. 25 dB/km, which correspond to a transmission of more than 94% of the incident power after traversing 1 km of the optical fiber [1].

In parallel with the development of the fiber waveguide, attenuation was also focused on the other optical components which would constitute the whole optical fiber communication system. Since optical frequencies are accompanied by extremely small wavelengths the development of all these optical components essentially required a new technology. Thus semi-conductor optical source (i.e. injection leaser and light emitting diodes) and detectors (i.e. photo diodes and to a lesser extent photo transistors) compatible in size with optical fibers were designed and fabricated to enable successful implementation of the optical fiber system.

1.2 Optical fiber communication system

Optical fiber communication system is a communication system in which information is transmitting through one place to another by sending pulses of light through optical fiber. A transmission system consists of a transmitter or modulator linked, transmits through a medium and a receiver or demodulator at the destination point where the information source provides an electrical signal. A transmitter comprises electrical or electronics components which converts the signal into suitable form for propagating over the light medium by modulating a carrier. The transmission medium consists of a pair of wires, a coaxial cable or a radio link. Through the

transmission medium signal is transmitted to the destination or receiver. Over a transmitted medium the signals are attenuated or loss. The general block diagram of optical fiber communication system is shown in the figure below:

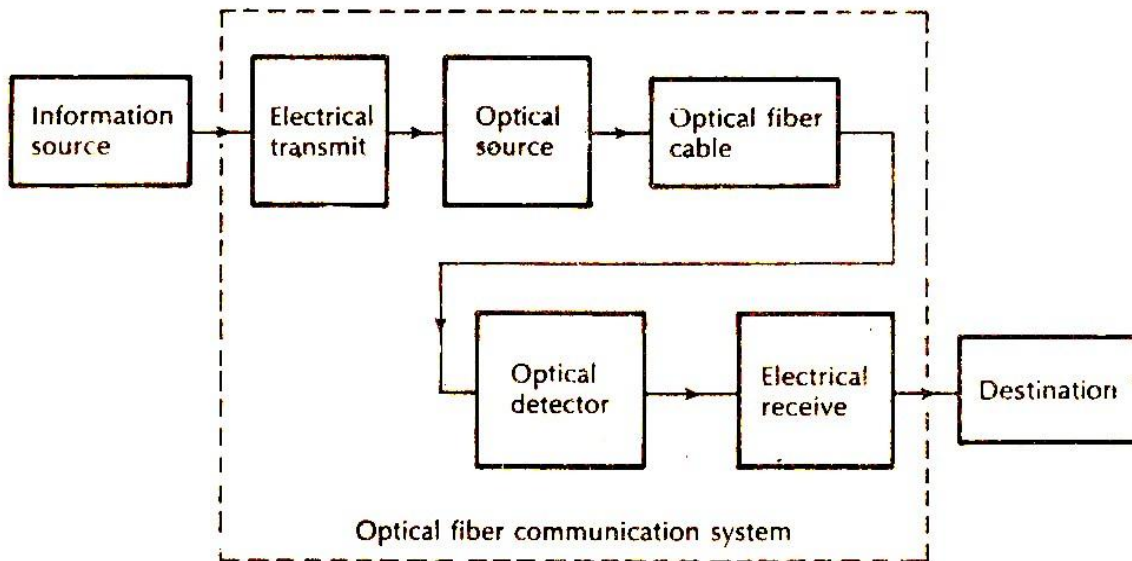


Fig. 1.1 Optical fiber communication system [2]

The source provides information in the form of electrical signal to the transmitter. The electrical stage of the transmitter drives an optical source to produce modulated light wave carrier. Semiconductor LASERS or LEDs are usually used as optical source here. The information carrying light wave passes through the transmission medium, for example optical fiber cables in this system. When it reaches to the receiver stage where the optical detector demodulates the optical carrier gives an electrical output signal to the electrical stage. The common types of optical detectors used are p-n, p-i-n and avalanche photodiode etc. Finally the electrical stage gets the real information back and gives it to the concern destination. The optical carrier may be modulated by either analog or digital information signal. In digital optical fiber communication system the information is suitably encoded prior to the drive circuit stage of optical source. It is more likely at the receiver end a decoder is used after amplifier and equalizer stage.

1.3 Optical spectral bands

Now-a-days a larger portion of electromagnetic spectrum was utilized to develop more reliable communication. For a more reliable communication system we have to increase data rates so that more information can be sent. So for these activities radio frequency, microwave and satellite links, under sea copper based wire lines are invented. Time-varying information bearing signal transferred over a communication channel by super imposing it on to a sinusoidal signal which is known as carrier and this is the reason for this trend. The baseband information is removed from the carrier at the destination and it is processed as desired. By increasing the carrier frequency increases the available transmission bandwidth and consequently provides larger information. The figure below shows the spectral band is used for radio transmission from high frequency (HF) to very high frequency (VHF) and very high to ultra high (UHF) with the nominal frequencies of 10^7 , 10^8 and 10^9 Hz, respectively. Optical frequencies are several orders of magnitude higher than those used in electrical communication system. Mainly optical band ranges from 10^{14} to 10^{15} Hz. The invention of laser arouses a development of using optical region of electromagnetic spectrum. The near-infrared spectral band ranging from 770 to 1675 nm as this is a low-loss region in silica glass fiber.

The technical advancement of optical communication is started in 1970. At this time researcher at Corning Glass demonstrated the feasibility of producing a glass fiber having an optical power loss that was low for a practical transmission link.

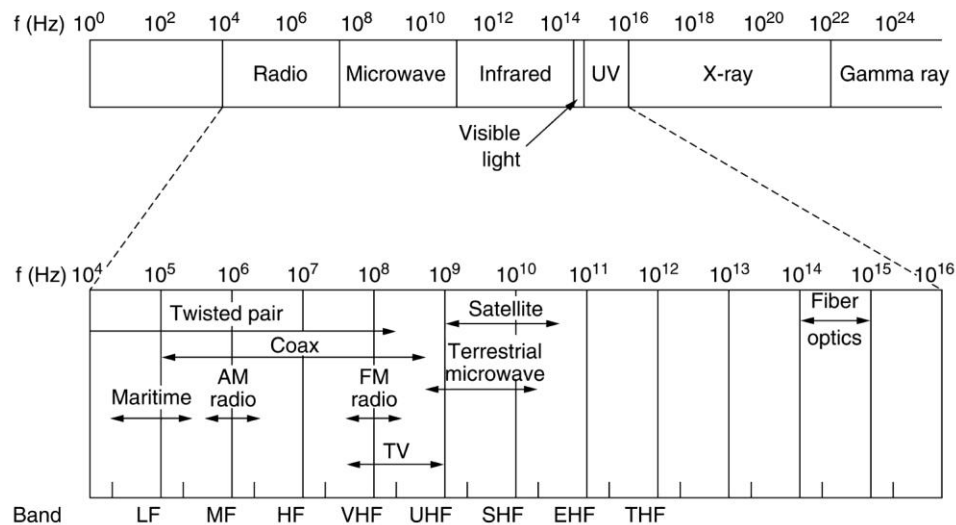


Fig. 1.2 Spectrum of electromagnetic radiation [3]

In the late 1970 the first installed optical fiber link appeared which uses 6 Mb/s over distances 10km. There is a huge development about 1980 where the link carrying data rates beyond terabits per seconds over the distances of 100km without restoring the signals fidelity along the path length. Optical fiber communications typically operate in a wavelength region corresponding to one of the following telecom windows:

- The first window at 800–900 nm was originally used. GaAs/AlGaAs-based laser diode and light emitting diodes (LEDs) served as transmitters, and silicon photodiodes were suitable for the receivers. However, the fiber losses are relatively high in this region, and fiber amplifiers are not well developed for this spectral region. Therefore, the first telecom window is suitable only for short-distance transmission.
- The second telecom window utilizes wavelengths around 1.3 μm , where the loss of silica fibers is much lower and the fiber's chromatic dispersion is very weak, so that pulse broadening is minimized. This window was originally used for long-haul transmission.
- The third telecom window, which is now very widely used, utilizes wavelengths around 1.5 μm . The losses of silica fibers are the lowest in this region, and erbium doped fibers are available which offer very high performance. Fiber dispersion is usually anomalous but can be tailored with great flexibility. The figure below shows the operating range of optical fiber systems.

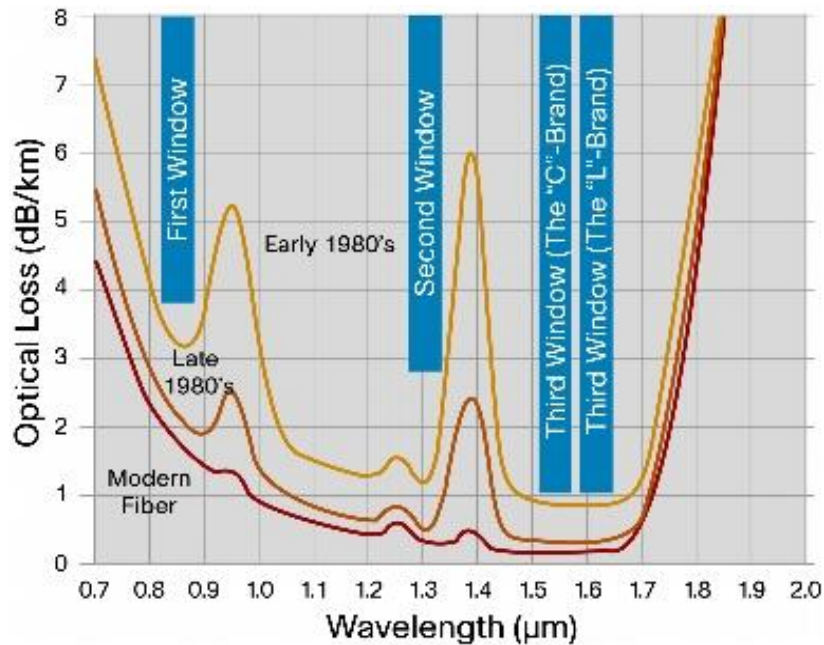


Fig. 1.3 Optical windows [4]

The second and third telecom windows are further subdivided into the following wavelength bands [5]:

Table 1.1
Subdivision of second and third window

Band	Description	Wavelength range
O band	original	1260–1360 nm
E band	extended	1360–1460 nm
S band	short wavelengths	1460–1530 nm
C band	conventional (“erbium window”)	1530–1565 nm
L band	long wavelengths	1565–1625 nm

1.4 Advantages of optical fiber communication

(a) **Enormous potential bandwidth:** The optical carrier frequency in the range 10^{13} to 10^{14} Hz offers the potential for a fiber information carrying capacity that is many orders of magnitude in excess of that obtained using copper cable or wideband radio systems. This enables fibers to simultaneously carry voice, data, image and video signals.

(b) **Small size and weight:** An optical fiber is often no wider than the diameter of a human hair; thus even after applying protective layers, they are far smaller and much lighter than corresponding copper cables. This is a tremendous boon to alleviating duct congestion in cities.

(c) **Immunity to interference and cross talk:** As optical fibers form a dielectric waveguide it is free from electromagnetic interfaces (EMI), radio frequency interfaces (RFI) or switching transients giving electromagnetic pulses (EMP). Therefore in a noisy environment optical fiber communication is unaffected where the fiber cable requires no shielding from EMI. It is fairly to ensure that there is no optical interface between fibers, and hence unlike communication using electrical conductors, cross talk is negligible even many fibers are cabled together.

(d) **Signal security:** As light from a fiber does not radiate significantly, a transmitted optical signal cannot be obtained non-invasively, thus ensuring a high degree of signal security.

(e) Low transmission loss: With losses as low as 0.2 dB/km, this feature alone has become a major advantage of optical fiber as extremely wide repeater spacing's (70 to 100km) may be used in long-haul communication links. This in turn reduces both system cost and complexity.

(f) System reliability and ease of maintenance: Due to the low loss property, system reliability is generally enhanced in comparison to conventional electrical conductor systems. Furthermore, reliability of optical components have predicted lifetimes of 20-30 years. Combined, these factors tend to reduce maintenance time and costs.

(g) Ease of Installation: Increasing transmission capacity of wire cables generally makes them thicker and more rigid. Such thick cables can be difficult to install in existing buildings where they must go through walls and cable ducts. Fiber cables are easier to install since they are smaller and more flexible. They can also run along the same routes as electric cables without picking up excessive noise.

(h) Enhanced safety: Optical fibers offer a high degree of operational safety, since they do not have the problems of ground loops, sparks, and potentially high voltages inherent in copper lines. However, precautions with respect to laser light emissions need to be observed to prevent possible eye damage.

1.5 Applications of optical fiber

If fiber optic technology had not emerged, extensive digitalization of the long-distance network would not have occurred as rapidly. High bandwidth coaxial cable transmission systems are too expensive to universally replace radio systems. Fiber transmission systems, on the other hand, provide dramatic savings in equipment and operational costs. Today, we are a world dependent upon a communications system that moves literally at the speed of light to deliver services in a variety of applications.

Enterprise and Private Networks: Exponential growth in data traffic is driving an ever-increasing demand for more bandwidth in enterprise and business networks around the world. To satisfy this ever-increasing need, service providers have adopted high-speed protocols and are looking toward a future that may require speeds of 40G to 100G or more. Network designers and planners need a multimode fiber specifically designed and tested for use with laser-based protocols to maximize the capabilities of bandwidth delivered in these high-speed systems.

FTTH and Access Networks: For millions of households, fiber-to-the-home (FTTH) is making the potential of broadband connectivity a day-to-day reality, enhancing their quality of life. Around the world, consumers are getting the secure, unsurpassed bandwidth capabilities of optical fiber waveguides to their home for always-on, affordable high-speed internet access, not to mention telecommuting, distance learning, telemedicine and video on demand (VOD).

Long-haul Networks: Long-haul terrestrial optical fiber networks connect countries and cities throughout the world. Today, these networks typically range from a few dozen to a few thousand kilometers, and have largely migrated to 10 Gb/s-based dense wavelength division multiplexed (DWDM) systems with 32 channels or more.

Submarine Networks: Given the harsh undersea environment, submarine telecommunications systems demand the most advanced optical technologies. The family of Vascade fibers enables high-speed, high-capacity solutions, providing the performance and reliability required in all undersea networks up to transoceanic distances. One example of this is the SEA-ME-WE 4 [6] project. The South East Asia-Middle East-West Europe 4 project is a next generation submarine cable system linking South East Asia to Europe via the Indian Sub-Continent and Middle East. The project aims to take these regions to the forefront of global communication by significantly increasing the bandwidth and global connectivity of users along its route between Singapore and France.

South East Asia–Middle East–Western Europe 4 (SEA-ME-WE 4) is an optical fiber submarine communications cable system that carries telecommunications between Singapore, Malaysia, Thailand, Bangladesh, India, SriLanka, Pakistan, United Arab Emirates, Saudi Arabia, Sudan, Egypt, Italy, Tunisia, Algeria and France.

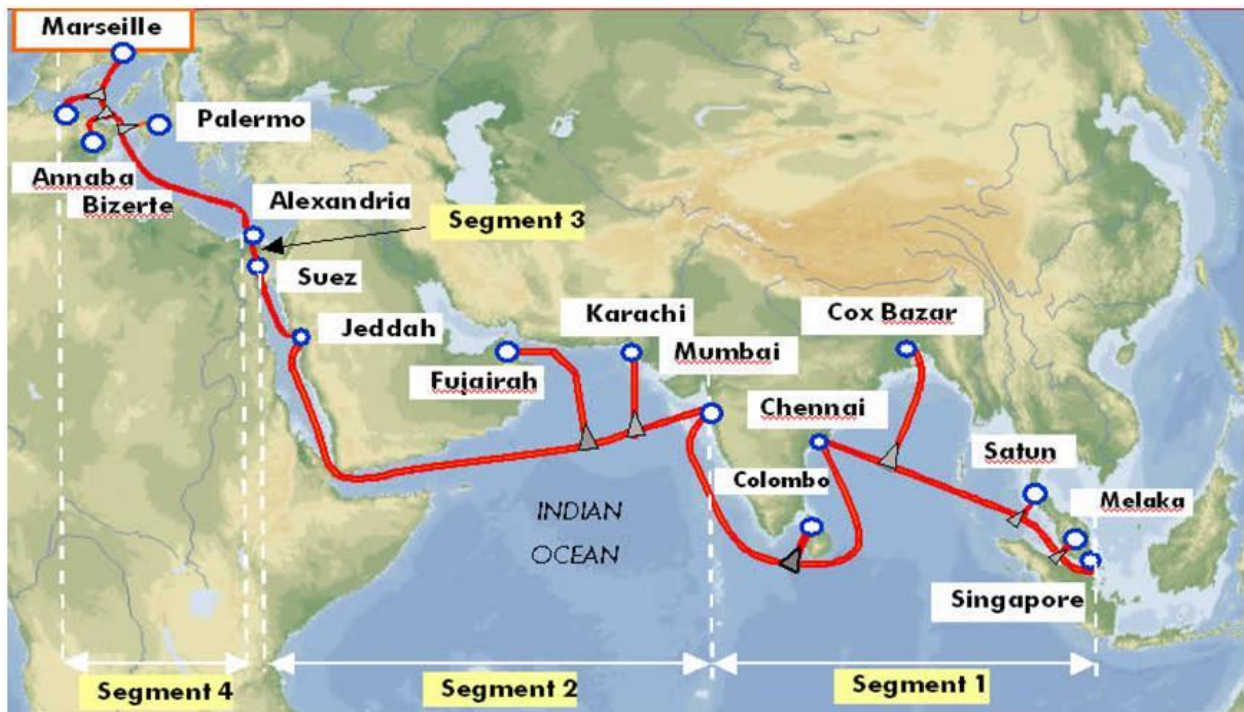


Fig. 1.4 The route of the submarine cable, SEA-ME-WE 4 [7]

1.6 Objective of the work

The significant restriction in optical fiber system is the dispersion. Dispersion affects the performance of the system and bit error rate. In this work the effect of temperature variations on fiber dispersion and on other modal behaviors are investigated. The refractive index, its dispersion, chromatic dispersion, and its variation as a function of temperature are important characteristics, which are necessary for the evaluation of optical fiber transmission system designs.

A knowledge of the refractive index as a function of temperature is necessary to evaluate chromatic dispersion at different temperatures, since it plays a vital role in the optical fiber communication system. We use the two-pole Sellmeier formula to represent the refractive index dependence on temperature [8-11]. The temperature effect is then introduced as a variation of Sellmeier coefficients, a method used by Ghosh and Bhar [12]. The two-pole Sellmeier formula is a meaningful model to represent refractive indexes with wavelengths.

The temperature effect on total dispersion is modeled for most popular materials used in the fabrication process of optical fiber, **Silica (SiO_2), Aluminosilicate (Al_2SiO_5) and Vycor glass (96.4% SiO_2 , 3% B_2O_3 , 0.5% Al_2O_3 , 0.1% Miscellaneous traces)**. Only the single mode step index fiber is considered. The results are investigated by using, COMSOL MULTIPHYSICS Version 4.2 [13] and MATLAB version 7.6.0 (R2008a) programs. However, the work is articulated within a particular framework to find out a comparative study within our limit.

1.7 Layout of the thesis

This paper is tried to develop logically and chronologically. The first chapter gives the introductory views followed by the second chapter, which provides a brief but a clear view on optical fiber. In the third chapter modal properties of optical fiber concern to this work are presented. The experimental work, comparative study along with analysis is depicted in chapter four.

In chapter four, to fulfill the requirements of this work, the dispersion characteristics of different optical fiber materials at different temperatures are studied using COMSOL MULTIPHYSICS version 4.2 and MATLAB version 7.6.0 (R2008a) programs. However, to ease the comparison, graphs are also drawn using the data of the analysis. The whole work gives comparative information among different optical fiber materials and their corresponding dispersion characteristics. Meanwhile, chapter five presents the concluding remarks of the work undertaken by us.

Chapter 2

Basics of Optical Fiber

2.1 Optical Fiber

At the heart of an optical communication system is the optical fiber, that acts as the transmission channel carrying the light beam loaded with information. Optical fibers are a kind of waveguides which are usually made of some kind of glass, can potentially be very long (hundreds of kilometers), and are in contrast to other waveguides fairly flexible. The most commonly used glass is Silica (quartz glass, amorphous silicon dioxide i.e. SiO_2), either in pure form or with some dopants. Silica is so widely used because of its outstanding properties, in particular its potential for extremely low propagation losses (realized with ultrapure material) and its amazingly high mechanical strength against pulling and even bending (provided that the surfaces are well prepared). Most optical fibers used in laser technology have a core with a refractive index which is somewhat higher than that of the surrounding medium (called the cladding). Light launched into the core is guided along the core, i.e., it propagates mainly in the core region, although the intensity distribution may extend somewhat beyond the core. Due to the guidance and the low propagation losses, the optical intensity can be maintained over long lengths of fiber.

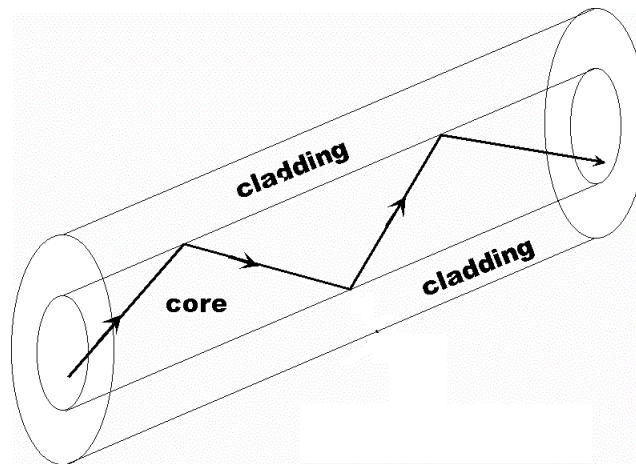


Fig 2.1: The optical fiber

The light beam is guided through the optical fiber due to phenomenon of total internal reflection. Fig 2.1 shows an optical fiber, which consists of a central dielectric core of refractive index n_1 cladded by a material of slightly lower refractive index $n_2 < n_1$.

2.2 Basic Structure of Optical Fiber

The basic structure of an optical fiber consists of three main parts; the core, the cladding, and the coating or buffer. Strength members and Jacket are used as the protection purpose in long haul communication. The basic structure of an optical fiber is shown in Fig. 2.2 below:

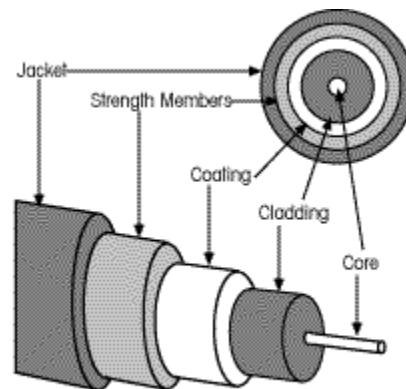


Fig 2.2: Basic structure of an optical fiber [14]

2.2.1 Core

The core is a cylindrical rod of dielectric material. Dielectric material conducts no electricity. Light propagates mainly along the core of the fiber. The core is generally made of silica glass or plastic with a high refractive index. The core is described as having a radius (a) and refractive index, n_1 .

2.2.2 Cladding

The core is surrounded by a layer of material with lower index of refraction called the cladding. Even though light will propagate along the fiber core without the layer of cladding material, the cladding does perform some necessary functions. The cladding layer is made of a dielectric material with an index of refraction n_2 . The index of refraction of the cladding material is less than that of the core material. This difference in index forms a mirror at the boundary of the core and cladding. Because of the lower index, it reflects the light back into the centre of the core, forming an optical wave guide. The cladding is generally made of glass or plastic. The cladding performs the following functions:

- Reduces loss of light from the core into the surrounding air
- Reduces scattering loss at the surface of the core
- Protects the fiber from absorbing surface contaminants
- Adds mechanical strength

2.2.3 Coating

For extra protection, the cladding is enclosed in an additional layer called the coating or buffer. The coating or buffer is a layer of material used to protect an optical fiber from physical damage. The material used for a buffer is a type of plastic. The buffer is elastic in nature and prevents abrasions. The buffer also prevents the optical fiber from scattering losses caused by microbends. Microbends occur when an optical fiber is placed on a rough and distorted surface.

2.2.4 Strength members

To further protect the fiber from stretching during installation, and to protect it from expansion and contraction due to temperature changes, strength member are added to the cable construction.

2.2.5 Jacket

The last item in the construction is jacket, and provides the final protection from the environment in which the cable is installed. Different jackets provide different solutions for indoor, outdoor, aerial, and buried installations.

2.3 Optical Fiber Materials

The fiber optic material must be transparent for efficient transmission of light, possible to draw long this fibers from the material. It must be compatible with the cladding material. Glass and plastic fulfills these requirements.

Glass optical fibers are almost always made from silica, but some other materials, such as fluorozirconate, fluoroaluminate, and chalcogenide glasses as well as crystalline materials like sapphire, are used for longer-wavelength infrared or other specialized applications. Silica and fluoride glasses usually have refractive indices of about 1.5, but some materials such as the chalcogenides can have indices as high as 3. Typically the index difference between core and cladding is less than one-two percent.

Plastic optical fibers (POF) are commonly step-index multi-mode fibers with a core diameter of 0.5 millimeters or larger. POF typically have higher attenuation coefficients than glass fibers, 1 dB/m or higher, and this high attenuation limits the range of POF-based systems. To select materials for optical fibers, a number of requirements must be fulfilled.

- It must be transparent to make long, thin, flexible fibers from the material.
- The material must be transparent at a particular optical length in order for the fiber to guide light efficiently.
- Physically compatible materials that have slightly different refractive indices for the core and cladding must be available.

Materials that satisfy these requirements are glasses and plastics. The variety of available glass fibers ranges from moderate loss with large cores used for short-transmission distances to very transparent (low loss) fibers employed in long-haul applications.

2.3.1 Fused Silica

Silica (SiO_2) is one of the chief constituents of the earth's crust. It is present in various forms, the most being quartz which is crystalline in character. Typical examples are siliceous sands and rock crystal. There are also various other crystalline forms such as tridymite and cristobalite. All types when fused at 2000°C give a vitreous material. Fused Silica is formed by chemical combination of silicon and oxygen. It is a unique material with an unrivalled combination of purity, high temperature resistance, thermal shock resistance, good electrical insulation, optical transparency and chemical inertness. The outstanding characteristic of silica glass is its very high degree of purity (99.99% SiO_2) [15]. Fused Silica is perfect optical material due to its good UV and IR transmission, low coefficient of thermal expansion. It has high stability and resistance to thermal shock over large temperature excursions, wide temperature operating range and high laser damage threshold. Typical of glasses, it lacks long range order in its atomic structure.

Fused Silica Properties [15] are:

- Transmission Range: 185 nm~2500 nm
- Thermal Expansion Coefficient: $0.54 \times 10^{-6}/\text{K}$
- Density: 2.20 g/cm^3

2.3.2 Vycor Glass (7913)

Vycor is the brand name of Corning's high silica, high temperature glass. It provides very high thermal resistance. Vycor is approximately 96% silica and 4% boron oxide, but unlike pure fused silica it can be readily manufactured in a variety of shapes. Vycor glass withstands harsh

environmental conditions like water, steam, low and high temperatures better than most other glass materials.

Vycor, Corning Code 7913 [16] is comparable to and sometimes used in place of fused silica. This glass is initially formed as a borosilicate type glass. It is then subjected to a chemical treatment that removes glass except silica. Glass is then reheated to eliminate microscopic holes caused by the chemical treatment. The Vycor (7913) glass composition is given below:

Table 2.1

Composition(%approx)	
SiO ₂	96.4
B ₂ O ₃	3
Al ₂ O ₃	0.5
Miscellaneous Traces	0.1

Vycor corning 7913 material is used in high temperature applications often in sight glasses due to its high thermal shock resistance and performance. It has also transmission in the UV and infrared range. Vycor is generally three times more resistance to abrasion than optical glass with higher expansion. Vycor quartz thickness ranges from 2mm to 12mm thick with 4mm a general stocked thickness.

Properties of Vycor glass [15, 16] are:

- Density 2.18 g/cm³
- Coefficient of Expansion (0 – 300⁰C): $7.5 \times 10^{-7}/^{\circ}\text{C}$

2.3.3 Aluminosilicate (Al₂SiO₅)

Aluminosilicate minerals are minerals composed of aluminium, silicon, and oxygen, plus other counteractions. They are a major component of kaolin and other clay minerals. An important type of glass, aluminosilicate, contains 20% aluminium oxide (alumina- Al₂O₃) often including calcium oxide, magnesium oxide and boric oxide in relatively small amounts, but with only very small amounts of soda or potash. It is able to withstand high temperatures and thermal shock and thus suitable for optical transmission in high temperature conditions.

2.4 Refraction of Light

Refraction is the bending of a wave when it enters where it's speed is different. The refraction of light when it passes from a fast medium to a slow medium bends the light ray toward the normal

or from a slow medium to fast medium bends the light ray outward the normal to the boundary between the two media. The bending is caused by one side of the wave changing speed before other side. As the speed of light is reduced in the slower medium, the wavelength is shortened proportionately. The frequency is unchanged; it's a characteristic of the source of the light and unaffected by the medium changes. Refraction of light is the main principle of optical waveguide communication system.

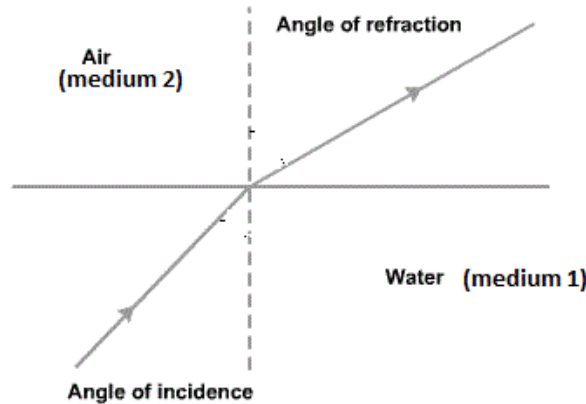


Fig 2.3: Refraction of Light

2.5 Refractive Index

Refractive index, also called index of refraction, measure of the bending of a ray of light when passing from one medium into another. Index of refraction of a material is the ratio of the speed of light in vacuum to the speed of light in that material.

$$n = \frac{c}{v} \quad (2.1)$$

Where, c is the velocity of light in vacuum ($3 \times 10^8 \text{ms}^{-1}$) and v is the velocity in that material. For example, the refractive index of water is 1.33, meaning that light travels 1.33 times slower in water than it does in vacuum. Refractive index of any material is a measure of the speed of light in that substance. As light exits a medium, such as air, water, or glass, it may also change its propagation direction in proportion to the refractive index. Refractive index of materials varies with the frequency of radiated light. This results in a slightly different refractive index for each color.

2.6 Snell's Law

Snell's law (also known as the Snell-Descartes law and the law of refraction) is used to describe the inter-relationship between the incidence angle of light and refraction, when referring to light

(or other waves) passing through a boundary between two different isotropic media, such as air, water, glass etc. When a ray is incident on the interface between two dielectrics of differing refractive indices (e.g. glass-air), refraction occurs. It is observed that the ray approaching the interface is propagating in a dielectric of refractive index n_1 and is at angle θ_1 to the normal at the surface of the interface. If dielectric on the other side of the interface has a refractive index n_2 which is less than n_1 , then refraction is such that the ray path in this lower index medium is at angle θ_2 to the normal, where θ_2 is greater than θ_1 . The angle of incidence n_1 and refraction n_2 are related to each other and to the refractive indices of the dielectrics. Snell's law states that the ratio of the angles of incidence and refraction is equivalent to the ratio of the phase velocities in the two media, or equivalent to the reciprocal of the ratio of the indices of refraction.

$$\frac{\sin \theta_1}{\sin \theta_2} = \frac{v_1}{v_2} = \frac{n_2}{n_1} \quad (2.2)$$

With each θ as the angle is measured from the normal of the boundary, where v as the velocity of light in the respective medium and n as the refractive index (which is unit less) of the respective medium.

2.7 Total Internal Reflection (TIR)

When light is incident upon a medium of lesser index of refraction, the ray is bent away from the normal, so the exit angle is greater than the incident angle. Such reflection is commonly called internal reflection.

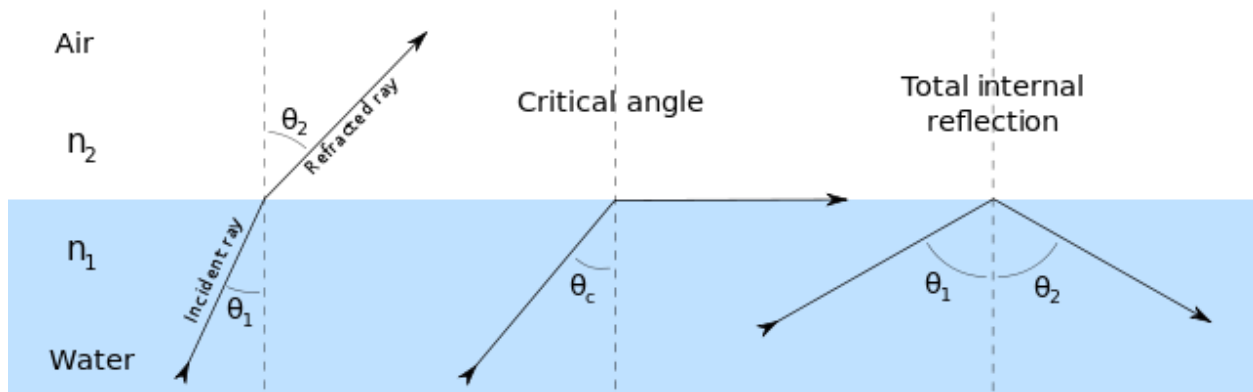


Fig 2.4: Total internal reflection [17]

Total internal reflection is a phenomenon that happens when a propagating wave strikes a medium boundary at an angle larger than a particular critical angle with respect to the normal to the surface.

According to Snell's law,

$$\sin\theta_2 = \frac{n_1}{n_2} \sin\theta_1 \quad (2.3)$$

Since $n_1/n_2 > 1$, it follows that $\theta_2 > \theta_1$. For relatively small angles of incidence, part of the light is refracted into the less optically dense medium, and part is reflected. When the angle of incidence θ_1 is such that the angle of refraction is θ_2 and $\theta_2 = 90^\circ$, the refracted ray runs along the interface between the two media. This particular angle of incidence is called the critical angle, θ_c . For $\theta_1 > \theta_c$, there is no refracted ray. Instead, the entire light incident on the interface is reflected. This effect is called total internal reflection, and occurs whenever the angle of incidence exceeds the critical angle.

2.8 Critical Angle

The critical angle is the angle of incidence above which total internal reflection occurs. The angle of incidence is measured with respect to the normal at the refractive boundary. Critical angle is defined as the angle of incidence beyond which rays of light passing through a denser medium to the surface of a less dense medium are no longer refracted but totally reflected. Consider a light ray passing from glass into air. The light emanating from the interface is bent towards the glass. When the incident angle is increased sufficiently, the transmitted angle (in air) reaches 90 degrees. It is at this point no light is transmitted into air. The critical angle θ_c is given by Snell's law,

$$n_1 \sin\theta_i = n_2 \sin\theta_t \quad (2.4)$$

Rearranging Snell's law, we get incidence

$$\sin\theta_i = \frac{n_2}{n_1} \sin\theta_t \quad (2.5)$$

To find critical angle, we find the value θ_1 when $\theta_t = 90^\circ$ and thus critical angle is as follows:

$$\theta_c = \theta_i = \arcsin\left(\frac{n_2}{n_1}\right) \quad (2.6)$$

2.9 Acceptance Angle

The maximum angle of incidence at the entrance aperture of the fiber for which the light ray suffers total internal reflection at the core-cladding interface and propagates through the fiber or waveguide is called the acceptance angle. The acceptance angle of an optical fiber is defined based on a purely geometrical consideration (ray optics) which is the maximum angle of a ray (against the fiber axis) hitting the fiber core which allows the incident light to be guided by the core. Optical fiber's capability to collect light not only determined by fiber size, but also by its

acceptance angle. Acceptance angle is the range of angles over which a light ray can enter the fiber and be trapped in its core.

$$\theta_o = \sin^{-1} \left[\frac{\sqrt{n_1^2 - n_2^2}}{n_o} \right] \quad (2.7)$$

Where, θ_o = acceptance angle

n_o = index of air (vacuum) = 1

2.10 Cone of Acceptance

The light rays contained within the cone having a full angle $2\theta_o$ (acceptance angle) are accepted and transmitted along the fiber. Therefore the cone is called ‘Acceptance cone’. In fiber optics, the cone within which, optical power may be coupled into the bound modes of an optical fiber. The acceptance cone is derived by rotating the acceptance angle, i.e. the maximum angle within which light will be coupled into a bound mode, about the optical fiber axis. The acceptance cone for a round optical fiber is a solid angle with an included apex angle that is twice the acceptance angle. Light rays that are within the acceptance cone can be coupled into the end of an optical fiber and be totally internally reflected as it propagates along the core.

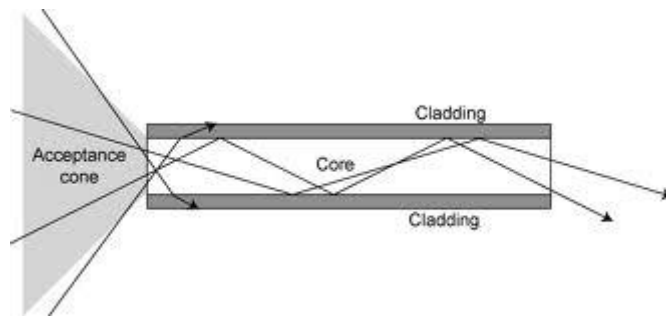


Fig 2.5: Cone of acceptance [18]

2.11 Numerical Aperture (NA)

The numerical aperture (NA) of a fiber is a figure of merit which measures the light gathering or accepting power of the fiber. Larger the numerical aperture, the greater the amount of light accepted by fiber. The acceptance angle also determines how much light is able to be entering the fiber and hence there is a relation between the numerical aperture and the cone of acceptance. The numerical aperture is defined as the sine of the acceptance angle.

$$\text{Numerical Aperture (NA)} = \sin \theta_o = \left[\frac{\sqrt{n_1^2 - n_2^2}}{n_o} \right] \quad (2.8)$$

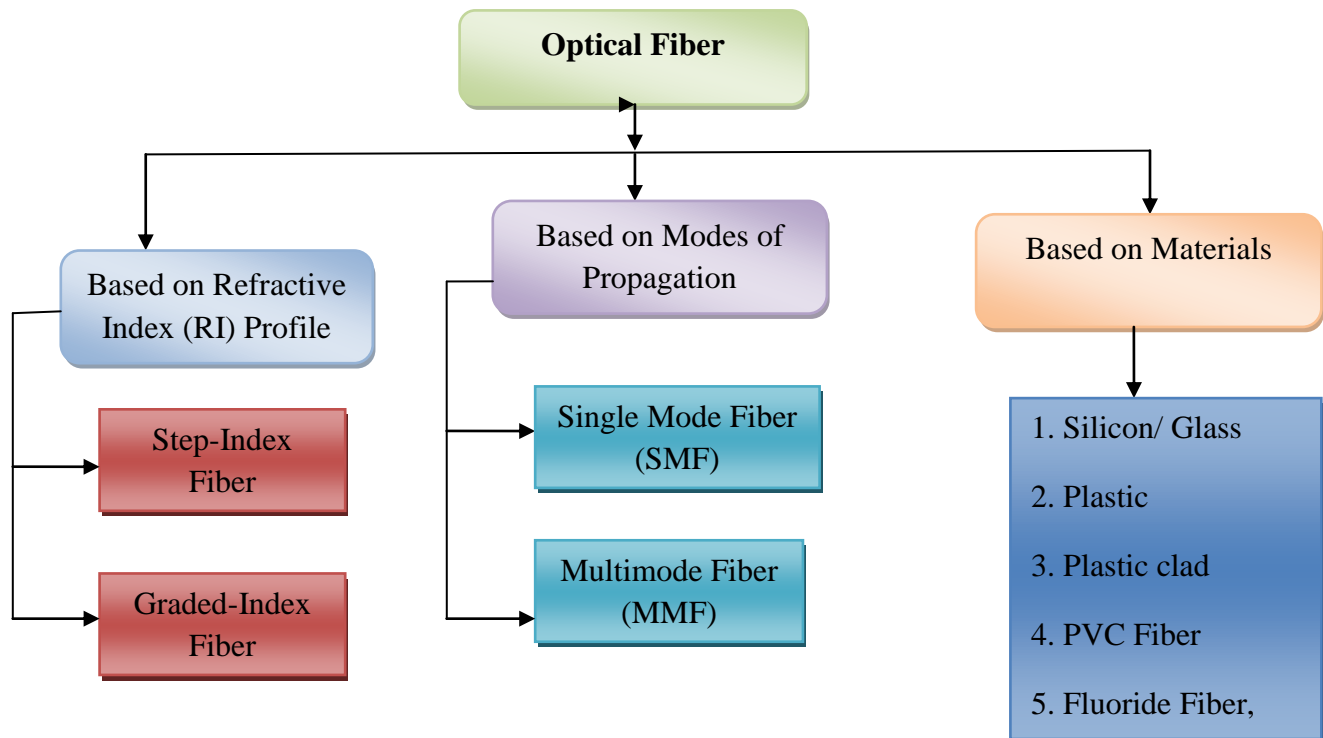
Numerical aperture is a measure of the amount of light that can be accepted by a fiber. If the light ray launching zone is air medium= 1.

$$\text{Numerical aperture (NA)} = \sin \theta_o = \sqrt{n_1^2 - n_2^2} \quad (2.9)$$

Then, the numerical aperture depends only on the refractive index of the core and the cladding.

2.12 Types of Optical Fiber

Optical fibers are characterized by their structure and by their properties of transmission. Basically, optical fibers are classified into two types basing on the modes of propagations. The first type is single mode fibers (SMF) and the second type is multimode fibers (MMF). However, besides modes of propagations, fibers are also categorized basing on their refractive index profile and materials of fabrication. Thus, all together optical fibers can be categorized as follows:



2.12.1 Based on mode of propagation

An optical fiber guides light waves in distinct patterns called modes. Mode describes the distribution of light energy across the fiber. The precise patterns depend on the wavelength of light transmitted and on the variation in refractive index that shapes the core. In essence, the variations in refractive index create boundary conditions that shapes how light waves travel through the fiber. Light rays propagate as an electromagnetic wave along the fiber. The two components, the electric field and the magnetic field form patterns across the fiber. These patterns are called modes of transmission. The mode of a fiber refers to the number of paths for the light rays within the cable. According to modes optic fibers can be classified into two types:

- Single Mode Fiber (SMF)
- Multi-mode Fiber (MMF)

2.12.1.1 Single Mode Fiber (SMF)

Single mode fiber allows propagation of light ray by only one path. Single mode fibers are best at retaining the fidelity of each light pulse over longer distance also they do not exhibit dispersion caused by multiple modes. Thus more information can be transmitted per unit time. This gives single mode fiber higher bandwidth compared to multimode fiber.

2.12.1.2 Multimode Fiber

Multimode fiber was the first fiber type to be manufactured and commercialized. The term multimode simply refers to the fact that numerous modes (light rays) are carried simultaneously through the waveguide. Multimode fiber has a much larger diameter, compared to single mode fiber; this allows large number of modes.

2.12.2 Based on Fiber Index Profile

A fiber is characterized by its profile and by its core and cladding diameters. Index profile is the refractive index distribution across the core and the cladding of a fiber. In other words, the index profile is graphical representation of value of refractive index across the core diameter. There are two basic types of index profiles:

- Step Index Fiber (SI)
- Graded index Fiber (GRIN)

2.12.2.1 Step Index Fiber

If the refractive index profile of a fiber makes a step change at the core cladding interface then it is known as step index fiber. The step index (SI) fiber is a cylindrical waveguide core with central or inner core has a uniform refractive index of n_1 and the core is surrounded by outer cladding with uniform refractive index of n_2 . The cladding index is less than the core refractive index. But there is an abrupt change in the refractive index at the core-cladding interface.

2.12.2.2 Graded Index Fiber (GRIN)

The graded index fiber has a core made from many layers of glass. In the graded index fiber the refractive index is not uniform within the core, it is highest at the center and decreases smoothly and continuously with distance towards the cladding. The graded index fibers have decreasing core index $n(r)$ with radial distance from a maximum value of n_1 at the axis to a constant value in n_2 beyond the core radius a in the cladding. The graded index fiber gives best results for multimode optical propagation for parabolic refractive index profile. Due to this special kind of refractive index profile multimode graded index fibers exhibit less intermodal dispersion than its counterpart i.e. multimode step index fibers.

A graded index fiber has lower coupling efficiency and higher bandwidth than the step index fiber. It is available in 50/125 and 62.5/125 sizes. The 50/125 fiber has been optimized for long haul applications and has a smaller numerical aperture (NA) and higher bandwidth. 62.5/125 fiber is optimized for LAN applications which is costing 25% more than the 50/125 fiber cable.

2.13 Fiber Optic Configuration

Depending upon the refractive index profile and modes of fiber there exist three types of optical fiber configurations. This optic-fiber configurations are-

- Single Mode Step Index Fiber
- Multimode Step Index Fiber
- Multimode Graded Index Fiber

The Table 2.2 below [19] shows typical dimensions of single mode and multimode fibers.

Table 2.2
Typical dimensions of single mode and multimode fibers

Type of fiber	Core diameter	Cladding thickness
Single mode step index	8-12 μm	125 μm
Multimode step index	50-200 μm	125-400 μm
Multimode graded index	50-100 μm	125-140 μm

2.13.1 Single Mode Step Index Fiber

The single mode step index fiber has a central core that is sufficiently small so that there is essentially only one path for light ray through the cable. The ray is propagated in the fiber through reflections. Typical core sizes are 2 to 15 μm . Single mode fiber is also known as fundamental or monomode fiber. Single mode fiber will permit only one mode to propagate and does not suffer from mode delay differences. These are primarily developed for the 1300nm window but they can be also used effectively with time division multiplex (TDM) and wavelength division multiplex (WDM) systems operating in 1550 nm wavelength region.

2.13.2 Multimode Step Index Fiber

Multimode step index fiber is most widely used type. It is easy to manufacture. Its core diameter is 50 to 100 μm i.e. large aperture and allows more light to enter the cable. Multimode step-index fibers trap light with many different entrance angles; each mode in a step-index multimode fiber is associated with a different entrance angle. Each mode therefore travels along a different path through the fiber. Different propagating modes have different velocities. There are many paths that a light ray may follow during the propagation. The light ray is propagated using the principle of total internal reflection (TIR). Since the core index refraction is higher than the cladding the cladding index of refraction, the light enters at less than critical angle is guided along the fiber.

2.13.3 Multimode Graded Index Fiber

The core size of multimode graded index fiber cable is varying from 50 to 200 μm range. The light ray is propagated through the refraction. The light enters the fiber at many different angles. As the light propagates across the core toward the center it is intersecting a less dense to more dense medium. Therefore, the light rays are being constantly being refracted and ray is bending continuously. This cable is mostly used for long distance communication.

The light rays no longer follow straight lines; they follow a serpentine path being gradually bent back towards the center by the continuously declining refractive index. The modes travelling in a straight line are in a higher refractive index so they travel slower than the serpentine modes. This reduces the arrival time disparity because all modes arrive at about the same time.

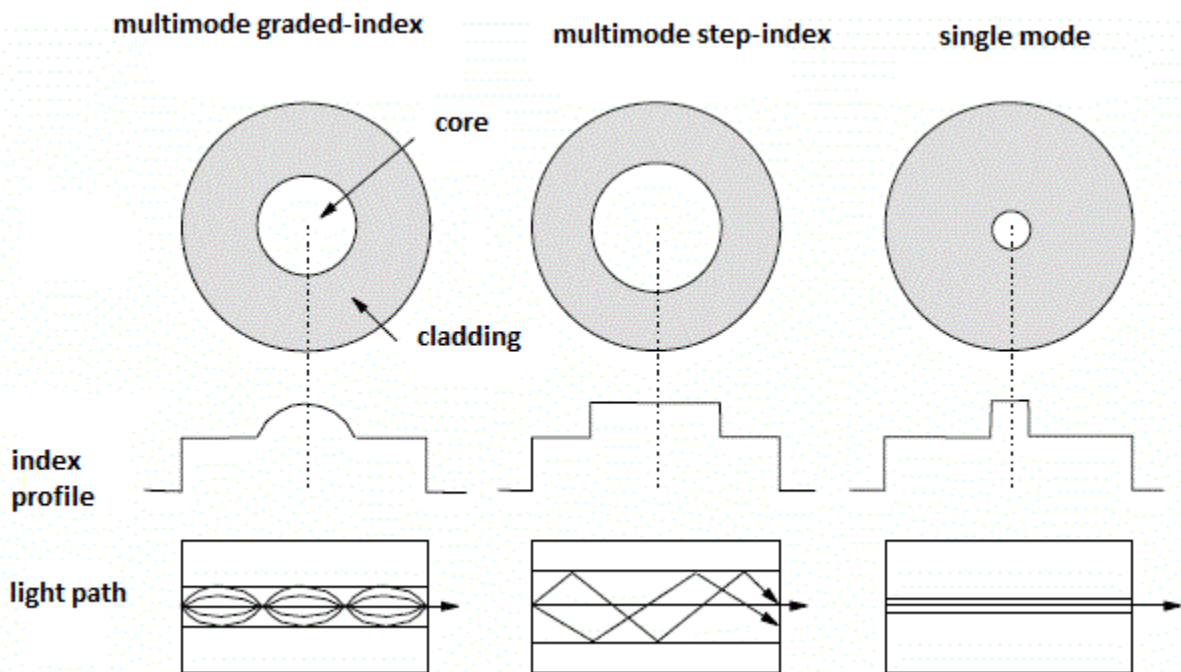


Fig. 2.6: Optical fiber configuration

2.14 Transmission Characteristics of Optical Fiber

The transmission characteristics of optical fiber play a major role in determining the performance of the entire communication system. Attenuation and bandwidth are the two most important transmission characteristics when the suitability of optical fiber for communication is analyzed. The various attenuation mechanisms are linear scattering, nonlinear scattering, material

absorption etc. The bandwidth determines the number of bits of information transmitted in a given time period and is largely limited by signal dispersion within the fiber.

2.14.1 Bandwidth–distance product (or bandwidth–length product)

The term bandwidth–distance product (or bandwidth–length product) is often used in the context of optical fiber communications. It is usually defined as the product of the length of a fiber-optic link and its maximum optical bandwidth. The latter is strongly related to the data rate (in Gbit/s), with a conversion factor which depends on the used modulation format. The bandwidth–distance product is typically limited by the fact that the bit error rate rises sharply for too high data rates. The concept of the bandwidth–distance product is helpful for comparing the performance of different types of fiber-optic links [20].

2.14.2 Material Absorption Losses

Absorption is a major cause of signal loss in an optical fiber. Absorption is defined as the portion of attenuation resulting from the conversion of optical power into another energy form, such as heat. Absorption in optical fibers is explained by three factors:

- Imperfections in the atomic structure of the fiber material
- The intrinsic or basic fiber-material properties
- The extrinsic (presence of impurities) fiber-material properties

Imperfections in the atomic structure induce absorption by the presence of missing molecules or oxygen defects. Absorption is also induced by the diffusion of hydrogen molecules into the glass fiber. Here there are two types of absorption losses in the fiber such as:

- Intrinsic absorption
- Extrinsic. Absorption

2.14.2.1 Intrinsic Absorption

Intrinsic absorption is caused by basic fiber-material properties. If an optical fiber were absolutely pure, with no imperfections or impurities, then all absorption would be intrinsic. Intrinsic absorption sets the minimal level of absorption. The below Figure shows the level of attenuation at the wavelengths of operation. This wavelength of operation is between two intrinsic absorption regions. The first region is the ultraviolet region (below 400nm wavelength). The second region is the infrared region (above 2000 nm wavelength).

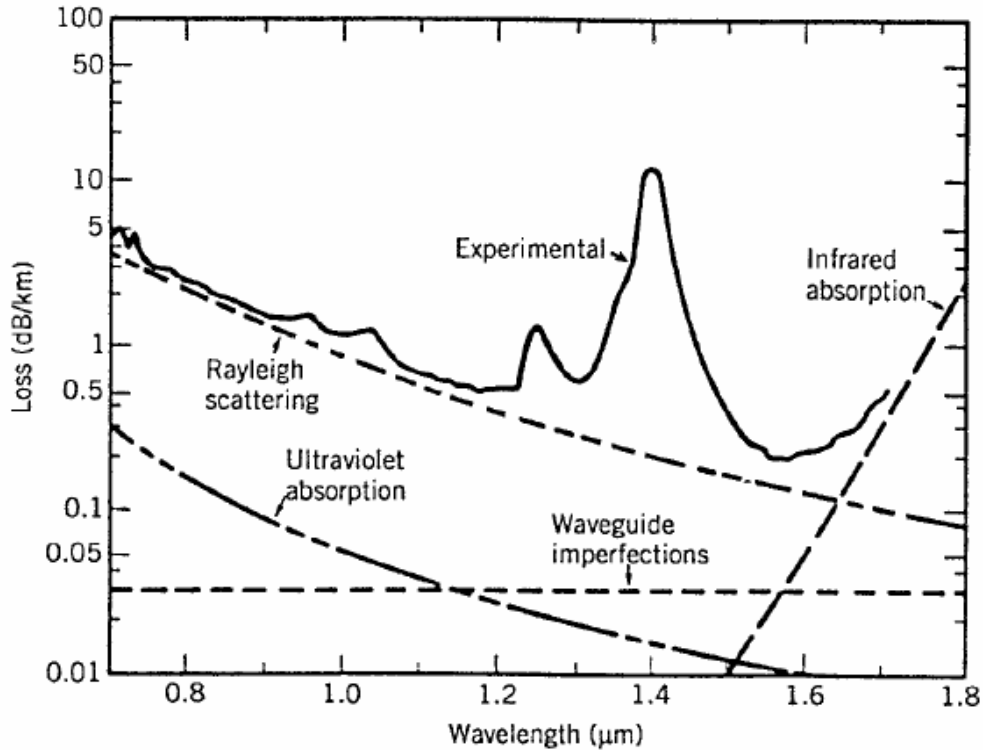


Fig 2.7 Absorption in optical fiber [5]

2.14.2.1.1 Ultra-Violet Absorption

Intrinsic absorption in the ultra-violet region is caused by electronic absorption bands. Basically, absorption occurs when a light particle (photon) interacts with an electron and excites it to a high energy level.

2.14.2.1.2 Infrared Absorption

The main cause of intrinsic absorption in the infrared region is the characteristic vibration frequency of atomic bonds. In silica glass, absorption is caused by the vibration of silicon oxygen (Si-O) bonds. The interaction between the vibrating bond and the electromagnetic field of the optical signal causes intrinsic absorption. Light energy is transferred from the electromagnetic field to the bond.

2.14.2.2 Extrinsic Absorption

Extrinsic absorption is caused by impurities introduced into the fiber material. Trace metal impurities, such as iron, nickel, and chromium, are introduced into the fiber during fabrication. Extrinsic absorption is caused by the electronic transition of these metal ions from one energy level to another. Extrinsic absorption also occurs when hydroxyl ions (OH^-) are introduced into the fiber. Water in silica glass form a silicon-hydroxyl (Si-OH) bond. This bond has a fundamental absorption at 2700 nm. However, the harmonics or overtones of the fundamental absorption occur in the region of operation. These harmonics increase extrinsic absorption at 1383 nm, 1250 nm, and 950 nm.

These absorption peaks define three regions or windows of preferred operation. The first window is centered at 850 nm. The second window is centered at 1300 nm. The third window is centered at 1550 nm. Fiber optic systems operate at wavelengths defined by one of these windows. The amount of water (OH^-) impurities present in a fiber should be less than a few parts per billion. Fiber attenuation caused by extrinsic absorption is affected by the level of impurities (OH^-) present in the fiber. If the amount of impurities in a fiber is reduced, then fiber attenuation is reduced.

2.14.3 Linear scattering losses

Through this mechanism a portion of optical power within one propagating mode is transferred to another. Now when the transfer takes place to a leaky or radiation mode then the result is attenuation. It can be divided into two major categories namely:

- Mie scattering
- Rayleigh scattering

2.14.3.1 Mie Scattering

Non perfect cylindrical structure of the fiber and imperfections like irregularities in the core-cladding interface, diameter fluctuations, strains and bubbles may create linear scattering which is termed as Mie scattering.

2.14.3.2 Rayleigh Scattering

The dominant reason behind Rayleigh scattering is refractive index fluctuations due to density and compositional variation in the core. It is the major intrinsic loss mechanism in the low impedance window. Rayleigh scattering can be reduced to a large extent by using longest possible wavelength.

2.14.4 Nonlinear scattering Losses

Especially at high optical power levels scattering causes disproportionate attenuation, due to nonlinear behavior. Because of this nonlinear scattering the optical power from one mode is transferred in either the forward or backward direction to the same, or other modes, at different frequencies. The two dominant types of nonlinear scattering are:

- Stimulated Brillouin Scattering
- Stimulated Raman Scattering

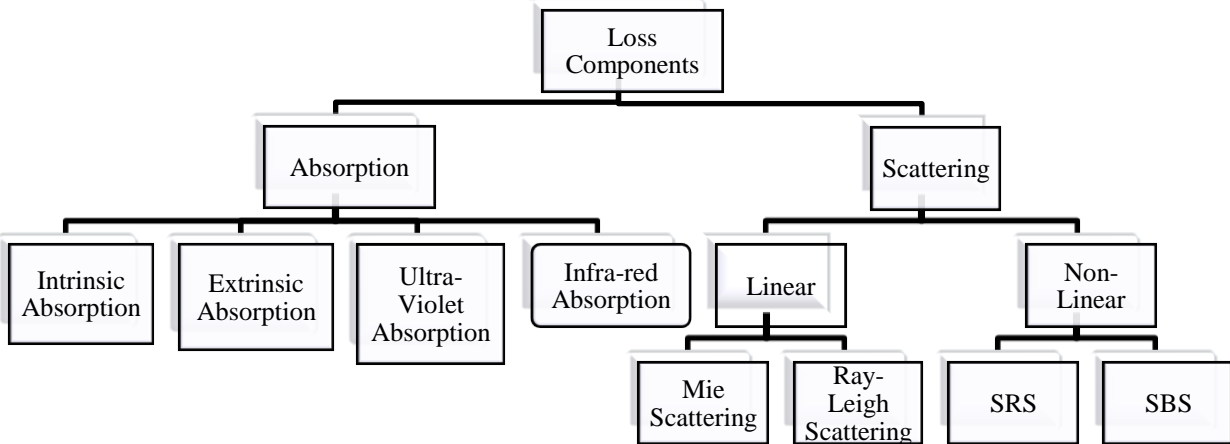
2.14.4.1 Stimulated Brillouin Scattering (SBS)

The SBS system is based on the measurement of the Brillouin Scattering characteristics. Brillouin scattering is a natural scattering process associated to the propagation of light in a medium like an optical fiber. The Brillouin interaction results in the generation of scattered light (Brillouin component) which shows a frequency shift compared to the light causing the interaction. This shift can be attributed to the presence of inhomogeneities associated to acoustic waves in the silica (acoustic phonons). A system based on the analysis of the Brillouin scattered light in optical fibers is naturally devoted to perform strain and temperature measurement. This can be achieved since the Brillouin shift depends on the acoustic velocity of the medium, which is temperature and strain dependent.

2.14.4.2 Stimulated Raman Scattering (SRS)

When light propagates through a medium, the photons interact with silica molecules during propagation. The photons also interact with themselves and cause scattering effects, such as stimulated Raman scattering (SRS), in the forward and reverse directions of propagation along the fiber. This results in a sporadic distribution of energy in a random direction. SRS refers to lower wavelengths pumping up the amplitude of higher wavelengths, which results in the higher wavelengths suppressing signals from the lower wavelengths. One way to mitigate the effects of SRS is to lower the input power. In SRS, a low-wavelength wave called Stoke's wave is generated due to the scattering of energy. This wave amplifies the higher wavelengths. The gain obtained by using such a wave forms the basis of Raman amplification.

All of these loss mechanisms are shown as follows:



Chapter 3

Modal properties of optical fiber

3.1 Optical fiber as a cylindrical waveguide

From Helmholtz [21, 22] equation we know that:

$$\nabla^2 \mathbf{E} + k^2 \mathbf{E} = 0 \quad (3.1)$$

Where,

$$\nabla^2 = \frac{\partial^2}{\partial x^2} + \frac{\partial^2}{\partial y^2} + \frac{\partial^2}{\partial z^2}, \text{ Laplacian operator and } k = \omega\sqrt{\mu\epsilon}$$

\mathbf{E} =Electric field vector

μ =Permiability

ϵ =Permittivity

We are interested in only the z component of the electric field vector and hence,

$$\nabla^2 E_z + k^2 E_z = 0 \quad (3.2)$$

Since the propagation of the wave is restricted only in the z – direction, we assume,

$$E_z = E_{z0} e^{-\gamma z} \quad (3.3)$$

Where,

$$\gamma = \alpha + j\beta$$

γ = Propagation constant

α = Attenuation constant

β = Phase constant

From equation (3.2) we have:

$$\nabla^2 E_z + k^2 E_z = 0$$

$$\Rightarrow \left(\frac{\partial^2}{\partial x^2} + \frac{\partial^2}{\partial y^2} + \frac{\partial^2}{\partial z^2} \right) E_z + k^2 E_z = 0$$

$$\Rightarrow \left(\frac{\partial^2}{\partial x^2} + \frac{\partial^2}{\partial y^2} \right) E_z + \frac{\partial^2}{\partial z^2} (E_{z0} e^{-\gamma z}) + k^2 E_z = 0$$

$$\begin{aligned}
&\Rightarrow \nabla_t^2 E_z + \gamma^2 E_z + k^2 E_z = 0 \\
&\Rightarrow \nabla_t^2 E_z + (\gamma^2 + k^2) E_z = 0 \\
&\Rightarrow \nabla_t^2 E_z + k_c^2 E_z = 0 \tag{3.4}
\end{aligned}$$

Where, $k_c^2 = \gamma^2 + k^2$

$$\begin{aligned}
&= (\alpha + j\beta)^2 + k^2 \\
&= (j\beta)^2 + k^2 \quad [\alpha = 0] \\
&= -\beta^2 + k^2 \\
&= k^2 - \beta^2
\end{aligned}$$

And, ∇_t^2 = transverse Laplacian [23]

For an optical fiber the electromagnetic wave in a guide will spread over at least two regions i.e. core and cladding of indices n_1 and n_2 ($n_2 < n_1$). The propagation occurs along the z-axis and the guiding structure confines light in the x-direction. The figure (3.1) shows the geometry of the wave vectors in the two regions of a slab waveguide.

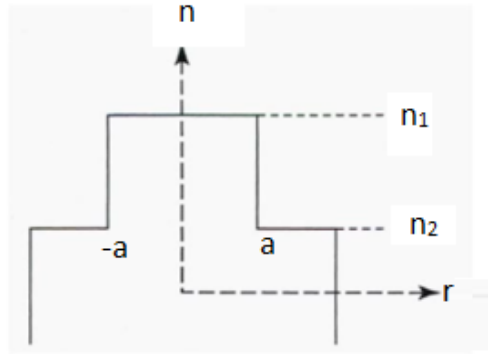


Fig 3.1: A step-index waveguide

For a step index fiber of the form shown in figure (3.1) with a core index n_1 and radius a , we can assume the electric field vector as follow:

$$\mathbf{E} = E_{z0}(r, \varphi)e^{-j\beta z} \tag{3.5}$$

Now, from equation (3.4) we can write,

$$\nabla_t^2 E_{z1} + k_c^2 E_{z1} = 0 \text{ For } r \leq a \tag{3.6}$$

Where,

$$k_c^2 = k_1^2 - \beta^2$$

$$\Rightarrow k_c^2 = \left(\frac{2\pi n_1}{\lambda}\right)^2 - \beta^2$$

$$\Rightarrow k_c^2 = k_0^2 n_1^2 - \beta^2 \quad (3.7)$$

Hence, from equation (3.6):

$$\nabla_t^2 E_{z1} + (k_0^2 n_1^2 - \beta^2) E_{z1} = 0 \quad \text{For } r \leq a \quad (3.8)$$

And, similarly:

$$\nabla_t^2 E_{z2} + (k_0^2 n_2^2 - \beta^2) E_{z2} = 0 \quad \text{For } r \geq a \quad (3.9)$$

For the notational convenience, we define the transverse propagation constants [23],

$$\beta^2 t_1 = n_1^2 k_0^2 - \beta^2 \quad (3.10)$$

$$\beta^2 t_2 = n_2^2 k_0^2 - \beta^2 \quad (3.11)$$

The normalized transverse propagation constants [23] are defined respectively as follows:

$$u = a\beta t_1 = a\sqrt{n_1^2 k_0^2 - \beta^2} \quad (3.12)$$

$$w = a|\beta t_2|$$

$$= a\sqrt{\beta^2 - n_2^2 k_0^2} \quad (3.13)$$

As in the case of the slab waveguide, βt_2 is imaginary for a guided mode since $\beta > n_2 k_0$. Thus,

$$u^2 = a^2 (n_1^2 k_0^2 - \beta^2) \quad (3.14)$$

$$w^2 = a^2 (\beta^2 - n_2^2 k_0^2) \quad (3.15)$$

The sum of the squares of the u and w define very useful quantity [2] which is usually referred to as the normalized frequency, V called the V -number. Thus,

$$V = \sqrt{u^2 + w^2}$$

$$= \sqrt{a^2 (n_1^2 k_0^2 - \beta^2) + a^2 (\beta^2 - n_2^2 k_0^2)}$$

$$= \sqrt{a^2 k_0^2 (n_1^2 - n_2^2)}$$

$$= k_0 a \sqrt{n_1^2 - n_2^2}$$

$$= \frac{2\pi}{\lambda} a \sqrt{n_1^2 - n_2^2} \quad (3.16)$$

Which is a dimensionless number that determines how many modes a fiber can support. A fiber with V number less than 2.405 supports only a single guided mode [19]. This mode is the HE_{11} mode. If the V number is less than 2.405 the other modes are not guided by the fiber. This type of fiber is called single mode fiber (SMF). We, now define a mode known as linearly polarized (LP) mode. A very useful feature of the LP-mode designation is the ability to readily visualize a mode. In a complete set of modes only one electric and one magnetic field component are significant. The electric field vector \mathbf{E} can be chosen to lie along an arbitrary axis, with the magnetic field vector \mathbf{H} being perpendicular to it [5]. The LP_{01} same as HE_{11} mode. The Table below [19] shows the construction of LP modes from actual TE, TM and hybrid modes support by the fiber.

Table 3.1

Construction of LP modes from actual TE, TM and hybrid modes support by the fiber

Linearly Polarized Mode	Combination of TE, TM and hybrid modes
LP_{01}	HE_{11}
LP_{11}	TE_{01}, TM_{01} and HE_{21}
LP_{21}	EH_{11} and HE_{31}
LP_{02}	HE_{12}
LP_{31}	EH_{21} and HE_{41}
LP_{12}	TE_{02}, TM_{02} and HE_{22}
LP_{41}	EH_{31} and HE_{51}

The number of modes that can exist in a waveguide as a function of V may be convenient to represent in terms of a normalized propagation constant, b defined by [2]:

$$\begin{aligned}
 b(v) &= a^2 w^2 / v^2 \\
 &= \frac{a^2 (\beta^2 - n_2^2 k_0^2)}{a^2 k_0^2 (n_1^2 - n_2^2)} \\
 &= \frac{k_0^2 [(\frac{\beta}{k_0})^2 - n_2^2]}{k_0^2 (n_1^2 - n_2^2)} \\
 b(v) &= \frac{(\frac{\beta}{k_0})^2 - n_2^2}{(n_1^2 - n_2^2)} \tag{3.17}
 \end{aligned}$$

3.2 Effective refractive index

The effective index of the fiber is the weighted average of the core and cladding indices, based on how much power propagates in each area. Effective refractive index is a number quantifying the phase delay per unit length in a waveguide, relative to the phase delay in vacuum. The rate of change of phase of the fundamental LP₀₁ mode propagating along a straight fiber is determined by the phase propagation constant β . It is directly related to the wavelength of the LP₀₁ mode, λ_{01} by the factor 2π , since β gives the increase in phase angle per unit length. Hence:

$$\beta\lambda_{01} = 2\pi, \text{ or } \lambda_{01} = \frac{2\pi}{\beta} \quad (3.18)$$

Moreover, it is convenient to define an effective refractive index for single-mode fiber, sometimes referred to as a phase index or normalized phase change coefficient [24] n_{eff} , by the ratio of the propagation constant of the fundamental mode to that of the vacuum propagation constant:

$$n_{eff} = \frac{\beta}{k} \quad (3.19)$$

Hence, the wavelength of the fundamental mode λ_{01} is smaller than the vacuum wavelength λ by the factor $1/n_{eff}$ where:

$$\lambda_{01} = \frac{\lambda}{n_{eff}} \quad (3.20)$$

It should be noted that the fundamental mode propagates in a medium with a refractive index $n(r)$ which is dependent on the distance r from the fiber axis. The effective refractive index can therefore be considered as an average over the refractive index of this medium [25]. At long wavelengths (i.e. small V values) the mode field diameter (MFD) is large compared to the core diameter and hence the electric field extends far into the cladding region. In this case, the propagation constant β will be approximately equal to n_2k (i.e. the cladding wave number) and the effective index will be similar to the refractive index of the cladding n_2 . Physically, most of the power is transmitted in the cladding material. At short wavelengths, however, the field is concentrated in the core region and the propagation constant, β approximates to the maximum wave number n_1k , the propagation constant in single-mode fiber varies over the interval $n_2k < \beta < n_1k$. Hence, the effective refractive index will vary over the range $n_2 < n_{eff} < n_1$.

The effective refractive index depends not only on the wavelength but also (for multimode waveguides) on the mode in which the light propagates. For this reason, it is also called modal index. Obviously, the effective index is not just a material property, but depends on the whole waveguide design. The effective index may be a complex quantity. In that case, the imaginary part describes loss.

3.3 Cutoff wavelength

The number of guided modes of a waveguide (for example: an optical fiber) depends on the optical wavelength [5]. The shorter the wavelength, the more modes can be guided. For long wavelengths, there may be only a single guided mode (single mode fibers) or even none at all, whereas multimode behavior is obtained at shorter wavelengths. When a particular mode ceases to exist beyond a certain wavelength, that wavelength is called its cut-off wavelength. For an optical fiber, the cut-off wavelength for the LP₁₁ mode sets a limit to the single-mode regime, as below that wavelength there is at least the LP₀₁ and the LP₁₁ mode.

$$\text{We know that, } V = \frac{2\pi}{\lambda} a n_1 (2\Delta)^{1/2} \quad (3.26)$$

Where, V = normalized frequency

n_1 =Refractive index of core

a =Core radius

λ =Operating wavelength

Δ = relative refractive index difference

It may be noted by rearrangement of Eq. (3.26) that single-mode operation only occurs above a theoretical cutoff wavelength λ_c given by:

$$\lambda_c = \frac{2\pi a n_1}{V_c} (2\Delta)^{1/2} \quad (3.27)$$

Where, V_c is the cutoff normalized frequency. Hence λ_c is the wavelength above which a particular fiber becomes single-moded. Dividing Eq. (3.27) by Eq. (3.26) for the same fiber we obtain the inverse relationship:

$$\frac{\lambda_c}{\lambda} = \frac{V}{V_c} \quad (3.28)$$

Thus for step index fiber where $V_c = 2.405$, the cut-off wavelength is given by [26]:

$$\lambda_c = \frac{V\lambda}{2.405} \quad (3.29)$$

Practical transmission systems are generally operated close to the cutoff wavelength in order to enhance the fundamental mode confinement.

3.4 Sellmeier Equation

This is an equation for the index of refraction of electromagnetic radiation as a function of wavelength in a medium whose molecules have oscillations of different frequencies. Therefore, it can be defined as an equation for calculating the wavelength dependent refractive index. Actually it is an empirical relationship between refractive index and wavelength for a particular medium. The equation is used to determine dispersion of light in the medium. The core refractive index, n_1 as a function of the operating wavelength, λ is defined through the Sellmeier equation which has the form [27-30]:

$$n^2(\lambda) = A + \frac{B\lambda^2}{\lambda^2 - C} + \frac{D\lambda^2}{\lambda^2 - E} \quad (3.30)$$

Where, λ is the wavelength in μm . The first and second terms represent respectively, the contribution to refractive indices due to the higher energy and lower energy band gaps of electronic absorption, while the first term accounts for the decrease in refractive indices due to the lattice absorption. The optical constants [8] A, B, C, D and E are called the Sellmeier coefficients of the optical materials.

The method of fitting a set of refractive index data to a Sellmeier in order to evaluate the optical constants was described by Malitson. However, his equation was of a slightly different form. To overcome such problem, the normal approach is to first find the initial value of the parameters and then to add corrections by an iterative process. Therefore, the deviation between the measured and computed values is minimum. Tsay et al. have given an excellent account of the variation of refractive index as a function of temperature in transparent crystals. Of the two factors, determining the temperature dependence, the electronic effect plays a dominant role over the lattice effect in semiconductor crystals. Recently, Lines has observed the physical origin of temperature dependence of chromatic dispersion in fused silica. But their analysis is not straightforward. Malitson has presented the spectral response of thermo-optic coefficients of fused silica by measuring the same for the temperature range 20-30⁰C. Matsuoka et al. have measured refractive indices of SiO₂ glass at seven temperatures from -165.4⁰C to 83.3⁰C for the UV and visible wavelength region and presented the constancy of thermo-optic coefficients at 20.5⁰C. These thermo-optic coefficients $\frac{dn}{dT}$ and their dispersion have been critically analyzed and smoothed by properly taking into account the band-edge dispersion [27].

The Sellmeier coefficients at any temperature T are computed from the room temperature Sellmeier equation and the smoothed $\frac{dn}{dT}$ values by calculating the refractive indices from the relation [27, 31]:

$$n_T = n_R + (T - R) \frac{dn}{dT} \quad (3.31)$$

Where, n_T = Refractive index at temperature T

n_R = Refractive index at Room temperature

T =temperature in degree centigrade

R =Room temperature

The Table below [8] shows the methods of finding Sellmeier coefficients at different temperatures:

Table 3.2

The linear fitted constants (m =slope, c_1 =intercept), of the least squares analysis of the temperature dependent Sellmeier coefficients (X) of fused Silica, Aluminosilicate and Vycor glasses ($X = mT + c_1$, T is the temperature in degree centigrade)

Sellmeier coefficients	Fitted constants	Fused silica SiO ₂	Aluminosilicate	Vycor glass
A	$m \times 10^6$ c_1	6.90754 1.31552	24.95380 1.41294	45.70720 1.27409
B	$m \times 10^5$ $c_1 \times 10$	2.35835 7.88404	-0.11466 9.50466	-1.47194 8.27657
C	$m \times 10^7$ $c_1 \times 100$	5.84758 1.10199	12.24700 1.32143	12.35900 1.06179
D	$m \times 10^7$ c_1	5.48368 0.91316	11.60740 0.90443	12.58560 0.93839
E	–	100.0	100.0	100.0

The Table 3.3 in shows Sellmeier coefficients for Fused Silica (fs), Aluminosilicate (as), and Vycor glasses at different temperatures we have done in our work.

Table 3.3

Sellmeier coefficients for fused Silica (fs), Aluminosilicate (as) and Vycor glasses at different temperatures $n^2 = A + B/(1 - C/\lambda^2) + D/(1 - E/\lambda^2)$

Material	Temp. (°C)	Sellmeier coefficients				
		A	B	C	D	E
SiO ₂	-120	1.3146910952	0.78557398	0.01012882904	0.91309419584	100
	-60	1.3151055476	0.78698899	0.01016391452	0.91312709792	100
	0	1.31552	0.788404	0.010199	0.91316	100
	10	1.3155890754	0.788639835	0.01020484758	0.91316548368	100
	20	1.3156581508	0.78887567	0.01021069516	0.91317096736	100
	25	1.3156926885	0.7889935875	0.01021361895	0.9131737092	100
	26	1.31569959604	0.789017171	0.010214203708	0.913174257568	100
	28	1.31571341112	0.789064338	0.010215373224	0.913175354304	100
	30	1.3157272262	0.789111505	0.01021654274	0.91317645104	100
	35	1.3157617639	0.7892294225	0.01021946653	0.91317919288	100
	40	1.3157963016	0.78934734	0.01022239032	0.91318193472	100

	45.2	1.315832220808	0.7894699742	0.0102254310616	0.9131847862336	100
	50	1.315865377	0.789583175	0.0102282379	0.9131874184	100
	60	1.3159344524	0.78981901	0.01023408548	0.91319290208	100
	70	1.3160035278	0.790054845	0.01023993306	0.91319838576	100
	80	1.3160726032	0.79029068	0.01024578064	0.91320386944	100
	90	1.3161416786	0.790526515	0.01025162822	0.91320935312	100
	100	1.316210754	0.79076235	0.0102574758	0.9132148368	100
	120	1.3163489048	0.79123402	0.01026917096	0.91322580416	100
Alumino-silicate	-120	1.409945544	0.950602592	0.013067336	0.9042907112	100
	-60	1.411442772	0.950533796	0.013140818	0.9043603556	100
	0	1.41294	0.950465	0.0132143	0.90443	100
	10	1.413189538	0.950453534	0.013226547	0.9044416074	100
	20	1.413439076	0.950442068	0.013238794	0.9044532148	100
	25	1.413563845	0.950436335	0.0132449175	0.9044590185	100
	26	1.4135887988	0.9504351884	0.0132461422	0.90446017924	100
	28	1.4136387064	0.9504328952	0.0132485916	0.90446250072	100
	30	1.413688614	0.950430602	0.013251041	0.9044648222	100
	35	1.413813383	0.950424869	0.0132571645	0.9044706259	100
	40	1.413938152	0.950419136	0.013263288	0.9044764296	100
	45.2	1.41406791176	0.95041317368	0.01326965644	0.904482465448	100
	50	1.41418769	0.95040767	0.013275535	0.904488037	100
	60	1.414437228	0.950396204	0.013287782	0.9044996444	100
	70	1.414686766	0.950384738	0.013300029	0.9045112518	100
	80	1.414936304	0.950373272	0.013312276	0.9045228592	100
	90	1.415185842	0.950361806	0.013324523	0.9045344666	100
	100	1.41543538	0.95035034	0.01333677	0.904546074	100
	120	1.409945544	0.950327408	0.013361264	0.013361264	100
Vycor glass	-120	1.268605136	0.829423328	0.010469592	0.9382389728	100
	-60	1.271347568	0.828540164	0.010543746	0.9383144864	100
	0	1.27409	0.827657	0.0106179	0.93839	100
	10	1.274547072	0.827509806	0.010630259	0.9384025856	100
	20	1.275004144	0.827362612	0.010642618	0.9384151712	100
	25	1.27523268	0.827289015	0.0106487975	0.938421464	100
	26	1.2752783872	0.8272742956	0.0106500334	0.93842272256	100
	28	1.2753698016	0.8272448568	0.0106525052	0.93842523968	100
	30	1.275461216	0.827215418	0.010654977	0.9384277568	100
	35	1.275689752	0.827141821	0.0106611565	0.9384340496	100
	40	1.275918288	0.827068224	0.010667336	0.9384403424	100
	45.2	1.27615596544	0.82699168312	0.01067376268	0.938446886912	100
	50	1.27637536	0.82692103	0.010679695	0.938452928	100
	60	1.276832432	0.826773836	0.010692054	0.9384655136	100
	70	1.277289504	0.826626642	0.010704413	0.9384780992	100
	80	1.277746576	0.826479448	0.010716772	0.9384906848	100
	90	1.278203648	0.826332254	0.010729131	0.9385032704	100
	100	1.27866072	0.82618506	0.01074149	0.938515856	100
	120	1.279574864	0.825890672	0.010766208	0.9385410272	100

3.5 Dispersion

In digital communication systems, information to be sent is first coded in the form of pulses and then these pulses of light are transmitted. The larger the number of pulses that can be sent per unit time, the larger will be the transmission capacity of the system. A pulse of light sent into a fiber broadens in time as it propagates through the fiber; this phenomenon is known as pulse dispersion. It is caused by the difference in the propagation times of light rays that takes different paths during the propagation through the fiber. Dispersion limits the information bandwidth. Dispersion occurs primarily because of the following mechanisms:

- In multi-mode fibers, dispersion is caused by different rays taking different time to propagate through a given length of fiber. In the language of wave optics, this is known as intermodal dispersion because it arises due to the different modes travelling with different group velocities.
- Any given light source emits over a range of wavelengths and because of the dependence of refractive index on wavelength, different wavelengths take different amount of time to propagate along the same path. This is known as material dispersion; and obviously, it is present in both single mode and multi-mode fibers.
- In single mode fibers, since there is only one mode, there is no intermodal dispersion. However, waveguide dispersion is present here.
- A single mode fiber can support two orthogonally polarized LP₀₁ modes. In a perfectly circular core fiber, the two polarizations propagate with the same velocity. However, due to the small random deviations from the circularity of the core or due to the random bends and twists in fiber, the orthogonal polarizations travel with slightly different velocities. This phenomenon leads to polarization mode dispersion (PMD).

3.5.1 Dispersion in single mode fibers

3.5.1.1 Material dispersion

Any given light source emits over a range of wavelengths and because of the dependence of refractive index on wavelength, different wavelengths take different amount of time to propagate along the same path. This is known as material dispersion. Material dispersion manifests through the wavelength dependence of the refractive index, $n(\lambda)$, by the following relation [27,28, 32]:

$$D_{mat}(\lambda) = -\frac{\lambda}{c} \frac{d^2 n_1}{d\lambda^2} \quad (3.32)$$

Where, $D_{mat}(\lambda)$ = material dispersion coefficient (ps/nm-km)

c = the light velocity (m/s)

λ = the wavelength (nm)

3.5.1.2 Waveguide Dispersion

It is due to the dependence of the group velocity of the fundamental mode on the V -number, which depends on the source wavelengths, λ even if n_1 and n_2 are constant. Waveguide dispersion arises as a result of the guiding properties of the wave guide, which impose a nonlinear $\omega - \beta$ relationship [33]. Therefore, a spectrum of source wavelengths will result in different V -numbers for each source wavelength and hence different propagation velocities. The waveguide dispersion in optical fibers is given by [32]:

$$D_w = -\frac{V^2}{2\pi c} \cdot \frac{d^2\beta}{dV^2} \quad (3.33)$$

Where,

V = Normalized frequency given by [25,43]

$$V = \frac{2\pi}{\lambda} a \sqrt{n_1^2 - n_2^2} \quad (3.34)$$

where,

n_1 = core refractive index

n_2 = Cladding refractive index

a = core radius (μm)

β = Propagation constant

For step-index fibers, the propagation constant, β is given by [34, 35]:

$$= \sqrt{\left(\frac{V^2}{2\Delta a^2} - \frac{\pi^2}{a^2}\right)}$$

For graded -index fiber the propagation constant, β is given by [34, 35]:

$$= \sqrt{\left(\frac{V^2}{2\Delta a^2} - \frac{6V}{a^2}\right)}$$

c = Free space speed of light

Δ = Relative refractive index difference between core and cladding

3.5.1.3 Chromatic dispersion or Total dispersion

In single mode fibers, the dispersion of a propagating pulse arises because of the finite width $\Delta\lambda$ of the source spectrum; it is not perfectly monochromatic. Dispersion mechanism is based on the fundamental mode velocity depending on the source wavelength, λ . This type of dispersion caused by a range of source wavelengths is generally termed chromatic dispersion and includes both material and waveguide dispersion since both depends on, $\Delta\lambda$.

It can be written as follows [5]:

$$D_{ch}=D_{mat} + D_w \quad (3.35)$$

Where,

D_{mat} =material dispersion

D_w =waveguide dispersion

3.5.1.4 Profile dispersion

Although material and waveguide dispersion are the cheap sources of broadening of a propagating light pulse there are other dispersion effects. There is an additional dispersion mechanism called profile dispersion [33] that arises because the group velocity of the fundamental mode also depends on the refractive index difference Δ , i.e. $\Delta=\Delta(\lambda)$. If Δ changes with wavelength, then different wavelengths from the source would have different group velocities and experience different group delays leading to pulse broadening. It is a part of chromatic dispersion because it depends on the input spectrum $\Delta\lambda$. Typically, profile dispersion D_p is less than 1 ps/km-nm and thus negligible compared with waveguide dispersion D_w . The profile dispersion can be expressed as follows [33].

$$D_p \approx -\frac{N_{g1}}{c} \left(V \frac{d^2(Vb)}{dV^2} \right) \left(\frac{d\Delta}{d\lambda} \right) \quad (3.36)$$

Where, b is the normalized propagation constant and the term $V \frac{d^2(Vb)}{dV^2} \approx 1.984/V^2$ and

N_{g1} =Group refractive index

$$= n - \lambda \frac{dn}{d\lambda}$$

Then the overall chromatic dispersion coefficients become [33]:

$$D_{ch}=D_{mat} + D_w + D_p \quad (3.37)$$

3.6 Effective area

The scenario where several wavelengths are coupled into a single mode fiber which runs through several tens or even hundreds of kilometers in a long-haul, high bit-rate optical communication system very often results in the manifestation of certain nonlinear effects in the fiber. All nonlinear effects depend on the field strength of the electromagnetic wave or the intensity of the field.

The severity of the manifestations of these nonlinear effects is often determined by a parameter of the single mode fiber identified as the effective area is defined as [36, 37]:

$$A_{eff} = \frac{(\iint |E|^2 dx dy)^2}{(\iint |E|^4 dx dy)} \quad (3.38)$$

The area integration is carried out over the cross section of the fiber and the electric field intensity is given by:

$$E = \sqrt{E_x^2 + E_y^2} \quad (3.39)$$

Where,

E_x = is the x-component of the electric field

E_y = is the y-component of the electric field

In optical fibers, the wave is guided mostly in the core area. Hence, it could be assumed that, the effective area corresponds to the core area of the fiber.

In our work, the effective area is calculated corresponds to both the core and the cladding area, because the field distribution is not uniform and hence a non-vanishing part of the propagates in the cladding region of the fiber.

3.7 Complex refractive index

The refractive index is a fundamental parameter of any optical material. For a transparent optical material, the refractive index, n is simply defined as the ratio of the velocity, c of the electromagnetic wave in vacuum to the phase velocity of the same wave in the material i.e.

$$n = \frac{c}{v} \quad (3.40)$$

Since the refractive index of air is only 1.0003, n is conventionally measured with respect to air instead of vacuum, and normally no correction is required. In practice, the optical materials are not purely a non-absorbing medium, and it is frequently convenient to define a complex refractive index [38]:

$$\tilde{n} = n + ik \quad (3.41)$$

Where, k is the imaginary part of the complex refractive index. Both n and k are wavelength dependent.

3.8 Perfectly Matched Layer (PML)

A perfectly matched layer is an absorbing boundary layer, which is a layer of artificial absorbing material that is placed adjacent to the edges of the grid, completely independent of the boundary

condition. When a wave enters the absorbing layer, it is attenuated by the absorption and decays exponentially. This layer absorbs waves of any wave-length and any frequency without reflection and thus can be used to artificially terminate the domain of scattering calculations. This layer can also be utilized to find out the complex part of effective index. There are several different PML formulations. However, all PML's essentially act as a lossy material. The lossy material, or lossy layer, is used to absorb the fields traveling away from the interior of the grid. The PML is anisotropic and constructed in such a way that there is no loss in the direction tangential to the interface between the lossless region and the PML. However, in the PML there is always loss in the direction normal to the interface.

The PML was originally proposed by J. P. Berenger in 1994. In that original work [39] he split each field component into two separate parts. Hence, it is called as split-field PML. The actual field components were the sum of these two parts but by splitting the field Berenger could create an (non-physical) anisotropic medium with the necessary phase velocity and conductivity to eliminate reflection at an interface between a PML and non-PML region. Since Berenger's first paper, others have described PML's using different approaches such as the complex coordinate-stretching technique put forward by Chew and Weedon, also in 1994.

Arguably the best PML formulation today is the Convolutional-PML (CPML). CPML constructs the PML from an anisotropic, dispersive material. CPML does not require the fields to be split and can be implemented in a relatively straightforward manner. In this work, we have considered cylindrical PML.

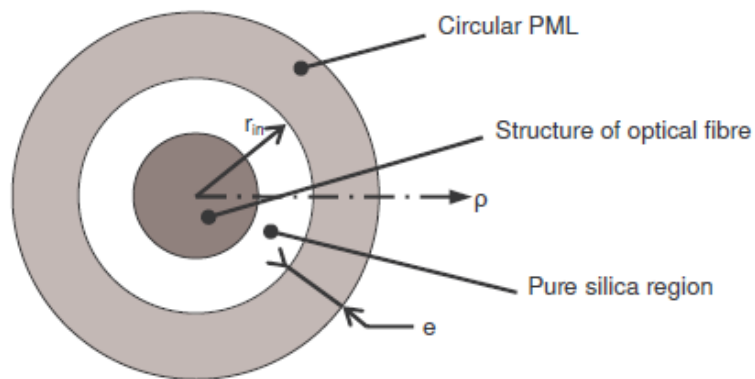


Fig 3.2: PML region surrounding the waveguide structure

3.9 Modal Birefringence

In practice due to disorder in the geometry of the fiber and uneven stresses and pressures on the fiber due to jacketing or any other such reason, a single mode step index optical fiber forms a set of principal axis. Single mode fibers with cylindrical symmetry about the core axis allow the propagation of nearly degenerate modes with orthogonal polarizations. They are therefore bimodal supporting HE_{11}^x and HE_{11}^y modes where the principal axes x and y are determined by the symmetry elements of the of the fiber cross section. Now, if the linearly polarized field at the input to the optical fiber is x polarized, it will experience propagation constant, β_x and if it is y polarized, it will experience a propagation constant, β_y the fiber behaves as a birefringent medium due to difference in the effective refractive indices, and hence phase velocities, for these two orthogonally polarized modes. If $\beta_x \neq \beta_y$, it indicates a state of birefringence. We know that mode effective index, n_{eff} should satisfy the condition [2] for guided modes,

$$n_2 < n_{eff} < n_1 \quad (3.42)$$

Since the propagation constants for the two orthogonally polarized modes are different, the effective mode indices experienced by these orthogonal polarized modes will also be different, with one of them being less than the other.

If $n_x < n_y$, then the mode polarized along the x axis will travel faster than the mode polarized along the y axis, and vice versa. Thus for this condition, the x axis is called as the fast axis and the y axis is called as the slow axis. So the optical signal which is coupled into a fiber optic link with an arbitrary state of polarization splits into its two orthogonal components along the fiber principal axis and propagate at different velocities resulting in phase difference between two components. This results in a change in state of polarization of the optical signal propagating through the fiber whereby at the output of a long fiber optic link with several sections of fiber, the state of polarization cannot be predicted. When the fiber cross section is independent of the fiber length L in the z direction, then the modal birefringence, B_F for the fiber, [2, 19]

$$B_F = \frac{(\beta_x - \beta_y)}{2\pi/\lambda} = (n_{eff_x} - n_{eff_y}) \quad (3.43)$$

Where, λ is the optical wavelength.

3.10 Polarization Mode Dispersion

A fundamental property of an optical signal is its polarization state. Polarization refers to the electric-field distribution of a light signal, which can vary significantly along the length of a fiber. This dispersion arises when the fiber is not perfectly symmetric and homogeneous, that is, the refractive index is not isotropic. When the refractive index depends on the direction of the electric field, the propagation constant of a given mode depends on its polarization. Due to

various variations in the fabrication process such as small changes in the glass composition, geometric and induced local strains (either during fiber drawing or cabling) the refractive indices n_1 and n_2 may not be isotropic leading to differential group delay and hence dispersion occurs even if the source wavelength is monochromatic. Polarization mode dispersion (PMD) is a source of pulse broadening which results from fiber birefringence and it can become a limiting factor for optical fiber communication. This is particularly critical for high-rate long-haul transmission links (e.g. 10 and 40 Gb/s over tens of kilometers). When considering a short section of single-mode fiber within a long fiber span it can be assumed that any disorders acting on it are constant over its entire length rather than varying along it. In this case the fiber becomes bimodal due to loss degeneracy for the HE_{11} modes. As these two modes have different phase propagation constants β_x and β_y they exhibit differential group delay. In the time domain for a short section of fiber, the differential group delay (DGD), [2]:

$$\Delta\tau = \delta\tau_g L \quad (3.44)$$

is defined as the group delay difference between the slow and the fast modes over the fiber lengths. The DGD can be obtained from the frequency derivative of the difference in the phase propagation constants [2],

$$\begin{aligned} \delta\tau_g &= \frac{\Delta\tau}{L} = \frac{d}{d\omega}(\beta_x - \beta_y) \\ &= \frac{d}{d\omega} \left(\frac{\omega n_x}{c} - \frac{\omega n_y}{c} \right) \\ &= \frac{d}{d\omega} \frac{\omega}{c} \Delta n_{eff} \\ &= \frac{\Delta n_{eff}}{c} + \frac{\omega}{c} \frac{d}{d\omega} \Delta n_{eff} \end{aligned} \quad (3.45)$$

Where $\delta\tau_g$, the differential group delay per unit length, i.e. the average value of the DGD is referred to as the polarization mode dispersion (PMD) of the fiber and usually expressed in units of picoseconds per kilometers (ps/km) for polarization-maintaining fibers $\delta\tau_g$ can be quite large at around 1 ns /km. A useful means of characterizing PMD for long fiber lengths is in terms of the mean value of the differential group delay. This can be calculated according to the relationship:

$$\Delta\tau = D_{PMD} \sqrt{L} \quad (3.46)$$

Where D_{PMD} is the RMS value of the polarization mode dispersion, measured in ps/\sqrt{km} , or is the PMD coefficient parameter. Typical values of D_{PMD} range from 0.05 to 1.0 ps/\sqrt{km} [5]. The PMD coefficient is a parameter that is typically specified for commercially available fiber. The PMD coefficient represents the PMD characteristics of one particular length of fiber. In a fiber link consisting of several successive joined of lengths of fiber is length will have a different PMD coefficient. The impact on system performance PMD increases with transmission distance [16], thus as the distance increases, it is more likely to observe large DGD at the receiver.

Chapter 4

Simulation Results and Discussions

4.1 The temperature dependence of the refractive indices

The temperature dependent Sellmeier coefficients using equation (3.30) are calculated for the three optical fiber glasses from which the refractive indices are calculated at any wavelength and at any operating temperature. The results are shown in Fig. (4.1) and Fig. (4.2).

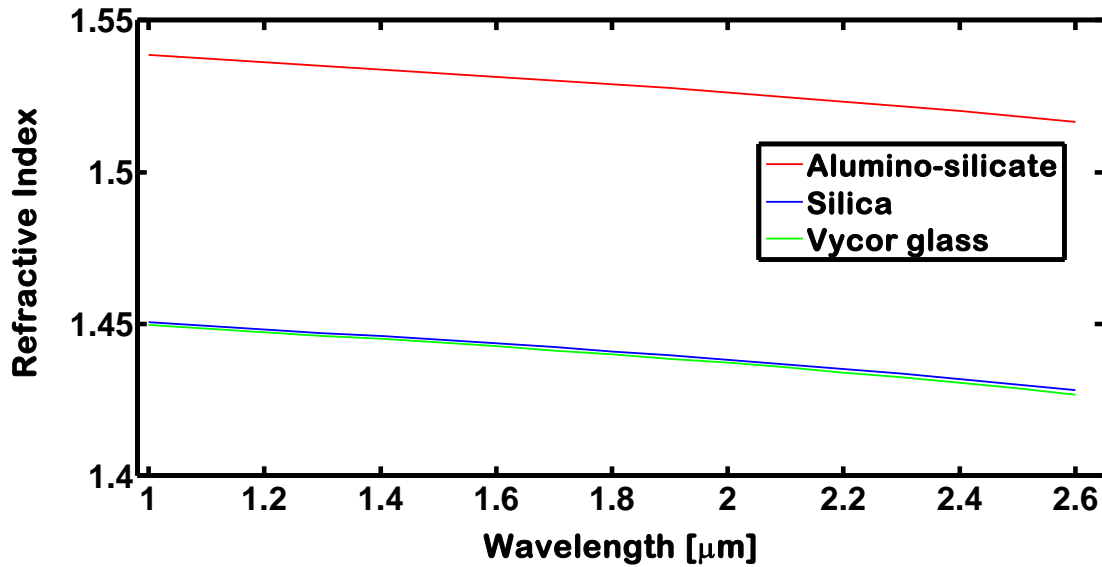


Fig. 4.1 Refractive index vs. wavelength for three optical glasses

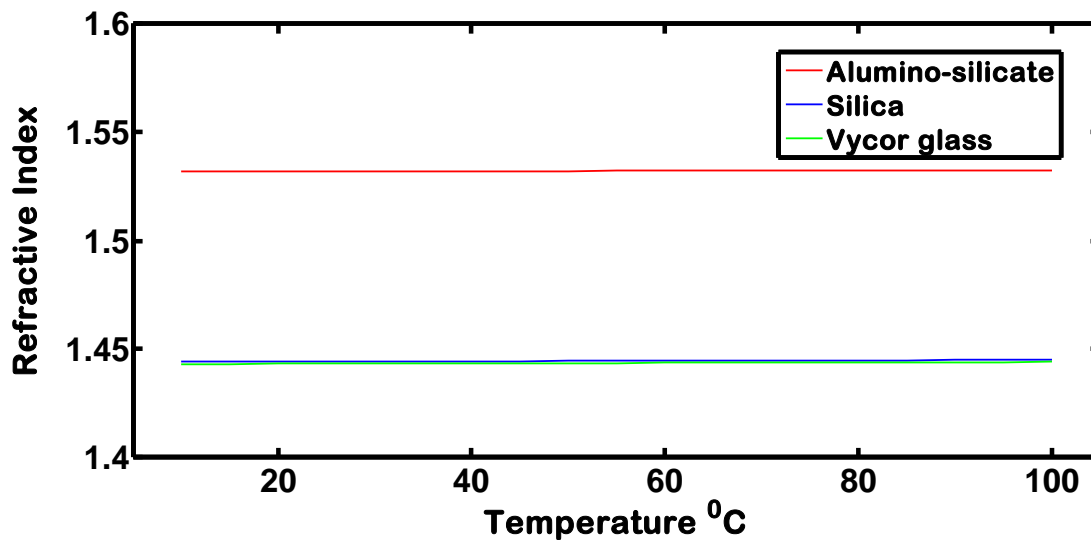


Fig. 4.2 Refractive index vs. temperature for three optical glasses

For all three types of glasses are found to follow a decreasing trend for refractive index vs. wavelength and nicely fit to straight line for refractive vs. temperature. For a given wavelength the refractive index of Aluminosilicate is high as compared to the others two, SiO₂ and Vycor respectively.

A typical plot of the temperature dependent Sellmeier coefficients (A, B, C, D) for all three types of materials is shown in Fig. (4.3), Fig. (4.4) and Fig. (4.5). It is evident that all are nicely fitted into straight lines. For fused silica (SiO₂) glass, the result is identical with [8].

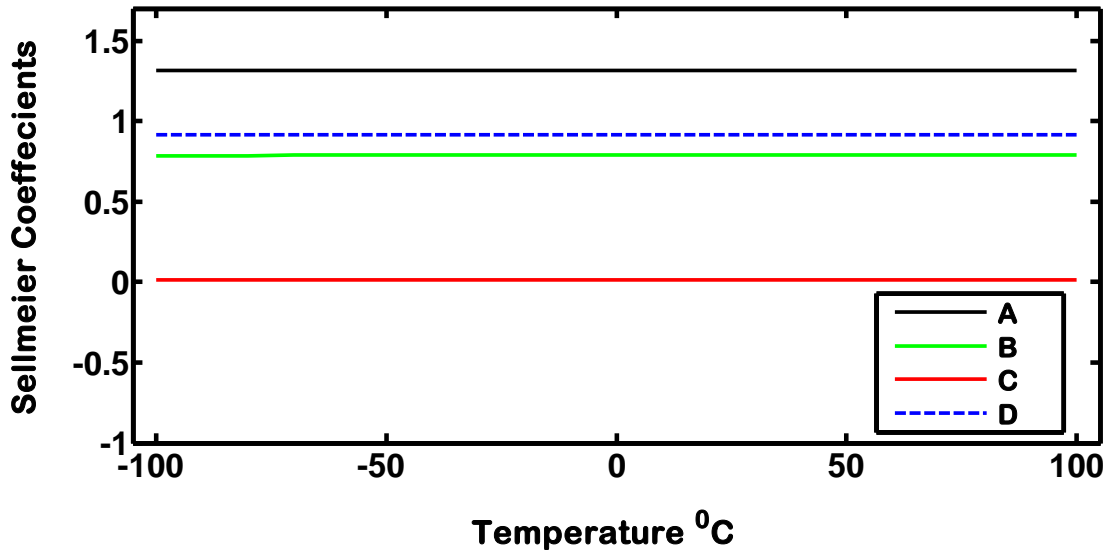


Fig. 4.3 Sellmeier coefficients vs. temperature for SiO₂ glass

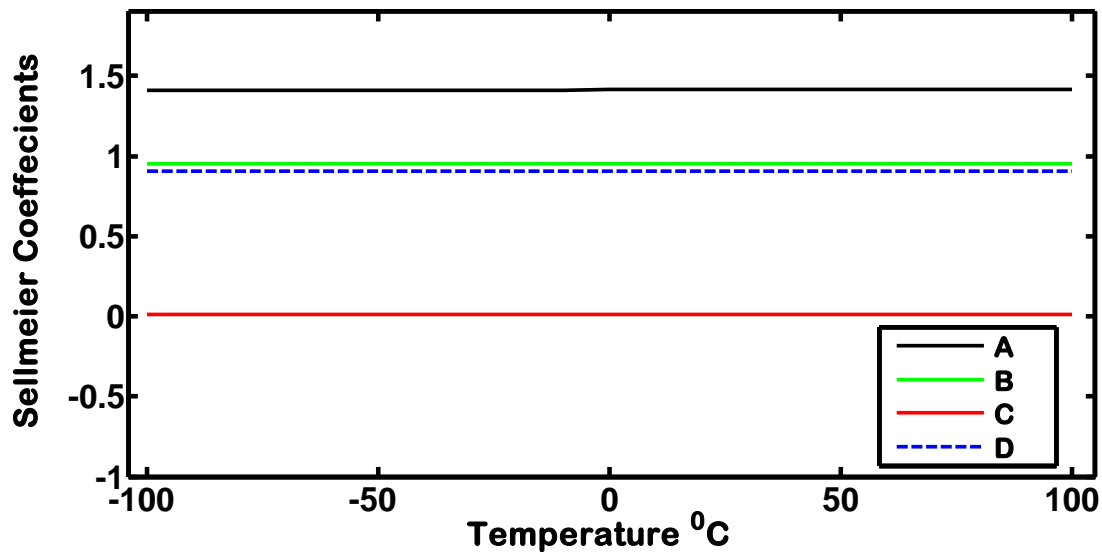


Fig. 4.4 Sellmeier coefficients vs. temperature Aluminosilicate glass

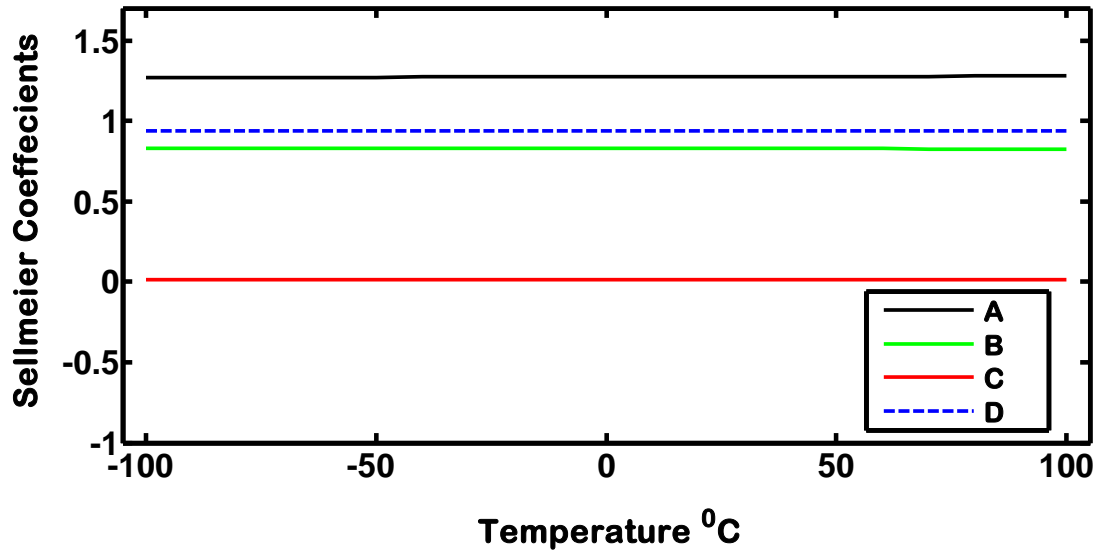


Fig. 4.5 Sellmeier coefficients vs. temperature Vycor glass

4.2 Effective Refractive Index

The effective refractive index for Aluminosilicate is simulated at 1.55 μm wavelength, 26°C with core $n_1 = 1.532$ and cladding 2% less than core. The simulation result is found shown in Fig. (4.6). It satisfies the condition for effective index [2]:

$$n_2 < n_{eff} < n_1$$

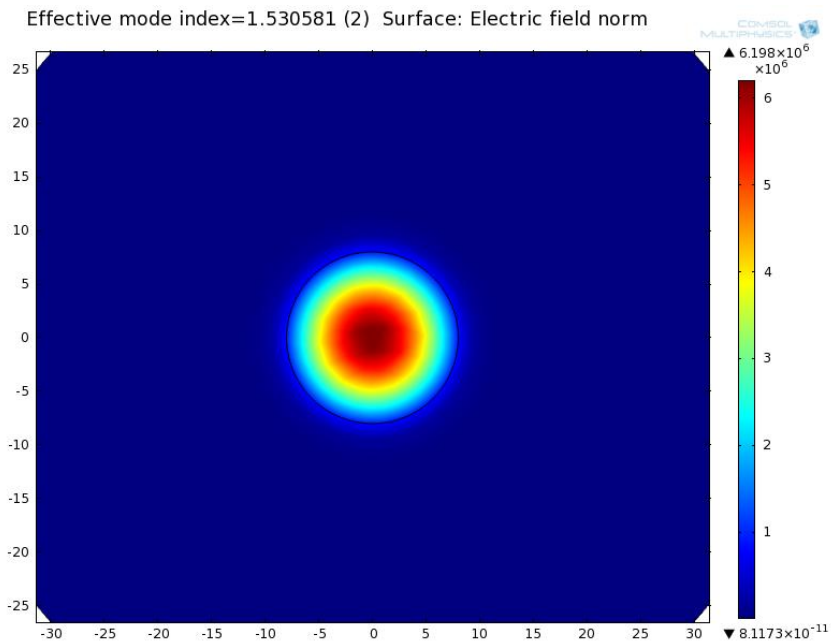


Fig. 4.6 Effective mode index for Aluminosilicate with normalized electric field.

Only the fundamental mode is found. For other two materials the same procedure is done. Also the normalized electric field is shown, which signifies that the electric field is maximum inside the core region and decreases far from the core. It is evident of strong guiding of light within the core of the step-index fiber where bend losses and others effect of external disturbances are weak [40].

A plot of effective mode index vs. wavelength at 26⁰C for SiO₂ glass is shown in Fig. (4.7), which decreases with the increase of wavelength.

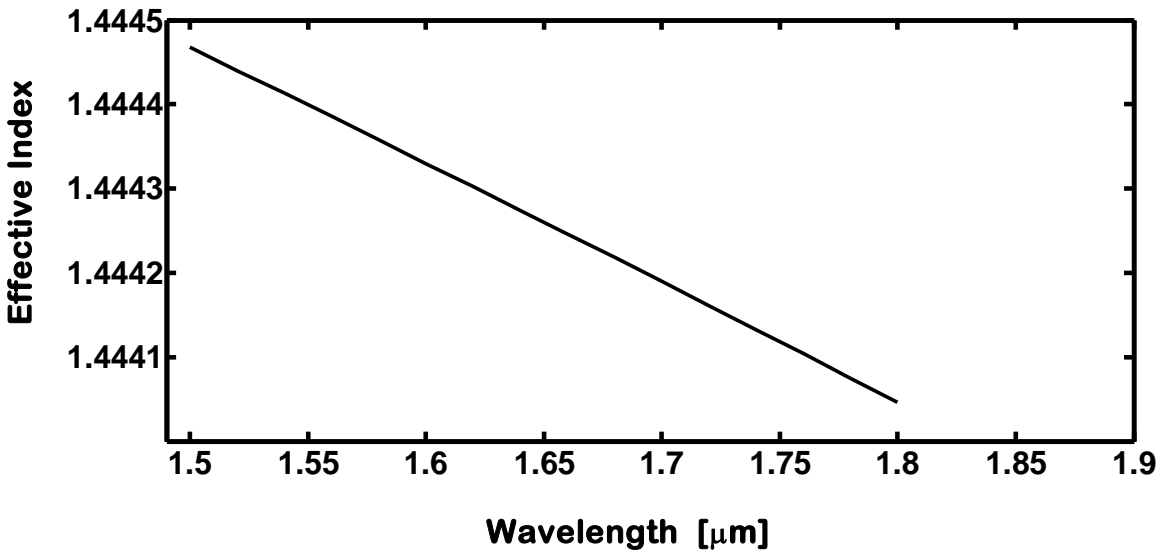


Fig. 4.7 Effective mode index vs. wavelength for SiO₂ glass at 26⁰C

The dependence of effective mode index is calculated in the temperature range of 0⁰C to 100⁰C at 1.55 μm wavelength is shown in Fig. (4.8), which is nicely fit into straight lines in the increasing trend for all three glasses.

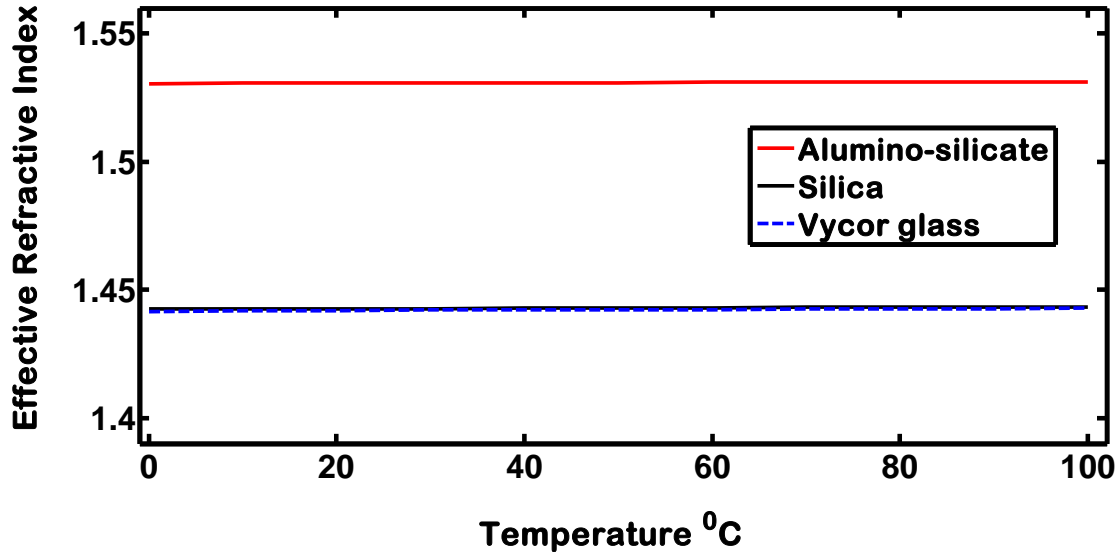


Fig.4.8 Effective mode index as a function of temperature

4.3 Dispersion

4.3.1 Material Dispersion

Material dispersion is calculated for the three optical fiber glass types (SiO₂, Aluminosilicate, Vycor glass) at 26°C using the temperature dependent Sellmeier coefficients in Equation (3.30). It is shown in Fig. (4.9).

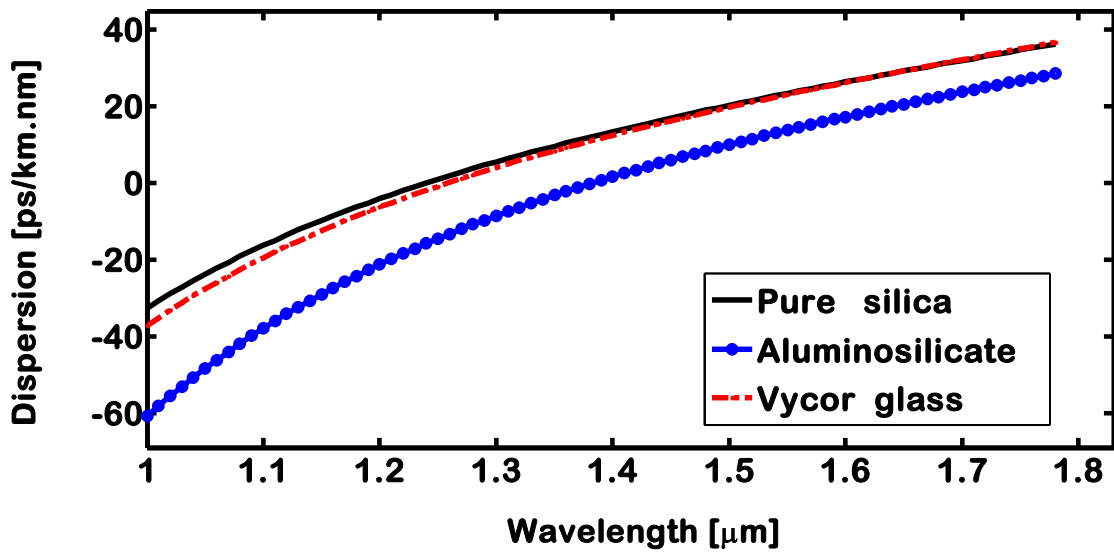


Fig. 4.9. Material dispersion at 26°C for all three glasses

The zero material dispersion wavelengths are 1.2726, 1.3921 and 1.2677 for SiO₂, Aluminosilicate and Vycor glass respectively which is nearly by shown [12]. The dispersion characteristics are not linear for whole spectral region. A sample of the results is shown in Fig. (4.10) for SiO₂ glass.

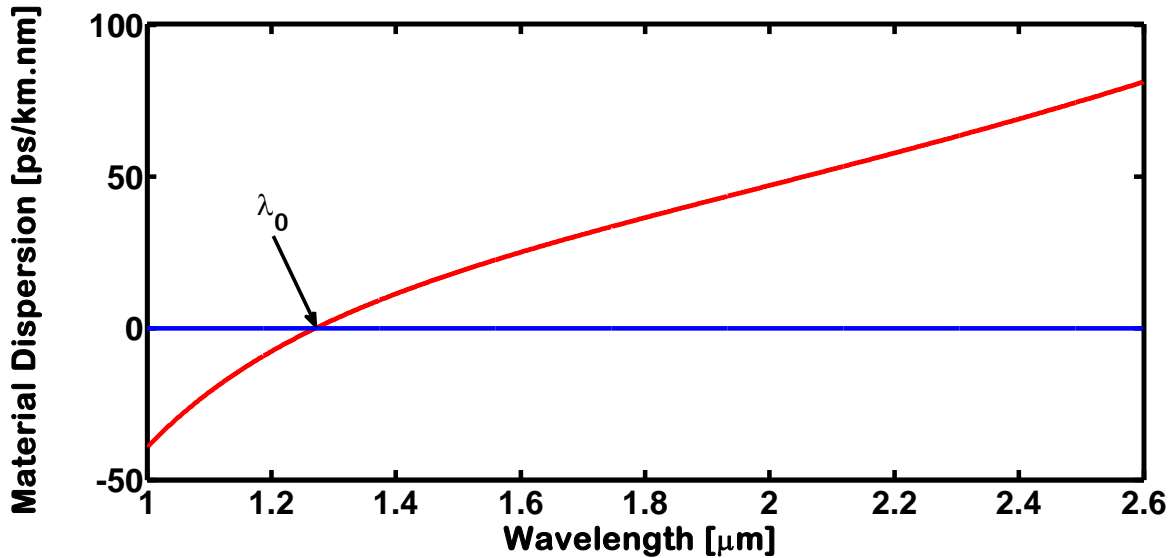


Fig. 4.10. Material dispersion for SiO₂ glass at 26°C with zero dispersion wavelength

For a wide of temperature (-120°C to 120°C), the material dispersion and the zero-material dispersion wavelength has been calculated for three glasses. The obtained results are shown in Fig. (4.11), Fig. (4.12) and Fig. (4.13) for SiO₂, Aluminosilicate, and Vycor glass, respectively. The material dispersion linearly related to temperature, and increases with the increase of wavelength for all three tested optical fiber materials.

The zero material dispersion wavelength as a function of temperature, T is displayed in Fig. (4.14) for all three types of glasses. It is seen that the temperature dependence is linear and $\frac{d\lambda_0}{dT}=0.025 \text{ nm}^{\circ}\text{C}$ for silica and this is perfectly matched with [9]. This value is fair agreement with the published experimental values of $0.029 \pm 0.004 \text{ nm}^{\circ}\text{C}$ and $0.031 \pm 0.004 \text{ nm}^{\circ}\text{C}$ for two dispersion shifted fibers within the experimental accuracy [41]. The corresponding values of $\frac{d\lambda_0}{dT}$ is found $0.03 \text{ nm}^{\circ}\text{C}$ for both Aluminosilicate and Vycor glasses [9].

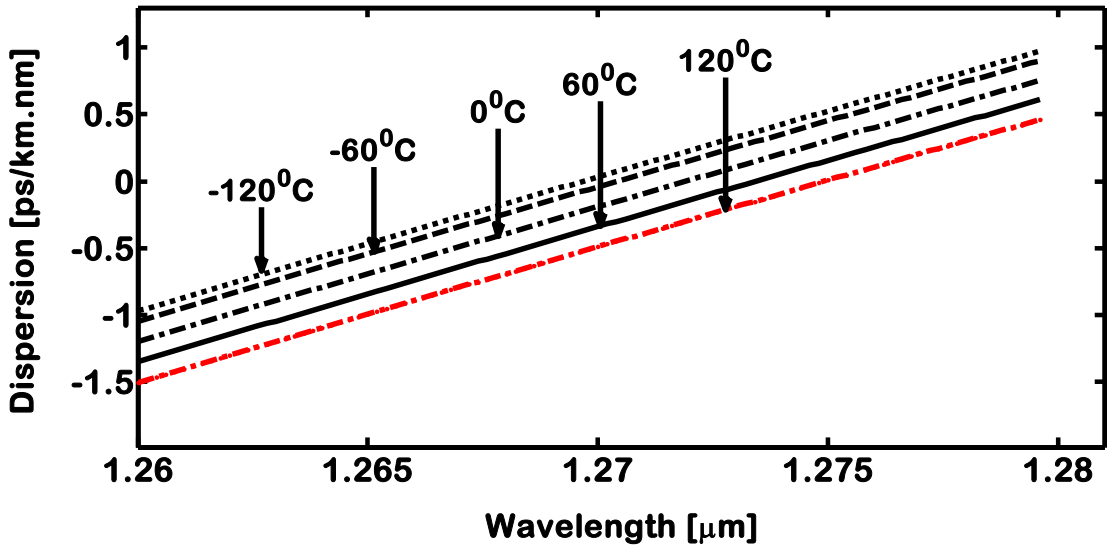


Fig. 4.11 Material dispersion vs. wavelength for a wide range of temperature for SiO₂ glass

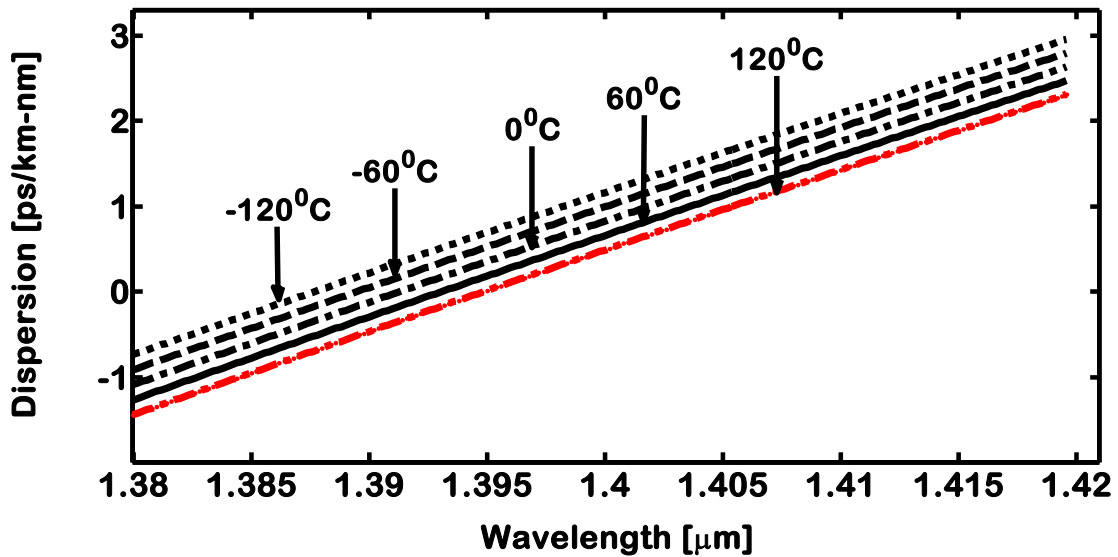


Fig. 4.12 Material dispersion vs. wavelength for a wide range of temperature for Aluminosilicate glass

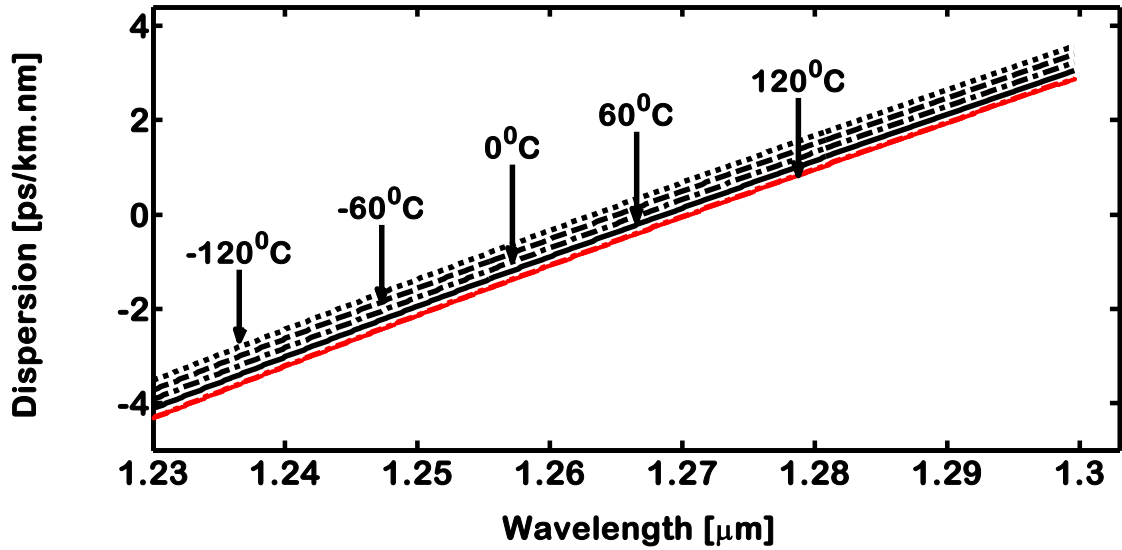


Fig. 4.13 Material dispersion vs. wavelength for a wide range of temperature for Vycor glass.

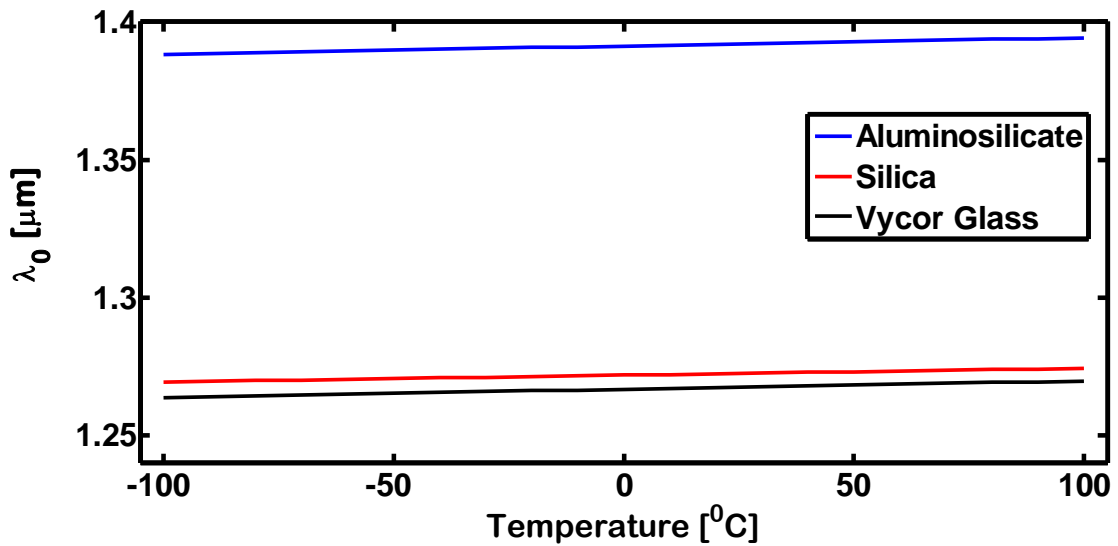


Fig. 4.14 Zero-dispersion wavelength vs. temperature

4.3.2 Chromatic Dispersion

Using the temperature dependent Sellmeier coefficients and the corresponding values of the V-number, waveguide dispersion and total dispersion for single mode step index fiber calculated a core radius, $a=5 \mu\text{m}$, and making a fixed relative refractive index difference, $\Delta=0.005$, for three types of glasses at temperature 26°C . Actually, the relative refractive index difference, is not fixed, since it is the difference between the indices of core and cladding. Moreover, these indices depend on temperature. Hence, the relative index difference must be a function of temperature which is later explained and termed as profile dispersion [33] due to this change.

The material dispersion is added to the waveguide dispersion parameter to get the total dispersion or chromatic dispersion. The Fig. (4.15), Fig (4.16), and Fig (4.17) shows the obtained results for SiO_2 , Aluminosilicate, and Vycor glass, respectively. The zero-total dispersion wavelengths obtained are 1.2982, 1.4111 and 1.2930 for SiO_2 , Alumino and Vycor glass respectively which are close to the values shown by [9]. These values are greater than that was obtained for zero-material dispersion solely. Hence, a shifted in total dispersion from the material dispersion curve

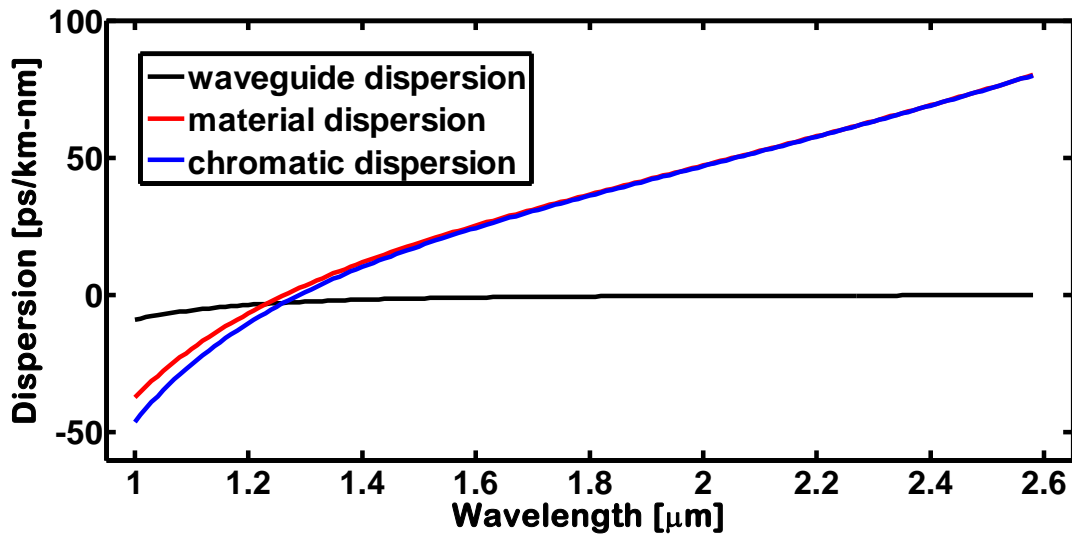


Fig. 4.15 Chromatic dispersion vs. wavelength for 26°C for SiO_2 glass.

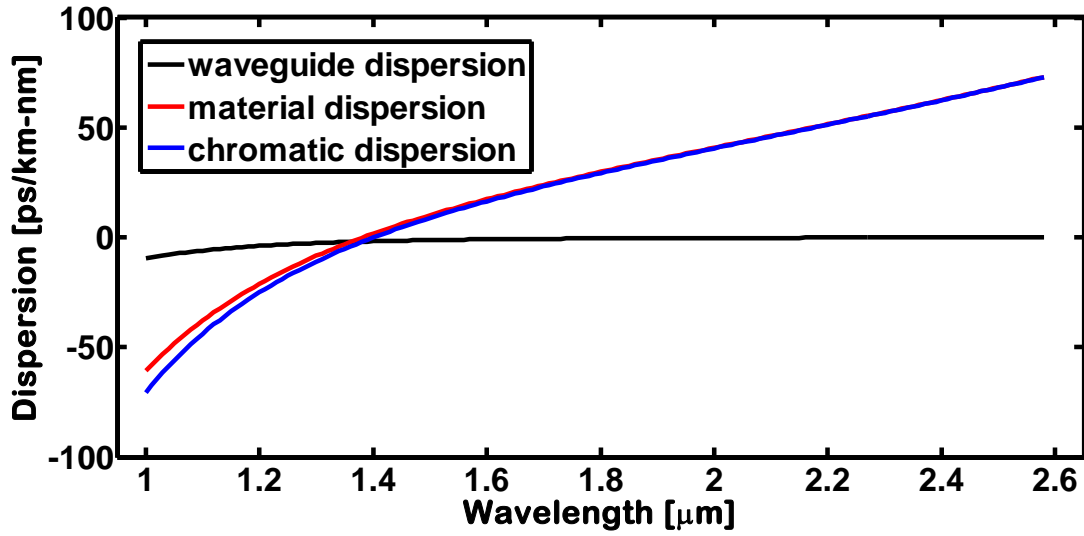


Fig. 4.16 Chromatic dispersion vs. wavelength for 26⁰C for Aluminosilicate glass.

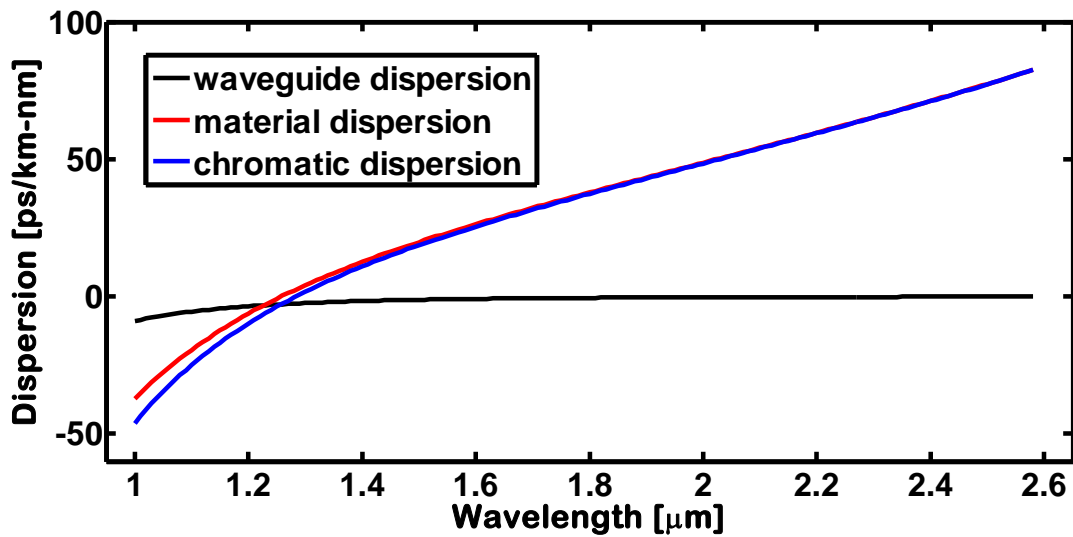


Fig. 4.17 Chromatic dispersion vs. wavelength for 26⁰C for Vycor glass

4.3.3 Profile Dispersion

The profile dispersion for all three types of glasses are shown in Fig. (4.18), fig. (4.19), and Fig. (4.20) for both temperatures 20⁰C and 45.2⁰C. It is shown that for such increase in temperature that is no effect of profile dispersion. Typically, profile dispersion is less than 1 ps/km-nm [33]. We get profile dispersion -7.36ps/km-nm for silica glass at 1.55 μm .

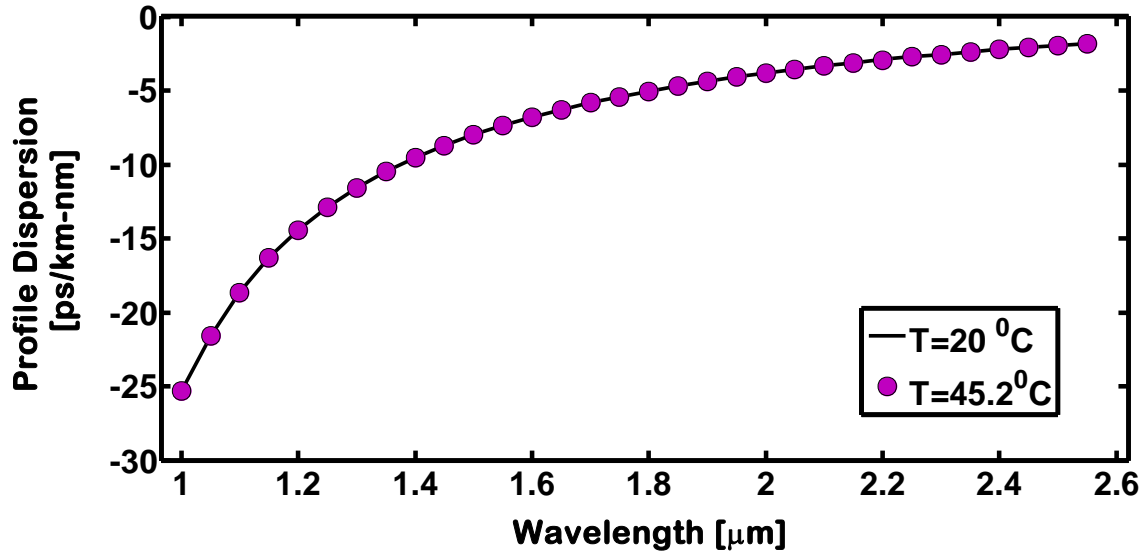


Fig. 4.18 Profile dispersion vs. wavelength for SiO₂ glass

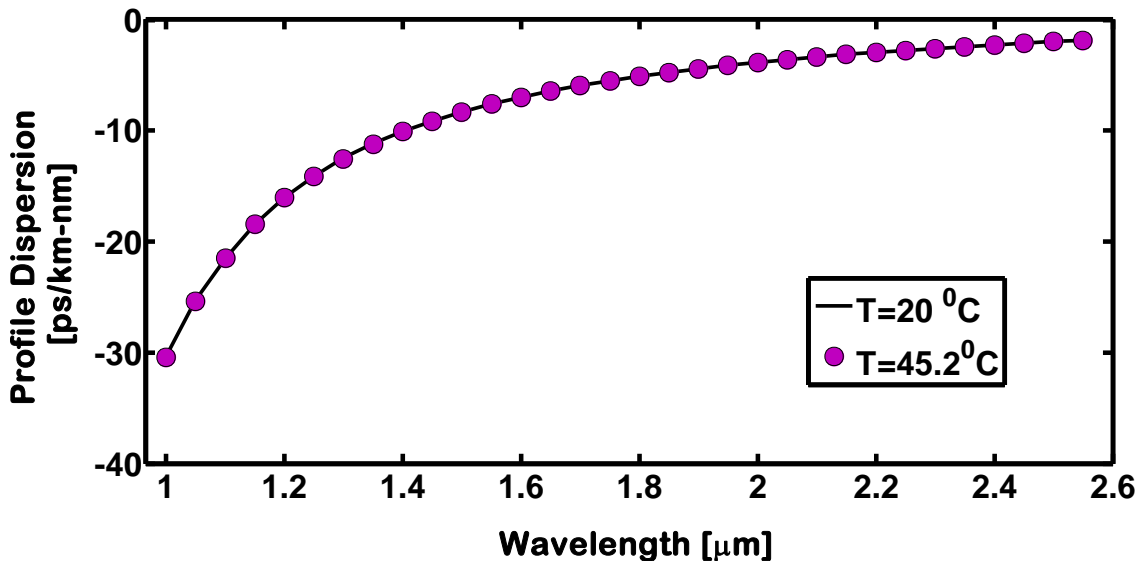


Fig. 4.19 Profile dispersion vs. wavelength for Aluminosilicate glass

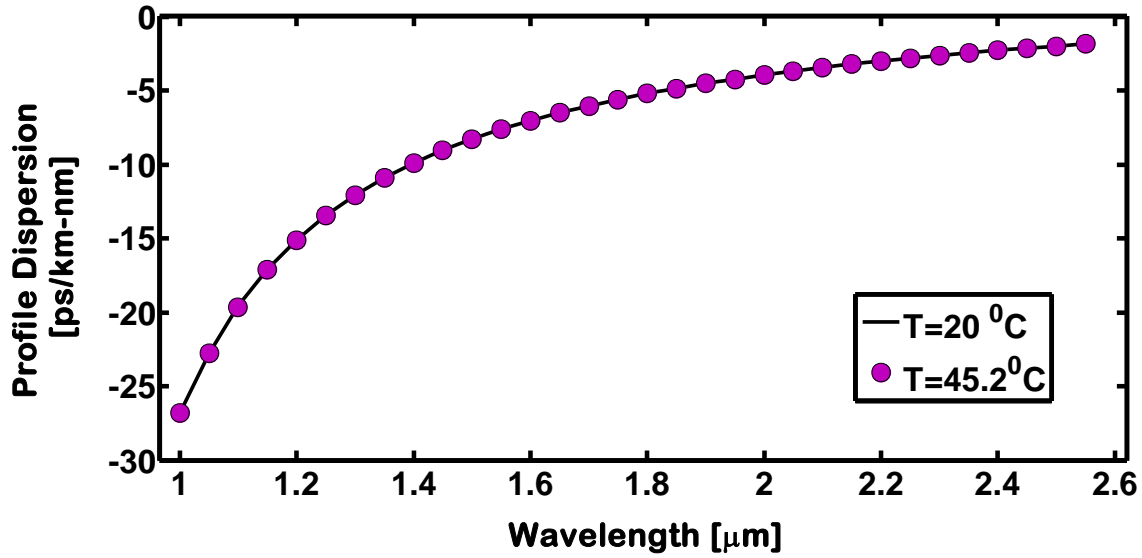


Fig. 4.20 Profile dispersion vs. wavelength for Vycor glass

Even for huge change in temperature, the profile dispersion is slightly shifted from its original position. It is displayed in Fig. (4.21), Fig. (4.22) and Fig. (4.23) at both temperatures 20⁰C and 1000⁰C for fused Silica, Vycor glass and Aluminosilicate glass respectively. At 1000⁰C, there is very trifle change in profile dispersion which concludes that for all three types of glasses profile dispersion is temperature independent.

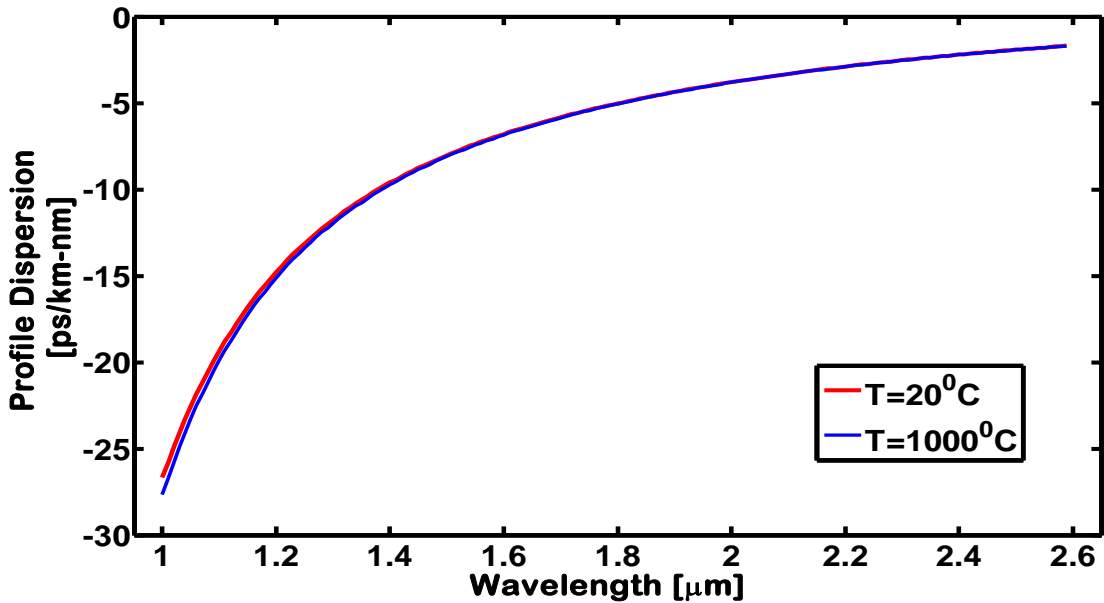


Fig. 4.21 Profile dispersion vs. wavelength for SiO₂ glass

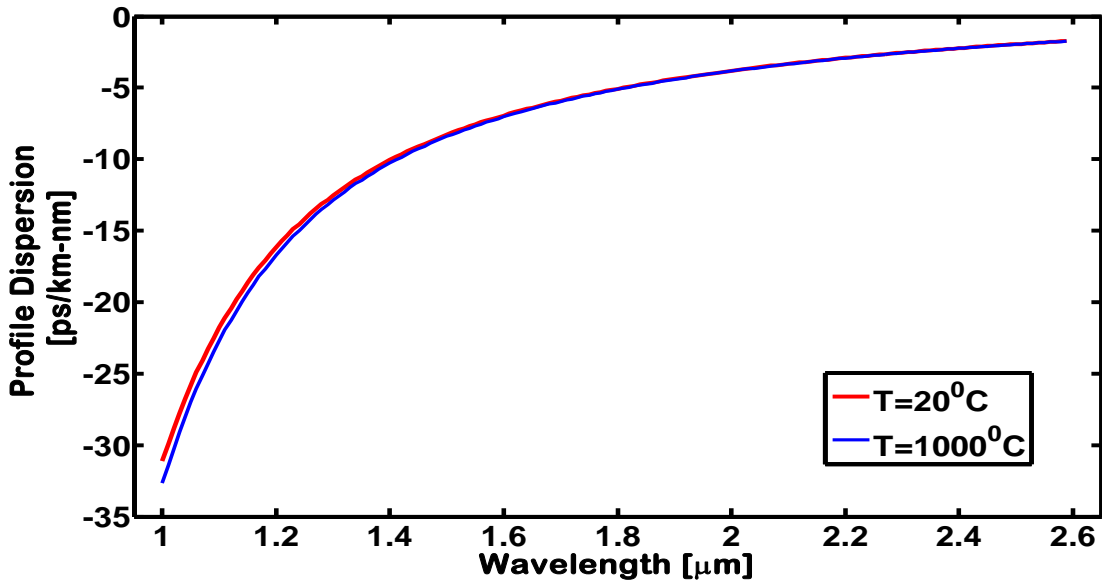


Fig. 4.22 Profile dispersion vs. wavelength for Aluminosilicate glass

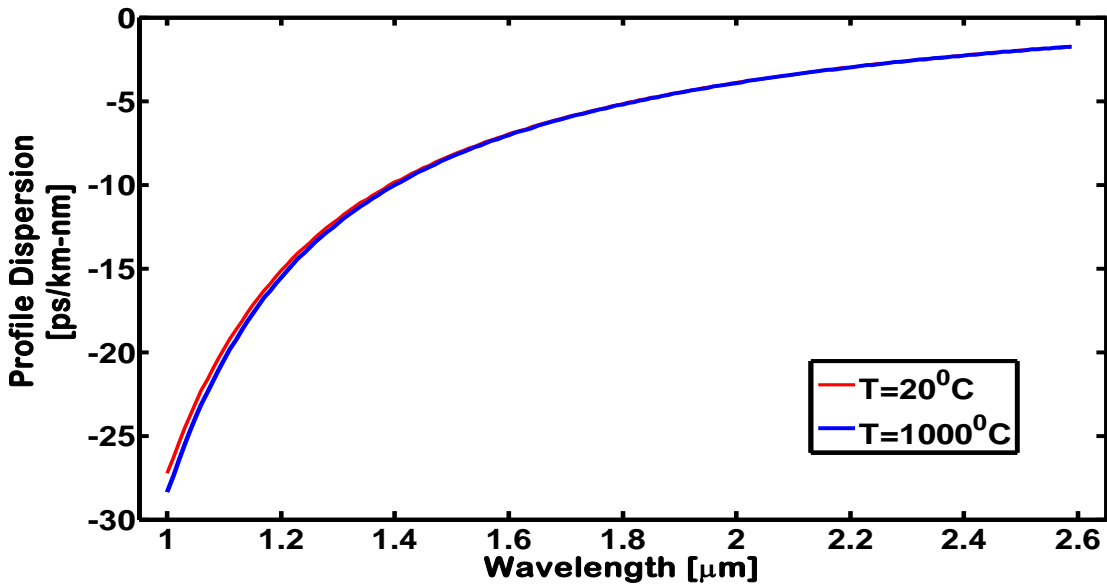


Fig. 4.23 Profile dispersion vs. wavelength for Vycor glass

Now the profile dispersion for a fixed temperature (26°C) for all three types of materials; Fused Silica, Vycor glass and Aluminosilicate is shown in Fig. (4.24). It is evident that, the profile dispersion for Aluminosilicate is higher while for the other two it is almost same.

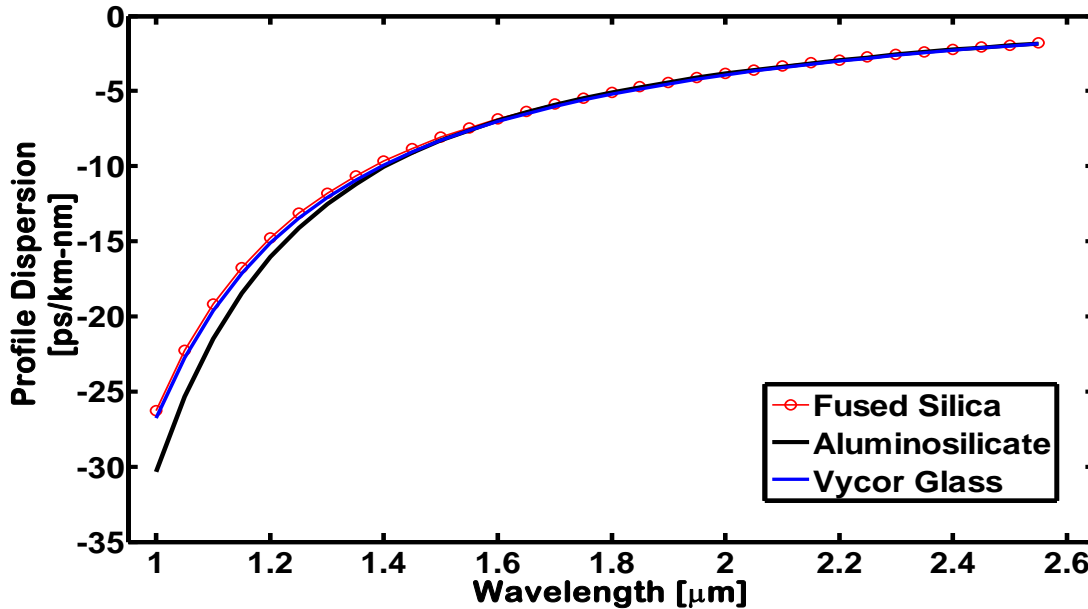


Fig. 4.24 Profile dispersion vs. wavelength for all three glasses

The total dispersion considering profile dispersion operating at 26°C is shown in Fig. (4.25). Here it is indicated that total dispersion is shifted due to profile dispersion and hence the zero total dispersion also. The zero total dispersion wavelengths are $1.3130\ \mu\text{m}$, $1.3081\ \mu\text{m}$, $1.4243\ \mu\text{m}$ for SiO_2 , Vycor glass and Aluminosilicate respectively which makes a variation from the stated values of zero-total dispersion wavelengths 1.2982 , 1.2930 and 1.4111 , not considering profile dispersion parameter.

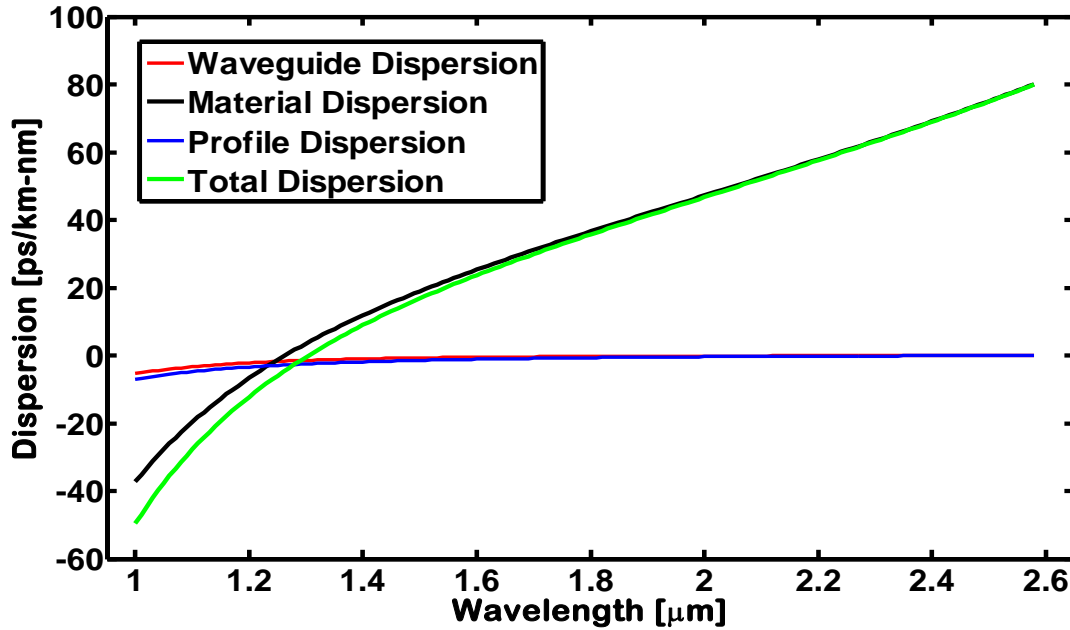


Fig. 4.25 Total dispersion vs. wavelength considering profile dispersion at 26⁰C for SiO₂ glass

4.4 Effective Area

The Fig. (4.26), Fig (4.27), and Fig (4.28) shows the wavelength -dependent effective area at three temperatures for three types of glasses. It is evident that, there is no effect of temperature on A_{eff} and solely A_{eff} depends on wavelength (λ) for all three types of glasses.

The A_{eff} increase with the increase of wavelength almost linearly. At longer wavelengths, the value of effective area is high as compared to lower wavelengths. The effective area at higher wavelengths is minimum for Aluminosilicate as compared to SiO₂ and Vycor glass.

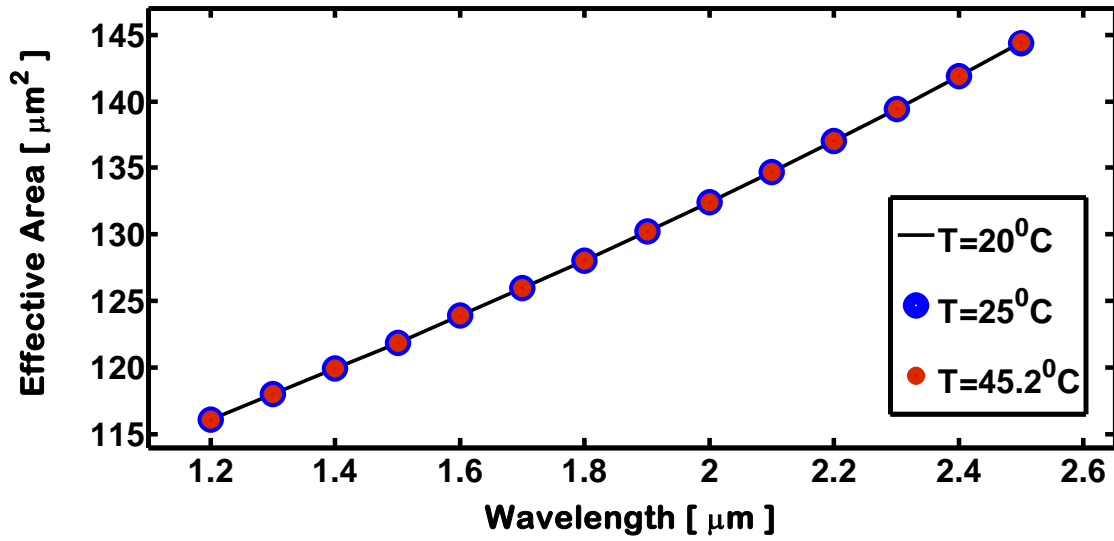


Fig. 4. 26 Effective area vs. wavelength of SiO₂ glass at different temperatures.

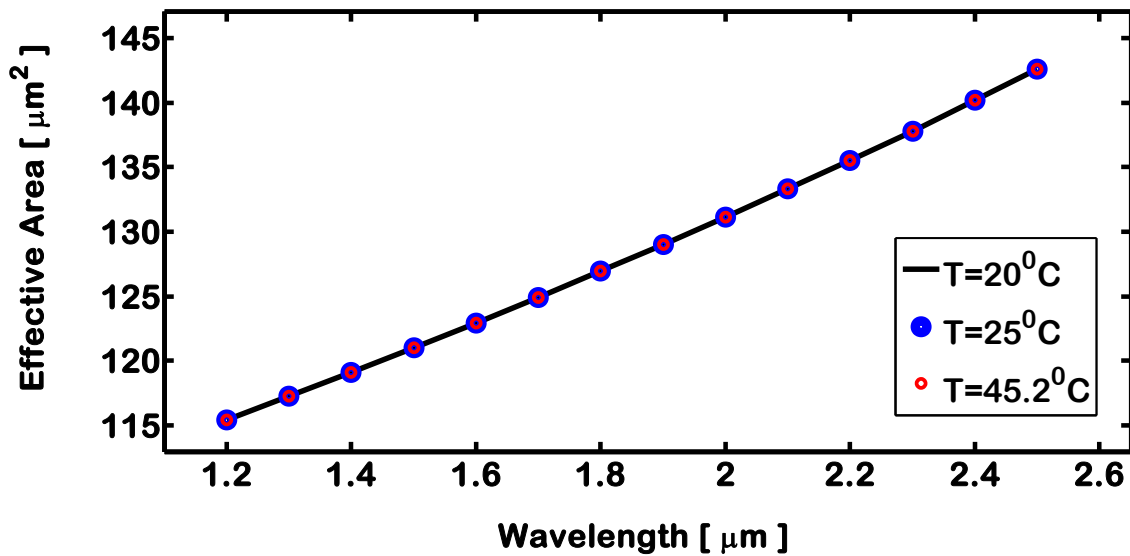


Fig. 4. 27 Effective area vs. wavelength of Aluminosilicate glass at different temperatures

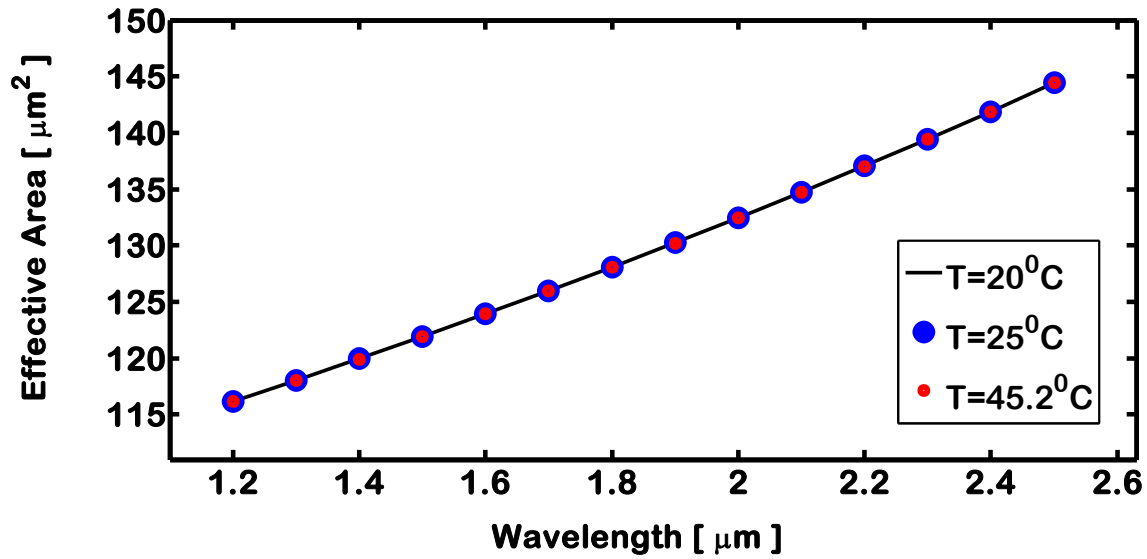


Fig. 4.28 Effective area vs. wavelength of Vycor glass at different temperatures

4.5 Power Flow

The Fig. (4.29) shows the simulation result of power flow. It is seen that the maximum power flow is along the core region indicates strong guiding of light. Meanwhile, the power is reduced far from the core and minimum at the cladding-air interface.

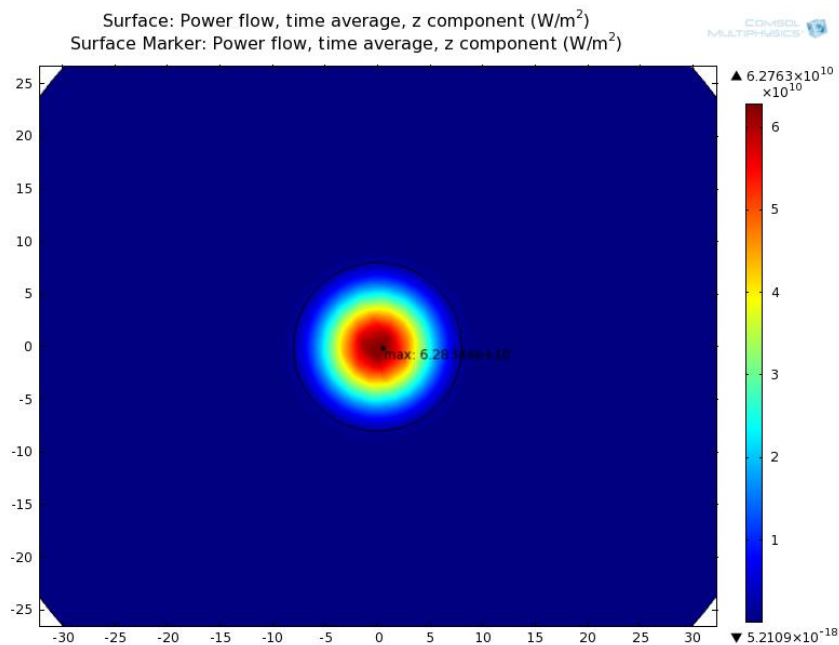


Fig. 4.29 Maximum power flow through the core

The Fig. (4.30), Fig.(4.31), and Fig.(4.32) shows the wavelength- dependent power flow in the both core and cladding region at three different temperatures for the three types of materials. It is evident that the power flow for all three types of materials is independent of temperature and absolutely depends on the wavelength and decrease with the increase of wavelength. The power flow at higher wavelengths is minimum for Aluminosilicate as compared to SiO₂ and Vycor glass.

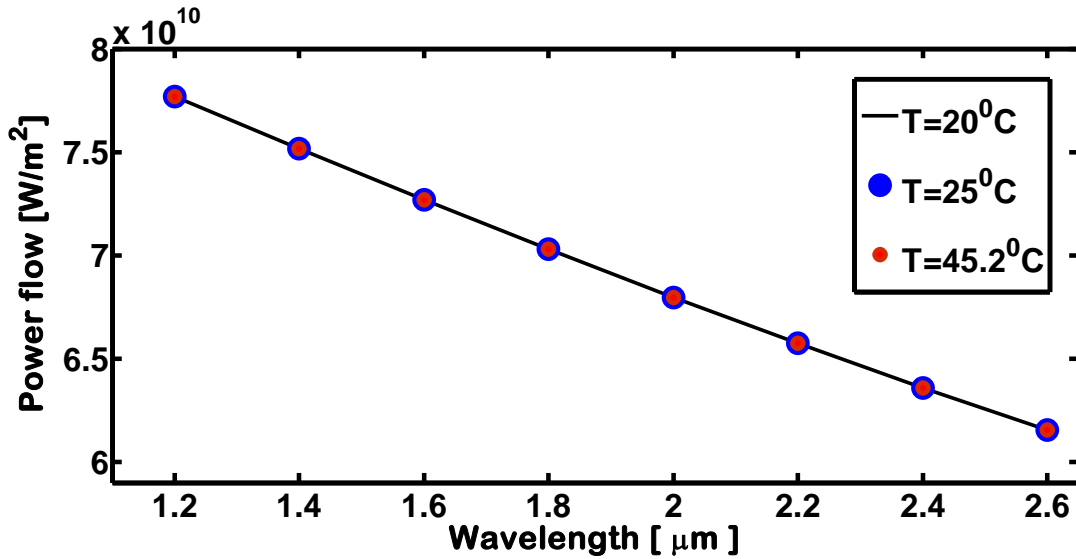


Fig. 4.30 Power flow vs. wavelength of SiO₂ glass at different temperatures.

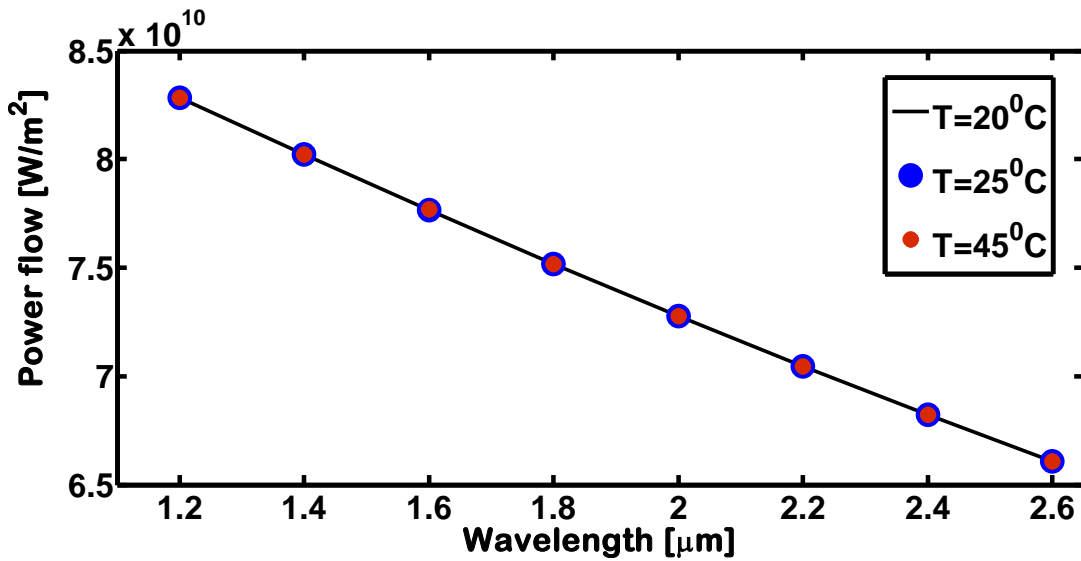


Fig. 4.31 Power flow vs. wavelength of Aluminosilicate glass at different temperatures

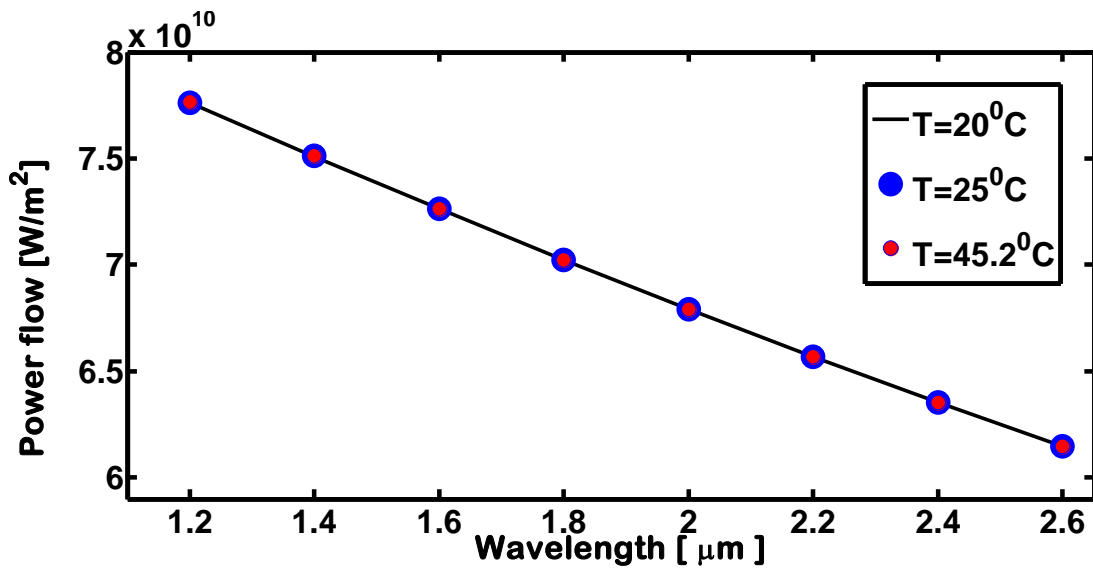


Fig. 4.32 Power flow vs. wavelength of Vycor glass at different temperatures

4.6 Perfectly Matched Layer (PML)

4.6.1 Effective Area and Power Using PML

When a wave enters in the absorbing layer, i.e. PML, it is attenuated and no reflection of wave occurs. Hence, the power confinement within the core is increased and corresponding effective area also decrease. The Fig. (4.33) shows the simulation result of a cylindrical perfectly matched layer with a complex refractive index.

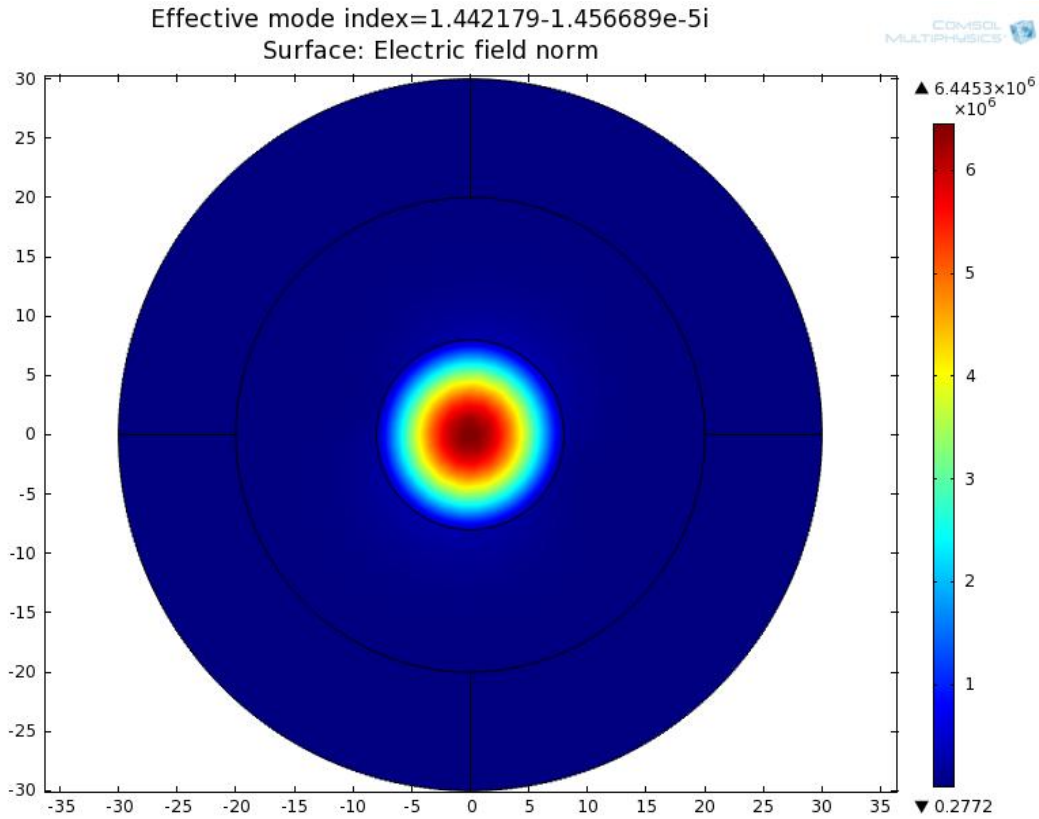


Fig. 4.33 Perfectly matched layer (PML)

The results for power and effective area using PML is shown in Fig.(4.34), Fig (4.35), Fig. (4.36) and Fig. (4.37).

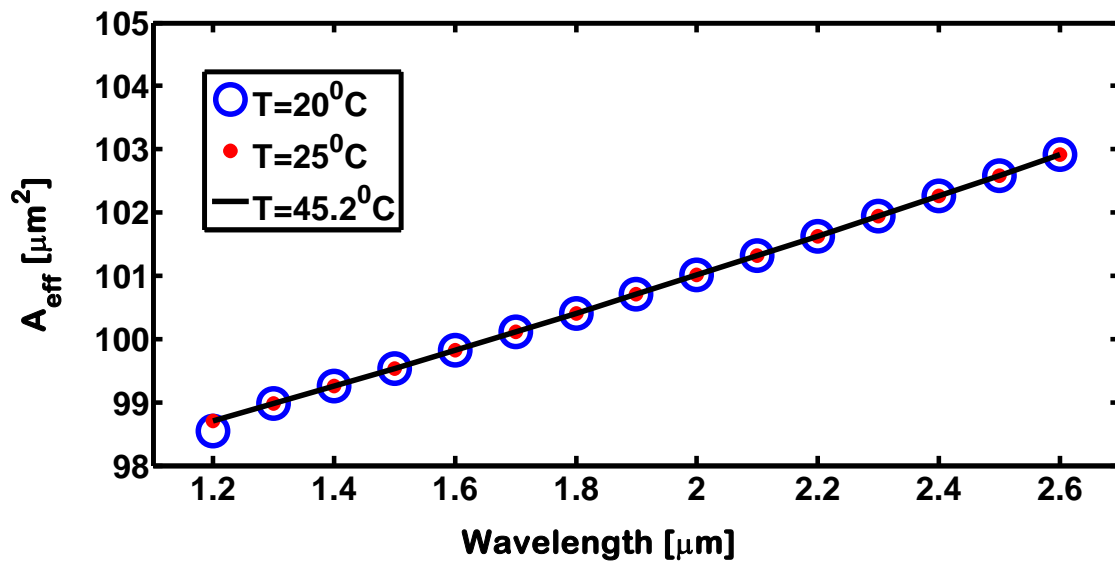


Fig. 4. 34 Effective area vs. wavelength of Aluminosilicate glass at different temperatures using PML

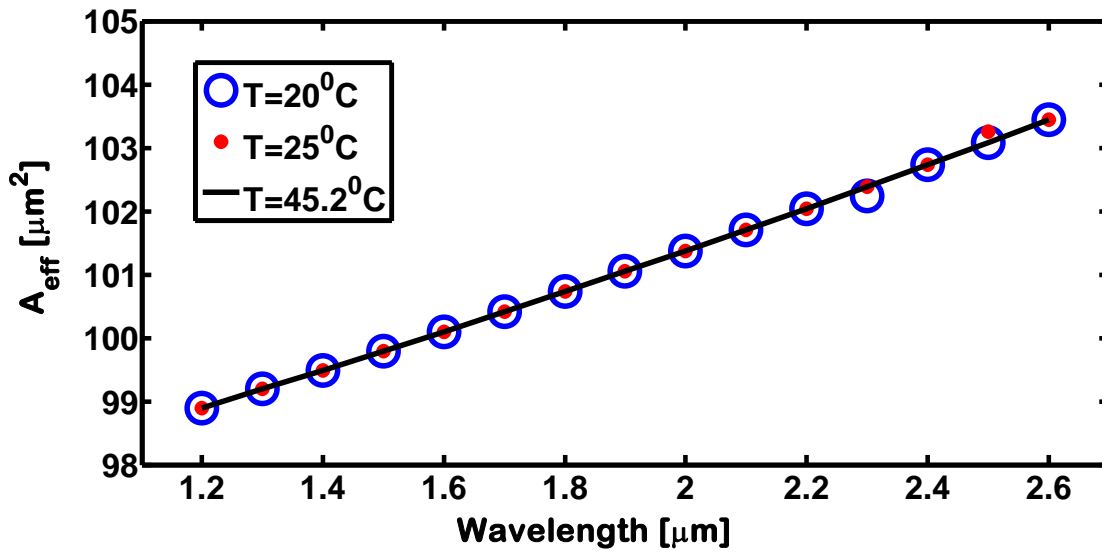


Fig. 4.35 Effective area vs. wavelength of Vycor glass at different temperatures using PML

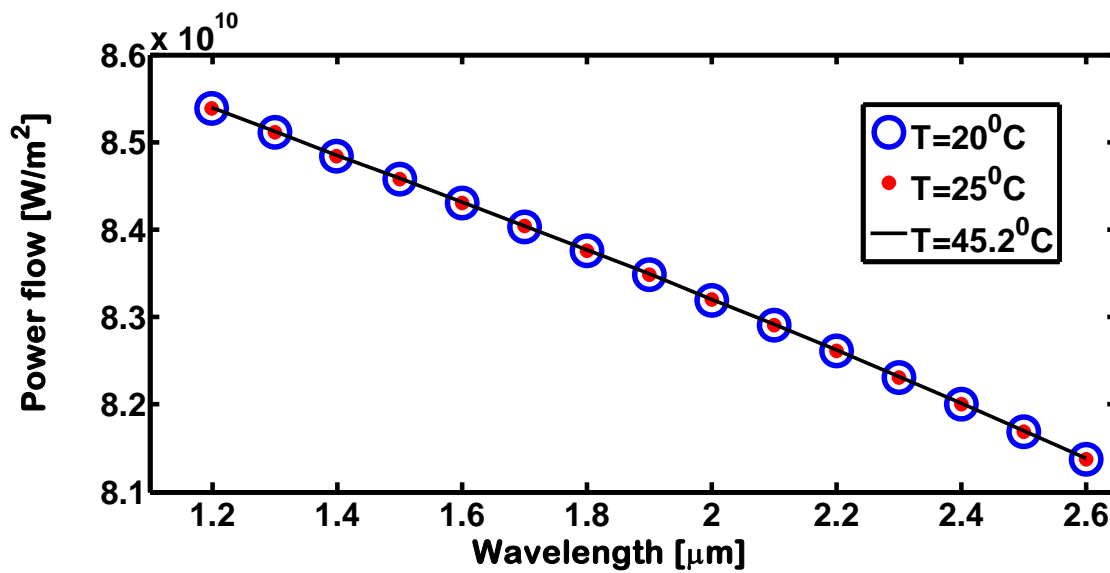


Fig. 4.36 Power flow vs. wavelength of Aluminosilicate glass at different temperatures using PML

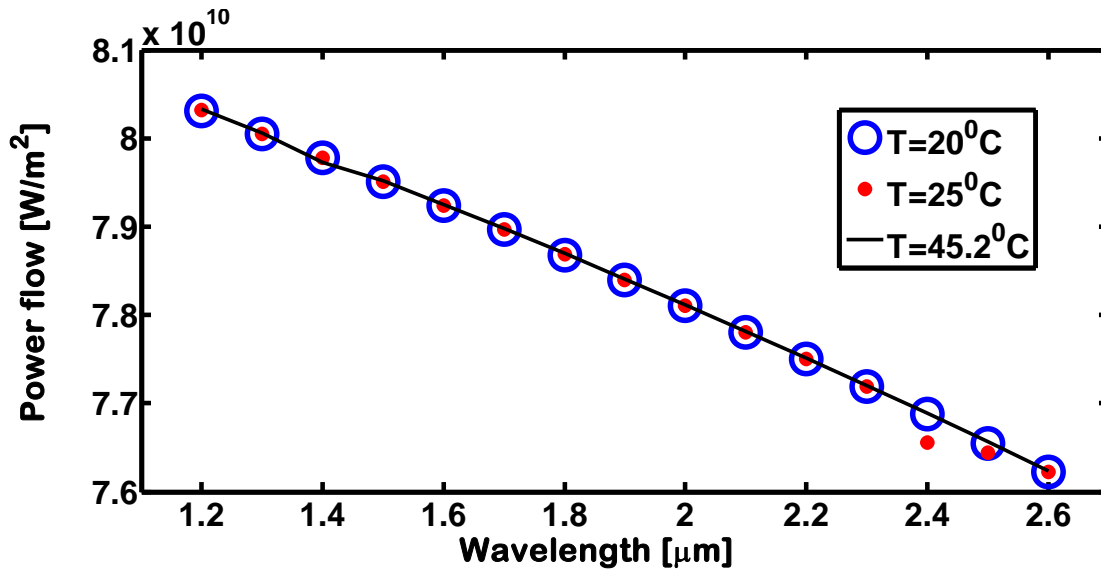


Fig. 4.37 Power flow vs. wavelength of Vycor glass at different temperatures using PML

4.7 Modal Birefringence

Ideally for a single mode step index fiber, modal birefringence is zero. In practice, for standard single mode fibers, it is order of 10^{-6} [42]. The characteristics of birefringence are showed in fig (4.38), fig (4.39) and fig (4.40) for all three types of materials, which are fitted by the simulated values from COMSOL MULTIPHYSICS 4.2 version [13]. From these figures, we see that birefringence is not dependent on temperature, follows a decreasing manner with the increase of wavelength. We should also mention it that the birefringence of Aluminosilicate is little bit higher than other materials. This result is identical with [43]

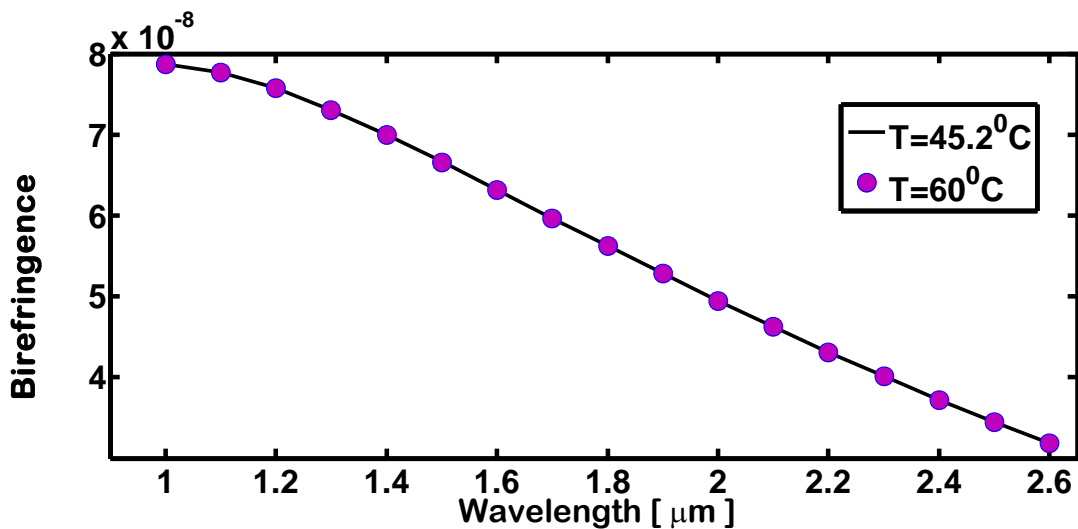


Fig. 4.38 Birefringence vs. wavelength for Aluminosilicate glass

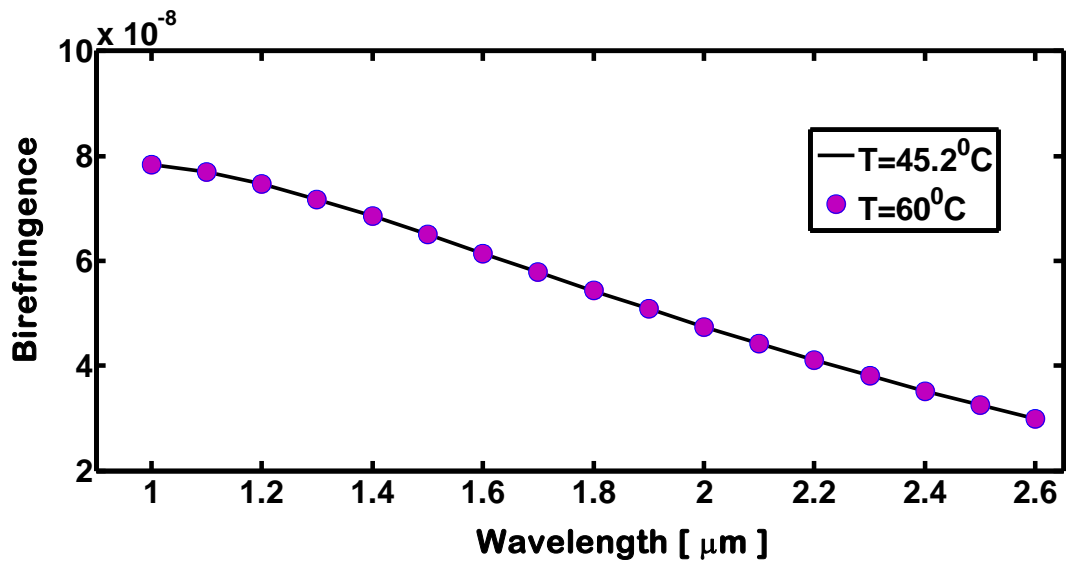


Fig. 4.39 Birefringence vs. wavelength for SiO₂ glass

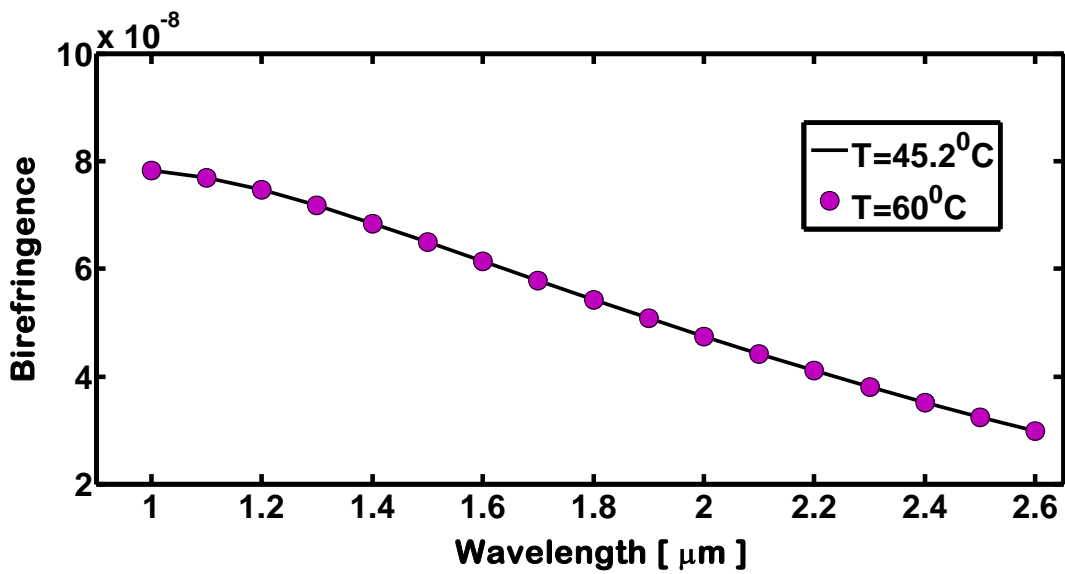


Fig. 4.40 Birefringence vs. wavelength for Vycor glass

4.8 Polarization mode dispersion

Polarization mode dispersion is measured in two manners—for short fiber length and long fiber length. As shown in Fig. (4.41), Fig. (4.42), and Fig. (4.43), PMD does not vary with low temperature variation (45.2°C and 60°C) and is a function of wavelength for short fiber length which satisfies the typical value 1 ns/km [2].

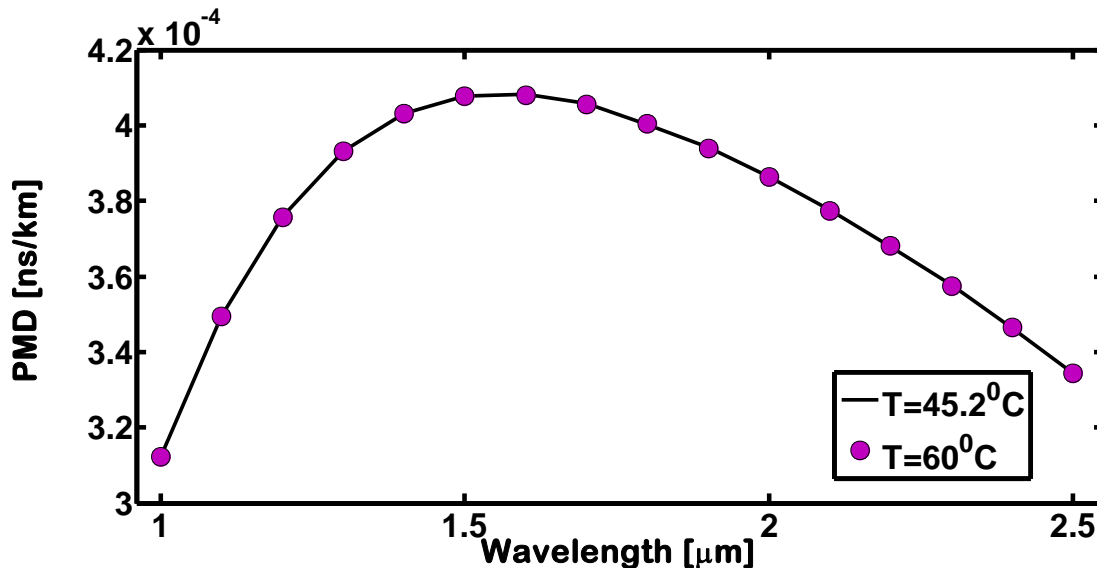


Fig. 4.41 PMD vs. wavelength for SiO_2 glass

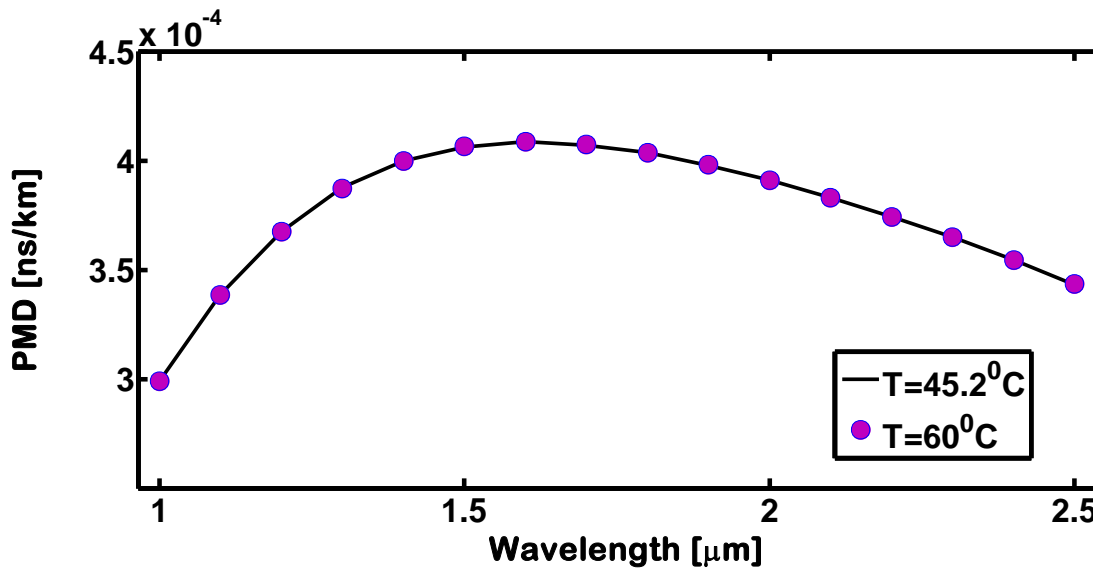


Fig. 4.42 PMD vs. wavelength for Aluminosilicate glass

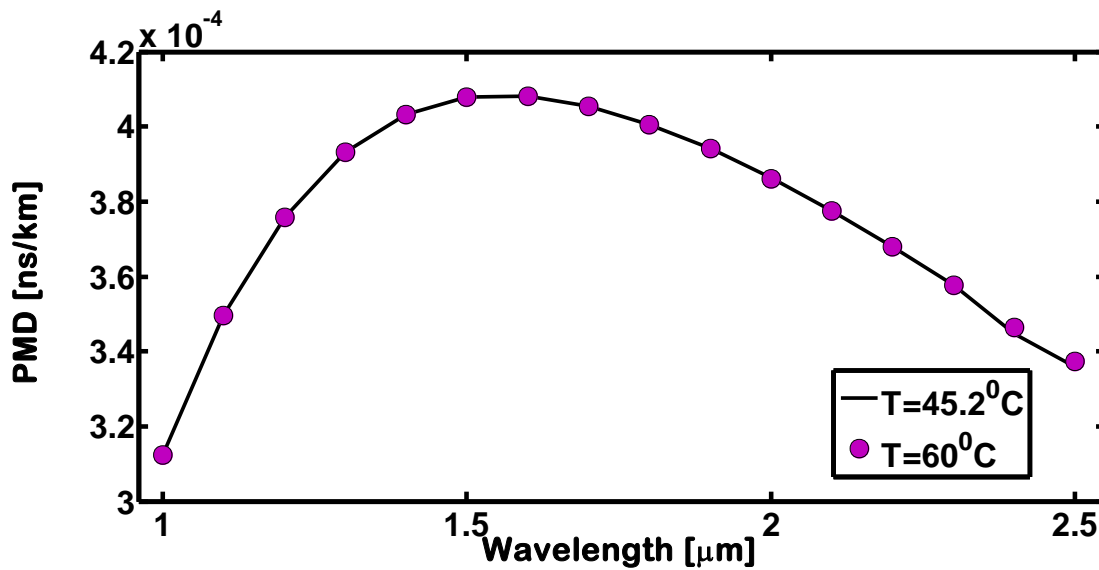


Fig. 4.43 PMD vs. wavelength for Vycor glass

The polarization mode dispersion for Aluminosilicate is higher than other materials (fused silica and vycor) due to higher value of birefringence. So, we can make a conclusion that, birefringence is the main reason of PMD. It is shown in Fig. (4.44), and Fig. (4.45) both at 45.2°C and 60°C .

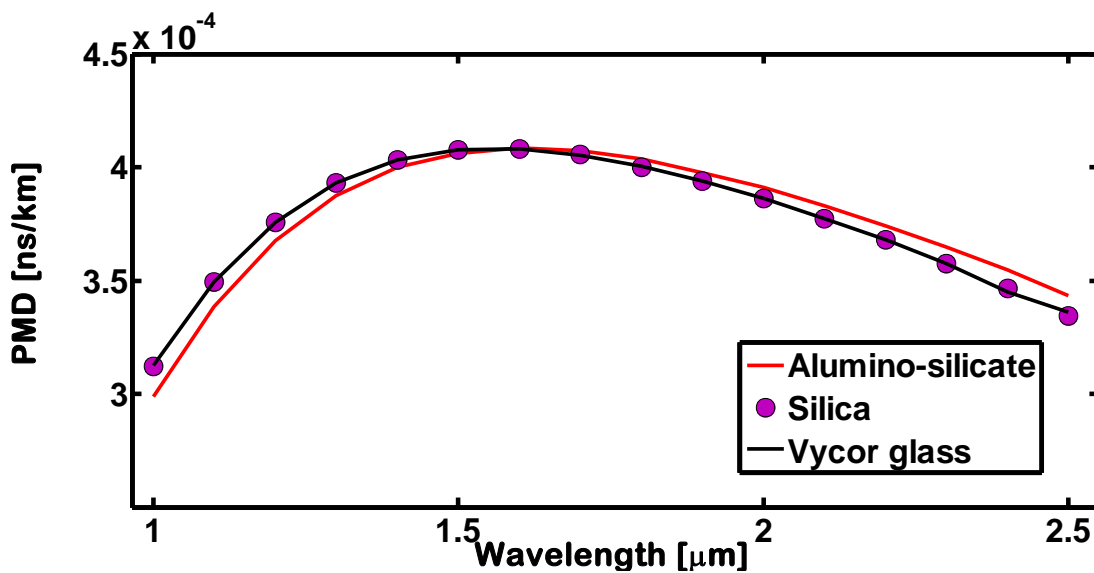


Fig. 4.44 PMD vs. wavelength for all three glasses at 45.2°C

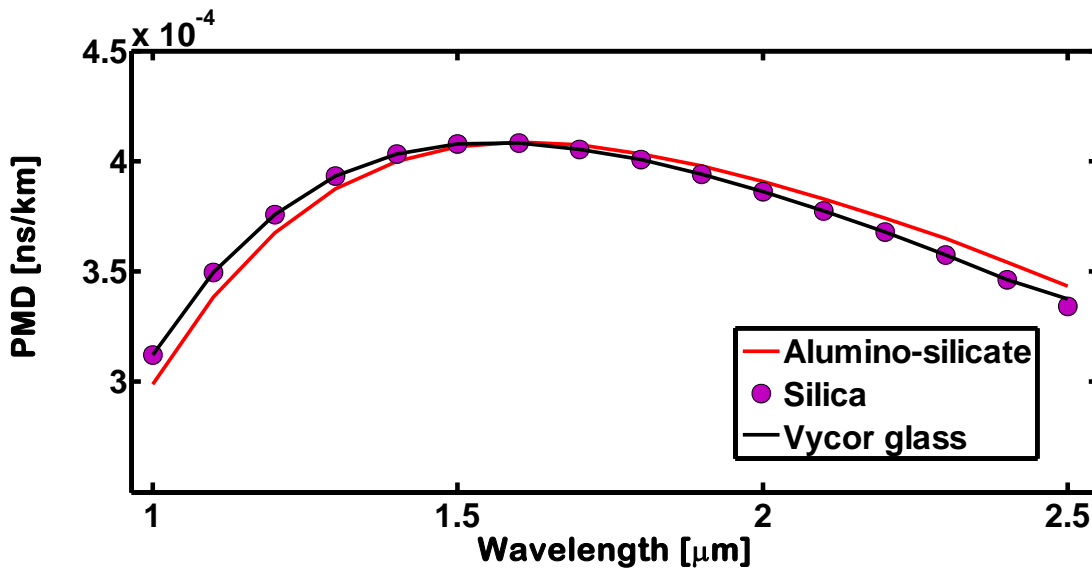


Fig. 4.45 PMD vs. wavelength for all three glasses at 60°C

For a long fiber length, polarization mode dispersion is a function of fiber length in terms of the mean value of the differential group delay. This is calculated according from the relationship [5]. It is measured in $\text{ps}/\sqrt{\text{km}}$ and sometimes called the PMD coefficient parameter. Typical values of D_{PMD} range from 0.05 to 1.0 $\text{ps}/\sqrt{\text{km}}$ [5]. The PMD coefficient is a parameter that is typically specified for commercially available fiber. The PMD coefficient represents the PMD characteristics of one particular length of fiber.

It is shown in Fig.(4.46), Fig. (4.47), Fig. (4.48), Fig. (4.49), Fig. (4.50), and Fig. (4.51) at 45.2°C and 60°C for Fused Silica, Vycor and Aluminosilicate. It is evident that PMD is increased with the increase length of fiber. For a particular length fiber, it violates the range of typical values from 0.05 to 1 $\text{ps}/\sqrt{\text{km}}$ [5]. Here, for fiber length up to 6 km, PMD satisfies the tolerable range at all operating wavelengths at 45.2°C and 60°C.

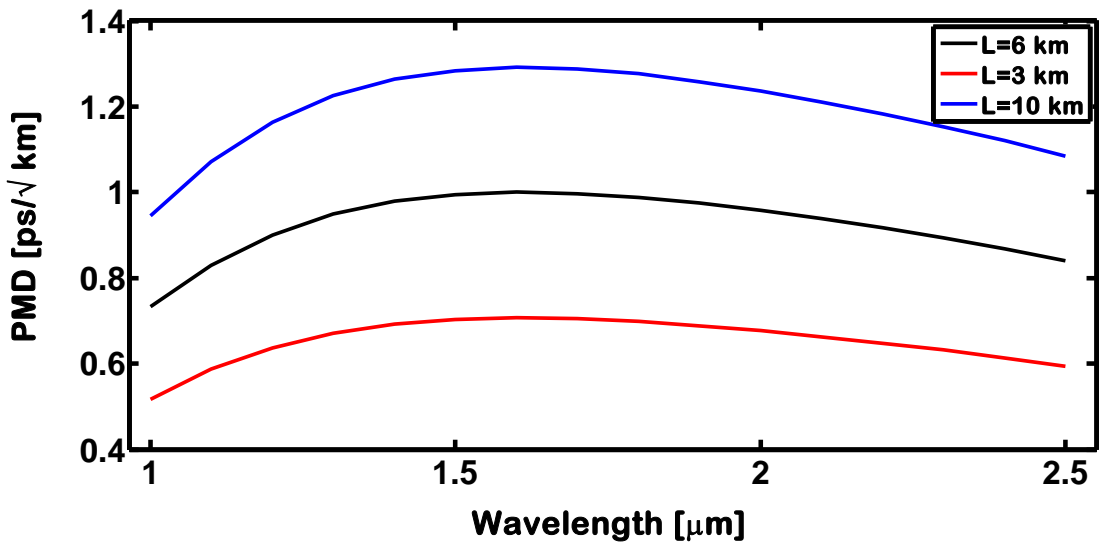


Fig. 4.46 PMD Coefficient vs. wavelength for Aluminosilicate glasses at 45.2°C

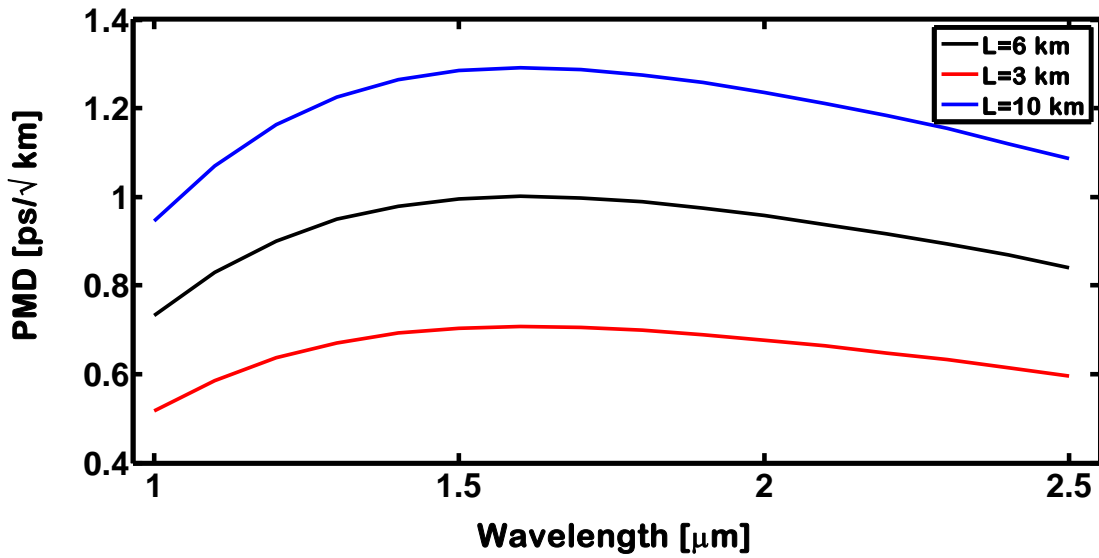


Fig. 4.47 PMD Coefficient vs. wavelength for Aluminosilicate glasses at 60°C

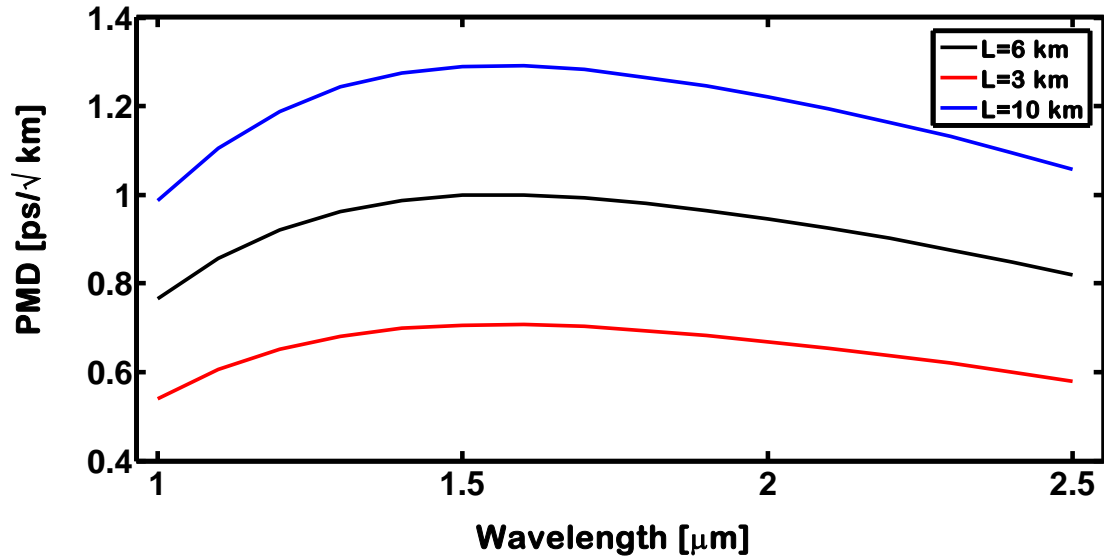


Fig. 4.48 PMD Coefficient vs. wavelength for SiO₂ glasses at 45.2⁰C

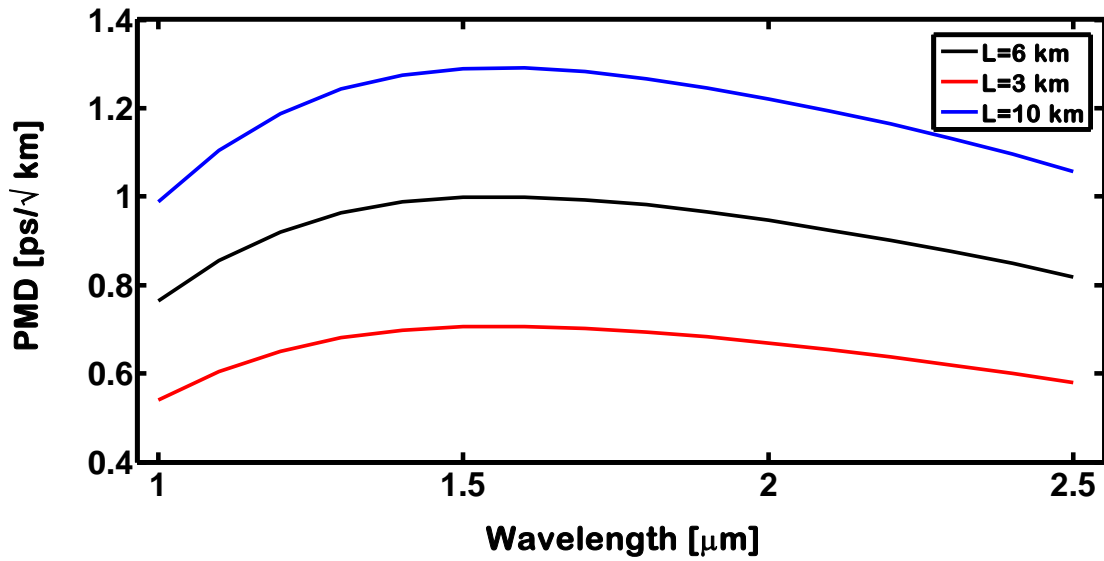


Fig. 4.49 PMD Coefficient vs. wavelength for SiO₂ glasses at 60⁰C

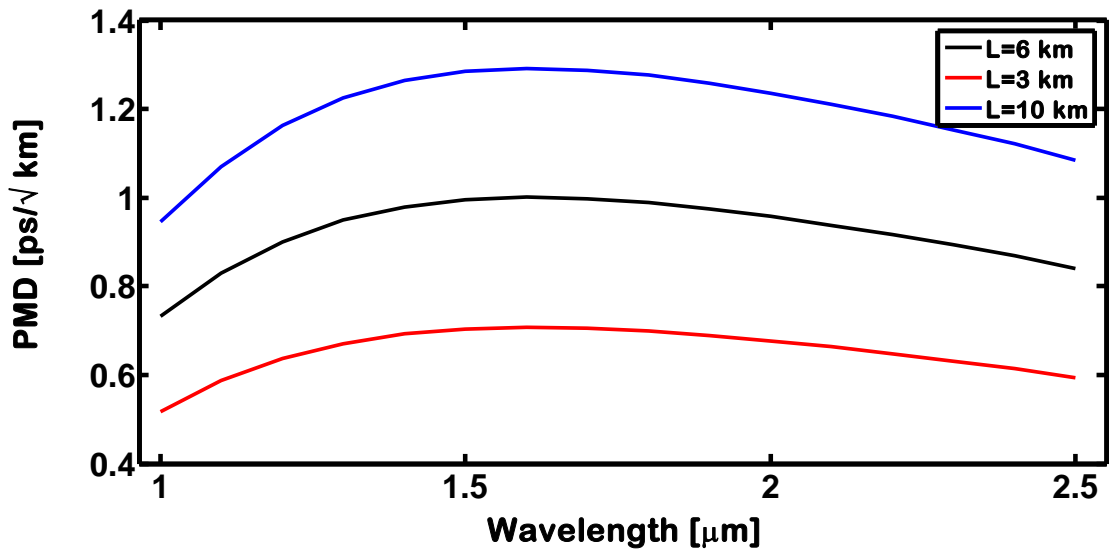


Fig. 4.50 PMD Coefficient vs. wavelength for Vycor glasses at 45.2°C

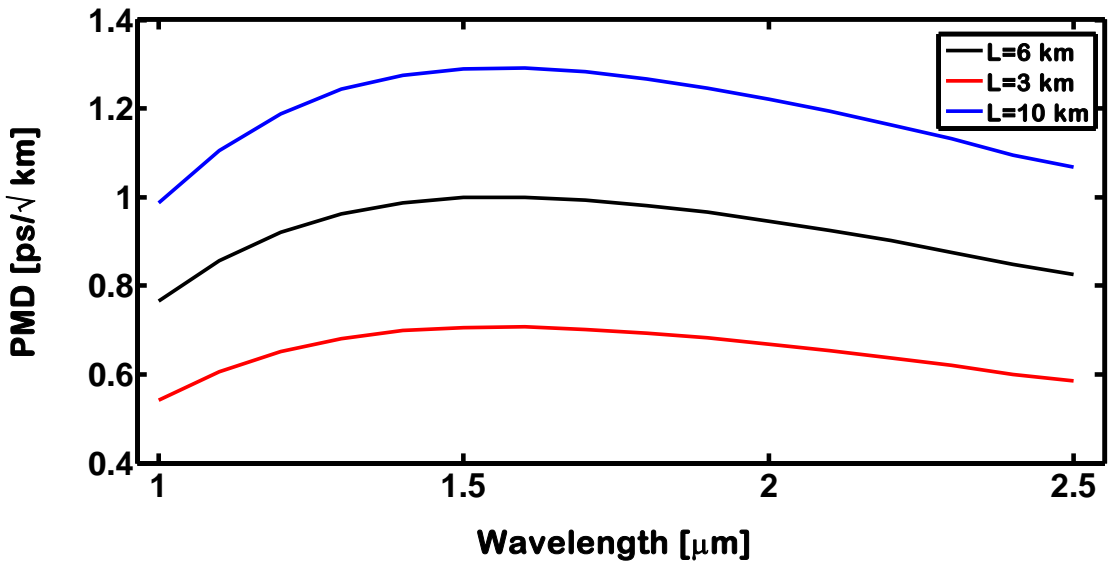


Fig. 4.51 PMD Coefficient vs. wavelength for Vycor glasses at 60°C

Chapter 5

Conclusion

5.1 Conclusion

The refractive index temperature dependence for all three fiber types are fitted in to straight line. The material dispersion and zero material dispersion wavelengths has approximately linear temperature dependence for all three types, SiO₂ and Vycor fibers give nearly similar results while Aluminosilicate give little difference one. For wide range of increasing temperature [-120⁰C to 120⁰C], SiO₂ and Vycor glass has less effect than for Aluminosilicate, since the zero material dispersion shifted by 0.012 for SiO₂ and Vycor glass while 0.024 for Aluminosilicate. The zero dispersion varies linearly with temperature is 0.03nm/⁰C for Aluminosilicate and Vycor glasses, whereas for SiO₂ it is 0.025nm/⁰C. It supports that the variation for SiO₂ is less than the others. The profile dispersion for a fixed temperature (26⁰C) is higher for Aluminosilicate than the two others. The analysis of birefringence shows higher values for Aluminosilicate as compared to SiO₂ and Vycor glass. Also the polarization mode dispersion for Aluminosilicate varies more, than the other materials as a function of wavelength. The above analysis supports that the SiO₂ is the best one among the three fiber types.

5.2 Scope of Future Work

The nonlinearity property like Raman amplification i.e. Raman Gain coefficient for different optical fiber materials may be calculated. The various factors like bending loss, splice loss etc. can be investigated. Photonic crystal fiber (PCF) structure for different fiber materials at different temperatures can be calculated.

References

- [1] Shaymol Badra, Ajoy Ghotok, Guided wave optics and photonic devices.
- [2] J. M. Senior, Optical Fiber Communications, Principles and Practice, (Publisher: Prentice Hall International, Hertfordshire,UK), 1992; 2nd Edition
- [3] <http://9-4fordham.wikispaces.com/Electro+Magnetic+Spectrum+and+light>
- [4] http://www.cisco.com/en/US/prod/collateral/modules/ps5455/white_paper_c11-463661.html
- [5] G. Kaiser, Optical fiber communications, 4th edition.
- [6] www.seamewe4.com
- [7] SEA-ME-WE 4 Network Administration System. Videsh Sanchar Nigam Limited. 2004. Archived from the original on 2007-07-06. Retrieved 2008-01-31.
- [8] G. Ghosh, M. Endo, T. Iwasaki, "Temperature-dependent Sellmeier coefficients and chromatic dispersions for some optical fiber glasses," *Journal of Lightwave Technology*, Vol. 12, No. 8, Aug. 1994.
- [9] W. EI Shirbeeny, Moustafa H. Aly, Ahmed E. EI-Samahy, Khaled M. Emad, " Temperature dependence of zero dispersion wavelength in single mode optical fibers for different materials," *International Journal of Pure and Applied Physics*, Vol. 3, No. 1, pp. 122-131, 2007
- [10] Aqeel Salim Raheem, "Dispersion in different single mode optical fiber materials at different temperature," *Al-Qadisiya Journal for Engineering Sciences*, Vol. 4, No. 3, 2011.
- [11] A. Rostami and S. Makouei, "Temperature dependence analysis of the chromatic dispersion in WII-type zero-dispersion shifted fiber (ZDSF)," *Progress In Electromagnetics Research B*, Vol. 7, pp. 209-222, 2008.
- [12] G. Ghosh and G. Bhar, "Temperature dispersion in ADP, KDP, and KD*P for nonlinear devices," *IEEE J. Quantum Electron*, Vol. QE-18, pp. 143-145, 1982.
- [13] COMSOL MULTIPHYSICS Version 4.2
- [14] http://www.consultants-online.co.za/pub/itap_101/images/fibrestructure.png
- [15] William J. Tropf , Michael E. Thomas, and Terry J. Harris, Properties of crystals and glasses.
- [16] www.corning.com

- [17] <http://upload.wikimedia.org/wikipedia/commons/thumb/5/5d/RefractionReflexion.svg/660px-RefractionReflexion.svg.png>
- [18] <http://www.fermaxuk.com/img/image/FODibujo2.jpg>
- [19] M. Satish Kumar, Fundamentals of Optical Fibre Communication.
- [20] Goralski, Optical Networking & Wdm
- [21] Samuel Y. Liao, Microwave devices and circuits, 3rd edition
- [22] David M. Pozar, Microwave Engineering, 4th edition.
- [23] A. Mendez, T. F. Morse, Specialty optical Fibers, Academic Press.
- [24] Tsai, Wan-Shao; Ting, San-Yu; Wei, Pei-Kuen, "Refractive index profiling of an optical waveguide from the determination of the effective index with measured differential fields," Optics Express, Vol. 20 Issue 24, pp.26766-26777 (2012)
- [25] E. G. Neumann, Single mode fibers; Fundamentals, Springer-Verlag, 1988.
- [26] L. B. Jeunhomme, Single mode fiber-optics, Marcel Dekker, 1983.
- [27] G. Ghosh, "Temperature-dependent Sellmeier coefficients and chromatic dispersions for some optical fiber glasses," *IEEE J.Lightwave Technology*, Vol. 12, No. 8, pp. 1338-1342,1994.
- [28] G. Ghosh, "Pressure-dependent Sellmeier coefficients and material dispersion for silica fiber glass," *IEEE J.Lightwave Technology*, vol. 16, no. 11, pp. 2002-2005,1998.
- [29] R. Gupta, "Absolute refractive indices and thermal coefficient of Fused Silica and Calcium Fluoride near 193nm," *Journal of Applied Optics* ,Vol. 37, No. 25 Sep. 1998.
- [30] Paul K.J. Park, "A novel chromatic dispersion monitoring technique using frequency-modulated and amplitude-modulated pilot tones," *Optical Fiber Communication Conference*, 5-10 May, 2006.
- [31] J. Matsuoka, N. Kitamura, S. Fujinaga, T. Kitaoka, and H. Yamashita, "Temperature dependence of refractive index of SiO₂ glass," *J. Non-Cry. Sol.*, vol. 135, pp. 86-89, 1991.
- [32] D. C. Agarwal, Fibre Optic Communications, 2nd edition, Wheeler Publishinhg, India, 1993.
- [33] Safa O. Kasap, Optoelectronics and photonics principles and practices.
- [34] Max Ming-Kang Liu, Principles and Applications of Optical Communications, 1st edition, IRWIN, Chicago, 1996.

- [35] G. Yabre, "Comprehensive theory of dispersion in graded-index optical fibers," *IEEE J. of Lightwave Technol.*, Vol. 18, No.2, pp. 166-176, 2000.
- [36] Saitoh, K. and Koshiha M., "Numerical modeling of photonic crystal fibers," *Lightwave Technology*, Vol. 23, No. 11, pp. 3580-3590, 2005.
- [37] Saitoh, K. and Koshiha M., "Chromatic dispersion control in photonic crystal fibers: Application to ultra-flattened dispersion," *Optic Express*, Vol. 11, pp. 843-852, 2003.
- [38] Gorachand Ghosh, Handbook of ther-optical constants of solids, Academic Press.
- [39] J. P. Bérenger, "A perfectly matched layer for the absorption of electromagnetic waves," *J. Comput. Phys.*, vol. 114, no. 1, pp. 185–200, 1994.
- [40] www.rp-photonics.com
- [41] Subir. K. Sarker, Optical fibers and fiber optic communication systems, 2nd edition, S. Chand and Company Ltd., India, 2001.
- [42] Norbert Grote, Herbert Venghaus, Fibre optical communication devices.
- [43] Petr Hlubina, Tadeusz Martynkien, and Waclaw Urbańczyk, "Dispersion of group and phase modal birefringence in elliptical-core fiber measured by white-light spectral interferometry," *Optics Express*, Vol. 11, Issue 22, pp. 2793-2798, 2003

